EQUINE IMMOBILIZATION WITH A LIMB RESTRAINT SYSTEM

A Thesis Submitted to the College of

Graduate Studies and Research

In Partial Fulfillment of the Requirements

For the Degree of Master of Science

In the Department of Mechanical Engineering

University of Saskatchewan

Saskatoon

By

Wei Cai

Keywords: Standing Horse, Mobility, Joint Restraints, Breaking Force, Immobilization,

PERMISSION TO USE

In presenting this thesis in partial fulfilment of the requirements for a Postgraduate degree from the University of Saskatchewan, I agree that the Libraries of this University may make it freely available for inspection. I further agree that permission for copying of this thesis in any manner, in whole or in part, for scholarly purposes may be granted by the professor or professors who supervised my thesis work or, in their absence, by the Head of the Department or the Dean of the College in which my thesis work was done. It is understood that any copying or publication or use of this thesis or parts thereof for financial gain shall not be allowed without my written permission. It is also understood that due recognition shall be given to me and to the University of Saskatchewan in any scholarly use which may be made of any material in my thesis.

Requests for permission to copy or to make other use of material in this thesis in whole or part should be addressed to:

Head of the Department of Mechanical Engineering

University of Saskatchewan

Saskatoon, Saskatchewan S7N 5A9

ABSTRACT

Mobility of the horse to initiate motion from the standing position is examined in this thesis. In particular, the thesis focuses on the study of the mobility of a horse with fixed hooves to the ground, and on how its musculoskeletal system is used to free the legs from restraints. Possible leg patterns to initiate motions are investigated. The breaking forces generated at front and hind hooves during static-pulling and dynamic jerking are evaluated. Design of the restraint system that uses ropes to immobilize certain joints in order to prevent the horse from generating these forces is the main objective of this thesis. Such a system could be applied as an alternative to rather massive mechanical devices, the main purpose of which is to block the breaking forces (which are quite large when fully developed).

Analysis of the mobility of the horse is based on the mechanics of a skeletal linkage system driven by muscle forces. Only major muscles involved in fighting the restraints are included in the analysis. The force generation capability of a muscle is determined by physiological cross sectional area (PCSA) of the muscle. Possible leg patterns are predicted with the kinematics analysis considering range of motion at each joint in the legs. Corresponding breaking forces generated in each pattern is evaluated with the kinetics analysis. Relationship between the characteristic parameter of the pattern and the breaking force at hoof are established.

The horse's computer model is used to justify the analytical result. Fighting mechanisms of the horse are simulated in the dynamic simulation software package. Patterns and the breaking forces developed by the horse model simulation agree well with the analytical results. To the

author's best knowledge, this is the first time a computer model is used in analyzing the method of restraining an animal.

The mobility of the animal with hoof restraints and methods to remove mobility were further confirmed with a preliminary animal restraint test conducted on a sheep. The sheep was chosen because the leg patterns to initiate motion on a horse are similar to that of sheep, but the sheep is more convenient to handle. The experiment showed that the mobility of the sheep could be removed completely by restraining its hooves, lower legs, and head with easily attached ropes.

ACKNOWLEDGMENTS

This thesis cannot be accomplished if not for the help from many people and their support.

I would like to take this opportunity to thank my supervisor Professor Walerian Szyszkowski, PhD, PEng, who guided me through the research with his enthusiasm, understanding and invaluable knowledge.

My appreciation also goes to my committee members Prof. Gregg Adams, Prof. Dean Chapman and Prof. Richard Burton for their valuable suggestions and continuing encouragement. Special thanks to Prof. Glen Watson for his support over the years.

The contributions of Prof. Peter Flood, Prof. Ronald Chaplin from the Western College of Veterinary Medicine and Mr. Hans Steinmetz from the Department of Mechanical Engineering in setting up the experiments and sharing of their expertise are truly appreciated.

During the course of this work, I was supported by NSERC and SSI grant through Prof. Glen Watson, Prof. Walerian Szyszkowski and Prof. Gregg Adams.

Sincere appreciation also goes to my husband Goh Wee Seng, parents Cai Fuhe, An Ping and sister Cai Jin for their love and support.

DEDICATION

This thesis is dedicated to the author's parents

Cai, Fuhe

&

An, Ping

TABLE OF CONTENTS

LIST OF TABLES

Table **Page**

LIST OF FIGURES

Figure **page**

LIST OF ABBREVIATION

A	Elbow joint (f) or stifle joint (h)
a	Acceleration
a_{arm}	Moment arm of muscle forces
B	Carpal joint (f) or hock joint (h)
b	Distance between elbow joint and biceps insertion point (f) or distance between stifle joint and biceps femoris (h)
BF	Breaking force at hoof
C	Fetlock joint (f) or metatarsus joint (h)
D	Pastern and hoof joint
E	Shoulder joint (f) or hip joint (h)
e_x	Vertical distance between shoulder joint and biceps insertion (f) or vertical distance between hip joint and biceps femoris insertion (h) in arbitrary pattern
e_y	Horizontal distance between shoulder joint and biceps insertion (f) or horizontal distance between hip joint and biceps femoris insertion (h) in arbitrary pattern
e_x^0	Vertical distance between shoulder joint and biceps insertion (f) or vertical distance between hip joint and biceps femoris insertion (h) in rest standing pattern
e_y^0	Horizontal distance between shoulder and biceps insertion (f) or horizontal distance between stifle and biceps femoris insertion (h) in rest standing pattern
F_1	Constraint force at carpal joint (f) or hock joint (h)
F_2	Constraint force at fetlock joint
F_{Ax}, F_{Ay}, F_A	Reaction force at joint A
F_{Bx}, F_{By} or F_B	Reaction force at joint B
F_{br}	Breaking force at hoof
F_{Cx}, F_{Cy} or F_C	Reaction force at joint C
F_{Dx}, F_{Dy}	Reaction force or breaking force at joint D
F_m, F_{mx}, F_{my}	Biceps muscle force
F_p	Force to move the leg in vertical direction
F_{xi}	External force applied in x direction
F_{yi}	External force applied in y direction

H	Length between elbow joint and hoof joint (f) or length between stifle joint and hoof joint (h) when the leg is stretched in a line
I	Biceps (f) or Biceps femoris (h) insertion point
i	Number of part in the system
J_{c1}	Moment of inertia about centroid of link1
J_{c2}	Moment of inertia about centroid of link2
j	Number of coordinate
k	Number of constraint equations
L	Lagranian
l_1	Length of link1
l_2	Length of link2'+ link3'
$l_2^{'}$	Length of metacarpus (f) or metatartus (h)
$l_3^{'}$	Length of pastern (f/h)
l_{c1}	Length between joint A and the center of mass of link1
l_{c2}	Length between joint D and the center of mass of link2
M	Mass on top of forelimb or hindlimb
M_i	Moment applied on each part
q	General coordinates
T	Kinetic Energy of the system
V	Potential Energy of the system
x	Displacement of joint A
x_{ci}	Displacement of centroid of a part in x direction
x_{stop}	Maximum displacement of joint A before it stops
v	Velocity
y_{ci}	Displacement of the centriod of a part in y direction
$v_{\max}$	Maximum velocity of joint A before it stops
α ,β,γ	Joint angle
$\dot{\alpha},\dot{\beta},\dot{\gamma}$	Joint angle velocity
$\ddot{\alpha},\ddot{\beta},\ddot{\gamma}$	Joint angle acceleration
θ_i	Angular displacement
λ	Lagrange multiplier
φ_1, φ_2	Restraint attachment angle
ϕ_k	Constraint equations

Note: f: forelimb
h: hindlimb

1. INTRODUCTION

1.1 Immobilizing a Horse

Immobilizing a horse is often required for medical imaging procedures, transportation and veterinary medical examinations, etc. Based on the handling experience, some simple restraint devices have been designed and used such as metal stocks, a table and straps, etc. Although horses may generally be positioned as required, none of these devices removes the horse's mobility sufficiently for imaging. Also, such restraints allow the horses to struggle within them. As a consequence, the animals very frequently injure themselves when fighting to break free and\or threatens the safety of handlers.

The other possibility to immobilize a horse is to use general anesthesia that will completely paralyze its muscles. However a support breathing system is always needed during general anesthesia. In addition, special treatment assisting the horse during recovery from general anesthesia, such as a cushioned room or water pool, are typically required to decrease the incidence and/or severity of post anesthetic complications. All of the complexity of administering general anesthesia can be avoided if a mechanical device can completely eliminate the animal's mobility, which is the object of this thesis. The novelty of such a design will be that instead of using mechanical devices to block large forces generated by a horse's muscle, this design will prevent the horse from generating such forces at all or will reduce them substantially. Therefore, this thesis focuses on mobility of the horse and designing the restraint system to

remove it. A thorough understanding of the horse's mobility is required for a successful design of such a system.

There is a perception that horses are designed by nature to run. Therefore, almost all research on the equine locomotion system focused on the study of the animal in motion. There are many studies analyzing walking, running or jumping horses [1, 2, 3, and 4]. Results from such studies do not help in the design of a restraint method since none of them examines how the animal initiates motion from standing. Mobility of the horse to initiate motion from the standing position is essentially a new concept introduced in this thesis. In particular, the thesis will focus on the study of a horse with removed mobility of the hoof. This is implemented by fixing horse hooves to the ground. The horse's body should remain motionless when mobility of the legs is removed by means of restraints.

Study of the mobility of the horse is based on understanding the musculoskeletal structure and the muscle functions of the horse. The skeletal system was considered as a simplified mechanical linkage system. Prediction of possible patterns of the initiation of motion was made by studying the linkage kinematics and dynamics.

Methods to remove mobility with external restraints were developed based on analytical calculations, computer simulations and experimental observations.

Due to the cost and safety involved, preliminary tests were preformed on sheep, which react somewhat similarly to restraints but are much easier to handle. Testing of the restraint methods with a sheep generally proves that this method works quite efficiently. Testing a horse should be done as future work. The computer model should help to design the restraint system which has to be strong enough to handle horses.

1.2 Mechanism of Initiating Motion with Fixed Hooves and the Method of Analysis

A standing horse must displace hooves (or a hoof) and move its legs to initiate horizontal motion. With the hooves fixed, it will try to pull one leg out of the hoof restraint in order to move it. As sketched in Figure1.1a, when the horse stands normally, the weight (W) carried by both forelimbs is distributed evenly on the two forelimbs. Weight W will be in order of 2,000N (which corresponding to a 100kg mass carried by each of the forelimbs).The ground reaction force (GRF) will be compressive and equal to half of the weight carried by the front legs. When the horse tries to free the right forelimb, for example, the weight will be switched from the right forelimb to the left forelimb. If the hoof is unconstrained, the right leg can be raised and moved forward (or backward) and the horse's weight will be supported by the remaining free legs during this time. If the hoof is constrained then the horse will use muscles to generate tensile forces to pull the leg from the ground. This force, referred to as the breaking force (BF) is not related to the horse's weight. The BF in the right leg is tensile, while the left leg will carry the compression force being the sum of weight W plus BF as shown in Figure1.1b. It is assumed that the leg's skeleton system is sufficiently strong to carry such a compression force without any damage. On the other hand, the tensile force BF can relatively easily either damage the hoof or break the restraint. Therefore, this force will be the main subject of the analysis presented. It is demonstrated that the situation at the hindlimb is similar (i.e.: the corresponding BF can be determined) to the forelimb. Due to the nature of BF, the horse's weight will not be included in the analysis of a limb fighting mechanism.

It should be noted that spreading the legs may be an efficient method of constraining the horse. In the position sketched in Figure 1.1c, the horse will not be able to shift the weight W from the right leg to the left leg. This is because a centered W supported by the left leg has to be

balanced with extra moment, otherwise the animal will fall. However, there are no sufficiently strong muscles to supply this extra moment (by twisting the upper body, for example). This extra moment must come from the ground reaction force supporting the leg. This force will obviously disappear at the moment when the horse makes any attempt to raise the leg. Therefore in the spread leg configuration, the animal is not capable of fighting the restraint as effectively as in the un-spread configuration.

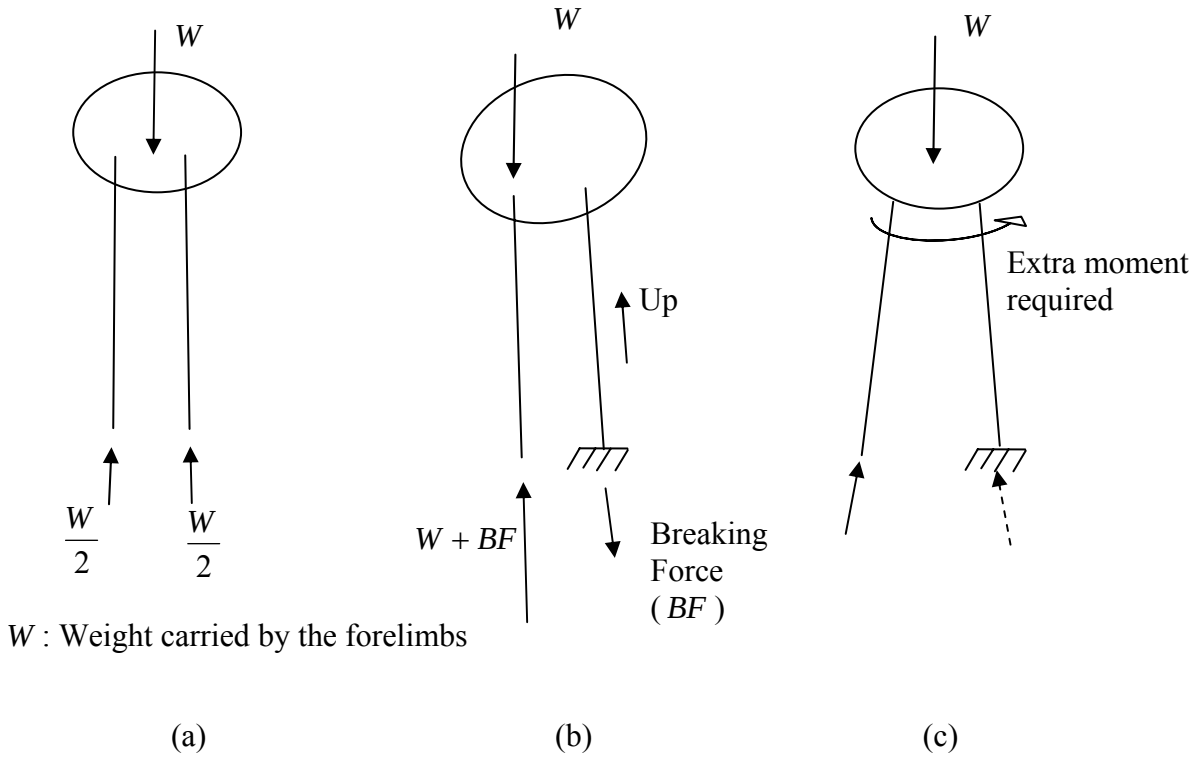

Figure 1.1: Weight shifting mechanism to free the forelimb

To obtain the breaking force, the steps of analysis approach outlined in Figure1.2 will be used. The analysis results will then be used for a better design of the restraint. The horse is modeled as a linkage system. The initial full mobility of such a system is reduced by fixing all four hooves to the ground. With the assumed range of motion at each joint, all possible leg

patterns that can be formed within the hoof restraints are identified. When muscle forces are applied, the quasi-static breaking force (*BF*) generated at the hoof restraint for each pattern is obtained. Then the pattern in which the maximum breaking force can be generated is determined. This pattern is assumed to be the 'best' for the horse in the sense that the horse will try to use it to free the leg. The breaking force under dynamic jerking is also obtained and will be compared with the quasi-static breaking force. Next, more restraints will be added to completely remove the mobility of the leg and to prevent forming the patterns that generate large *BF* at the hoof. Finally, the constraint forces will be minimized by adjusting the restraint angles at each joint.

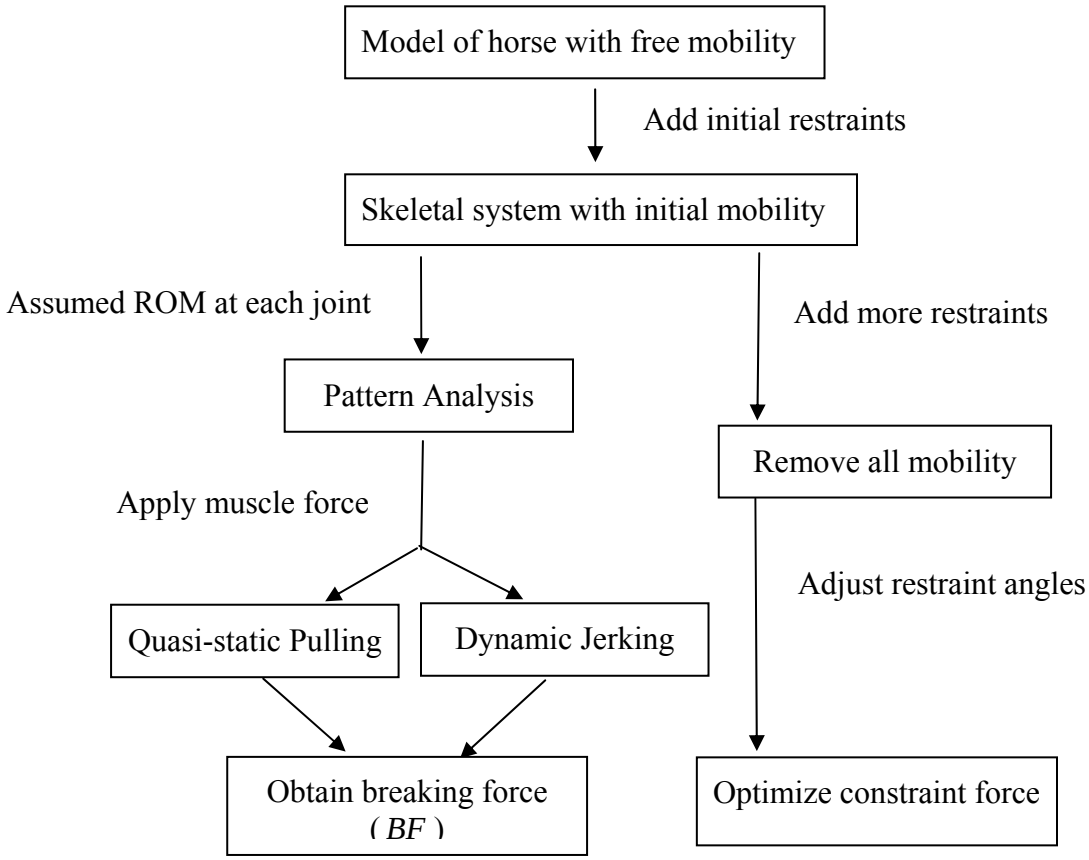

Figure 1.2: Scheme of analyzing restraint method

1.3 The Musculoskeletal System of a Horse

Horses move mainly by rotating the limb members around adjacent joints. There are, however, certain limitations placed on the rotation of joints. The shape of the articular surfaces, tension in extra capsular ligaments, contraction or passive tension in muscles and other soft structures around a joint may arrest movement [5]. The limit of rotation is referred as Range of Motion (ROM). The ROM of each joint of the limbs will be discussed next. When a hoof is constrained to the ground, the degree of freedom of the limb is reduced and the corresponding patterns of the leg motion, which include ROM of each joint of the leg, can be identified.

Muscle contraction is the driving force of animal locomotion. This study assumes the animal can fight against the restraints with its peak isometric muscle force. Force generation capacity of major horse muscles was reported [6,7]. The peak isometric muscle force is defined by $F_0^M = C \times PCSA$, where C is the maximum isometric stress of the horse skeletal muscle taken as 0.3MPa [6] and PCSA is the physiological cross sectional area of the muscle. The action of a particular muscle force is assumed to be in line with the muscle.

1.4 Mechanics of the Limb Linkage System

In this chapter, only motions of the limb linkage system on the sagittal plane are considered. Motion off this plane is relatively insignificant and contributes very little to fighting the restraints.

The geometric patterns of the limb's motion as well as velocity and acceleration of each part of the linkage system is studied by applying the methods of kinematics. The maximum breaking force is calculated. It is believed that the horses may intuitively find the best geometrical pattern

to generate such a force. Relationship between the pattern and the breaking force can be predicted either by the kinetics or by the quasi-static analysis.

There will be no motion in the limb if the muscle forces are balanced by the reactions at the restraint or if the ROMs of joints are reached. Then the quasi-static breaking force can be calculated from equilibrium equations in the form:

$$\sum F = 0 \text{ and } \sum T = 0 \qquad (1.1)$$

The first equation represents equilibrium of forces, where the second represents equilibrium of moments.

With some mobility still present, the animal may struggle violently against the hoof restraint to generate some dynamic jerking force. The dynamic breaking force at hoof can be analyzed with the help of Newton's law of motion in translation and rotation for each limb, written symbolically as:

$$\sum F = ma \text{ and } \sum T = I\alpha \qquad (1.2)$$

where a and α are respectively the translational and rotational accelerations of the members considered. The breaking force can be determined either by solving the static equation (1.1) or the dynamic equation (1.2).

Simulation software such as ADAMS solves the dynamic problem (1.2) using the Lagrangian approach which is equivalent to Newton's equation. Details of the equations of motion in the Lagrange's form can be found in Appendix D.

1.5 Computer Model of the Horse

Dynamic analysis software can be used to simulate the motion of a horse and its interaction with the restraints. A computer based horse model was used previously [4] to study horse free

locomotion. This thesis is the first attempt to use a computer animal model to study the animal's mobility with initial restraints.

Simple linkage models and anatomical model are built in SolidWorks and its dynamic simulation package COSMOS which solves the dynamics problem using the ADAMS solver. The dynamic analysis method used is identical to those used in the analysis of ordinary dynamic mechanical systems. Each part in the anatomical model is treated as a rigid body and is characterized by its geometric profile, mass, center of gravity and moment of inertia. A system of Lagrangian equations, which is equivalent to (1.2), is automatically generated and solved by the computer using a formal description of the constraints, loading forces and initial conditions. The results are used in the computer simulation of the motion. More details about creating the model can be found in Appendix B and C.

2. FORELIMB RETRAINT METHOD

2.1 Forelimb Musculoskeletal Structure and Mobility

A horse forelimb is composed of long bones suitable for rotation. Bones of the forelimb include [5]: Scapula, Humerus, Radius & Ulna, Metacarpus, Proximal, Middle and Distal phalanges. These bones are linked at shoulder, elbow, carpas, fetlock, pastern and coffin joints [9] as shown in Figure 2.1.

The range of motion at each joint is shown in Figure 2.2 [10, 11, and 12]. In free locomotion, the forelimb can develop various configurations that are within these ranges. However, fixing the hooves of the limbs will significantly reduce the number of possible configurations and the horse's mobility. For a linkage system, fixing the distal end of it will eliminate two degrees of freedom. The horizontal direction freedom of the proximal end of the limb is limited by fixing all the hooves. In addition, the radius and the ulna are only allowed to rotate forward from the natural standing position since the extruded olecranon of the humerus limits the ROM of elbow joint. Moreover, the carpal and fetlock joints can not extend further. As a result, the only mechanism the horse can use to fight the hoof restraint is to flex the elbow.

Flexing the elbow joint is driven by the powerful biceps which is the most important flexor on a forelimb. Maximal force generation capability is estimated to be about 11,000N. [6] This biceps force can be transmitted to generate a breaking force at the hoof. The forces generated by other muscles of the forelimb to fight the hoof restraint

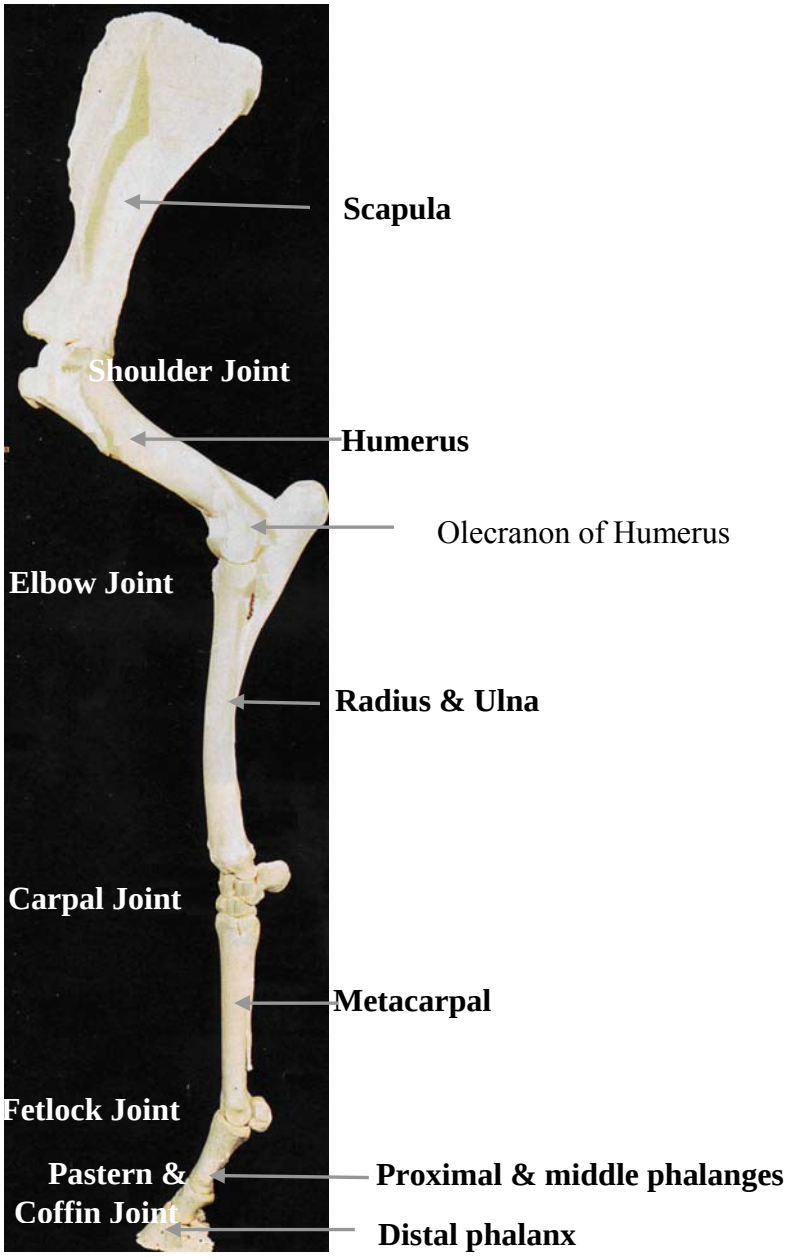

Figure 2.1: Skeleton of the horse forelimb

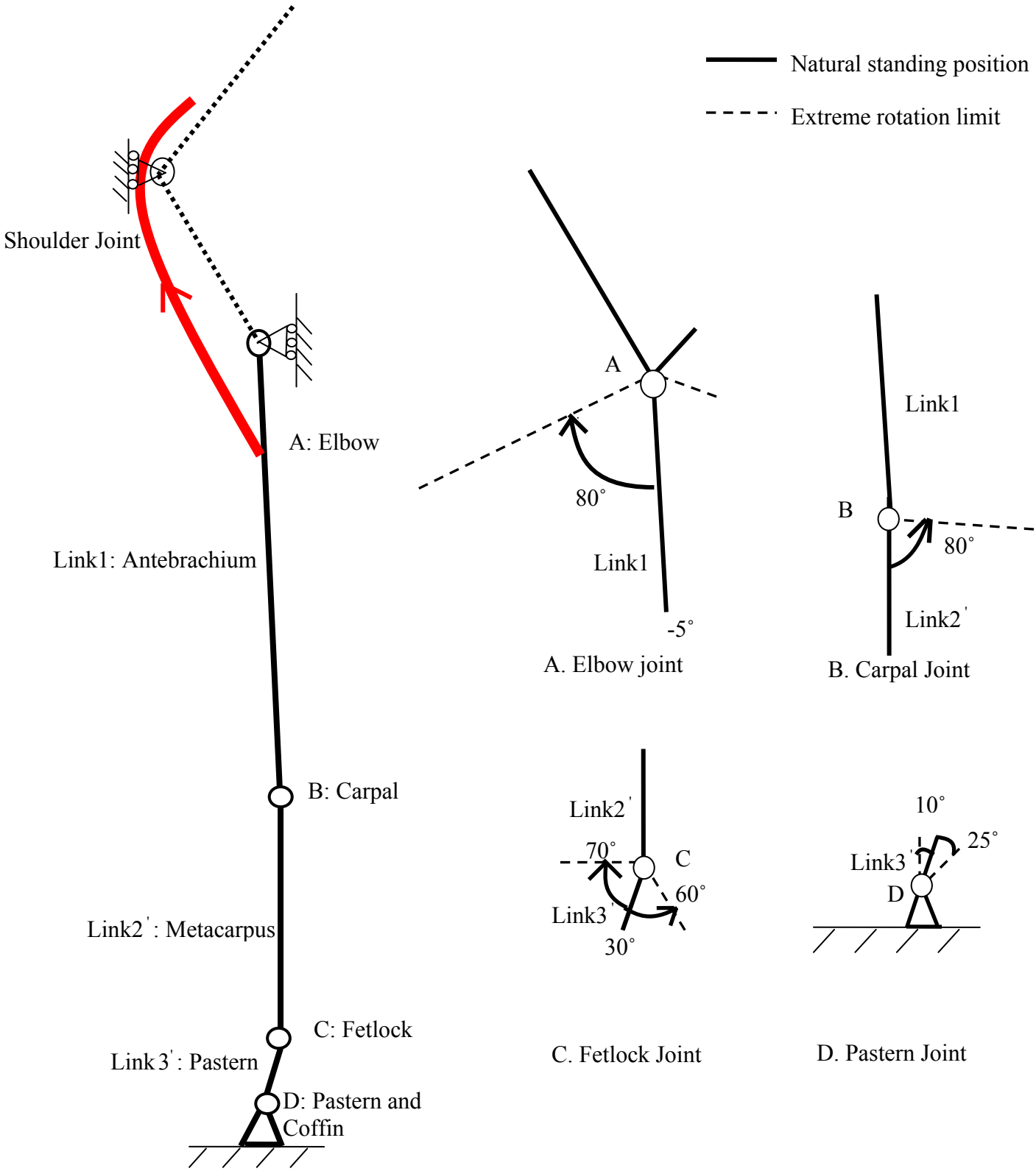

Figure 2.2: Linkage system of the horse forelimb and the ROM at each joint

are significantly smaller. Evaluation of these forces in fighting the hoof restraint can be found in Appendix A.

The animal can pull the hoof slowly with the biceps force (quasi-static action). The animal can also pull the hoof by dynamic jerking (i.e. by dynamic action) as observed in the experiment with the restrained sheep. These two ways of generating the BF will be analyzed in the next section.

2.2 Mechanical Model of the Horse Forelimb in the Standing Configuration

The musculoskeletal system of the forelimb has been discussed in the previous chapter. In this section, the restrained forelimb of the horse is modeled as a simplified linkage system. Based on anatomic analysis, it has been assumed that the forelimb mobility is driven by the biceps muscle. The hoof is attached to the ground and the upper body is allowed to move vertically.

This mechanical model should be helpful in answering the following questions:

- What are the possible leg patterns of initiating the motion and the forces to lift the hoof?
- What is the best pattern for the horse to develop the maximum force in fighting the hoof restraint?
- What are the effects of dynamic jerking in striking against the hoof restraint?
- How to remove the mobility of the forelimb in initial restraints by applying more restraints?

2.2.1 The Forelimb Mechanical Model

The forelimb of the horse with hoof restraint can be modeled as a three link system with a mass at the top as shown in Figure 2.3. The links were considered undeformable. In general, the rules of mechanics (statics and dynamics) of rigid bodies will be applied.

The top mass, estimated at 100kg, is added to represent a portion of the horse's trunk and the upper arm (scapula and humerus) which may be involved in the forelimb motion. It is assumed

that in dynamics, the horse can relocate this mass up or down to maximize the breaking force at the constrained hoof. This mass can also be locked at a particular vertical position by using the upper body muscles. In particular, a quasi-static configuration to produce maximum force will be developed by allowing the top mass to move freely in vertical direction. The motion could be generated with the force F_p, coming from upper body as shown in Figure 2.3.

Link1 (l_1), link2$'$ (l_2') and link3$'$ (l_3') represent antebrachium, metacarpus and pastern accordingly. The member of length l_2 indicates link2 formed when tension on members l_2' and l_3' align them together. Joint A, B, C, D stand for elbow, carpal, fetlock and pastern respectively. Each joint is assumed to be a planar revolute joint.

As discussed previously, it is assumed that only the biceps will be used when the horse is attempting to break the hoof's restraint. The action line of the force is the line from biceps insertion point (I) on the antebrachium to the origin point E at the shoulder joint.

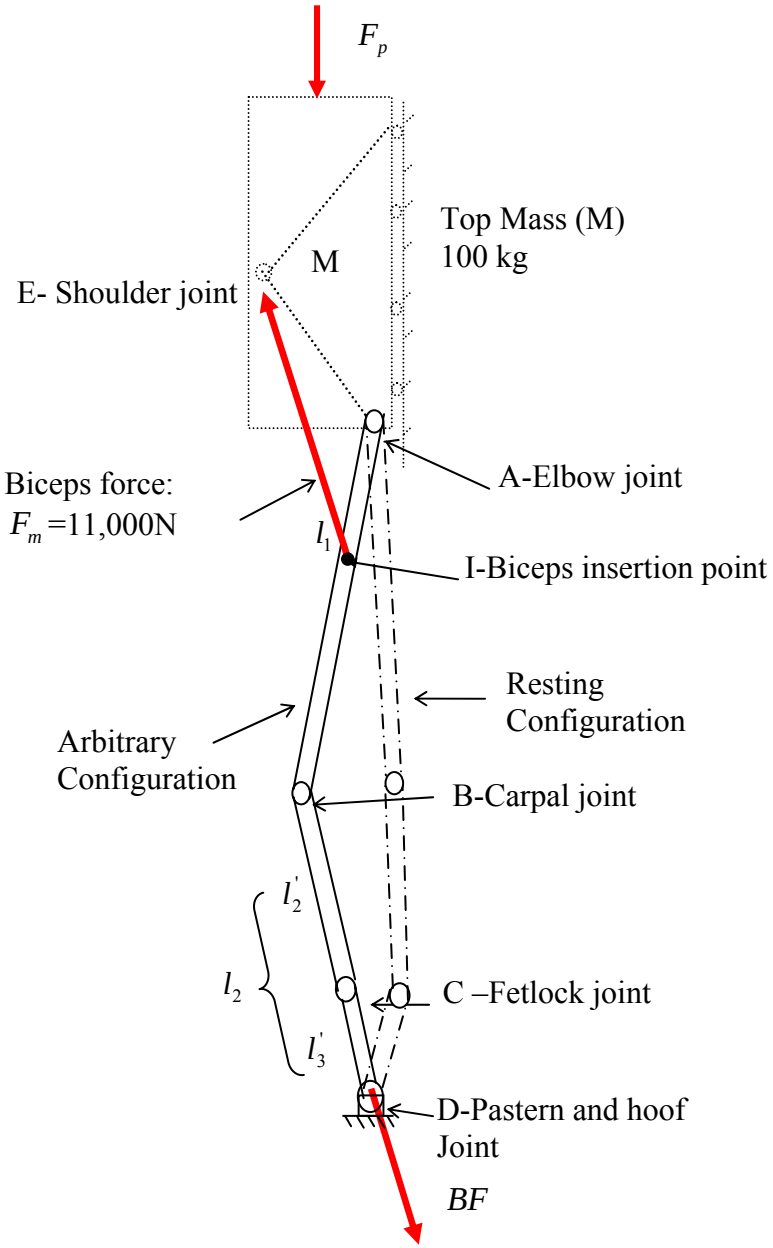

Figure 2.3: Mechanical model of the forelimb

2.2.2 The Forelimb Anatomical Computer Model

A computer model of the mechanical system of the horse forelimb build up in SolidWorks is shown in Figure 2.4. Motion analysis is implemented in COSMOS, a software package using the ADAMS solver.

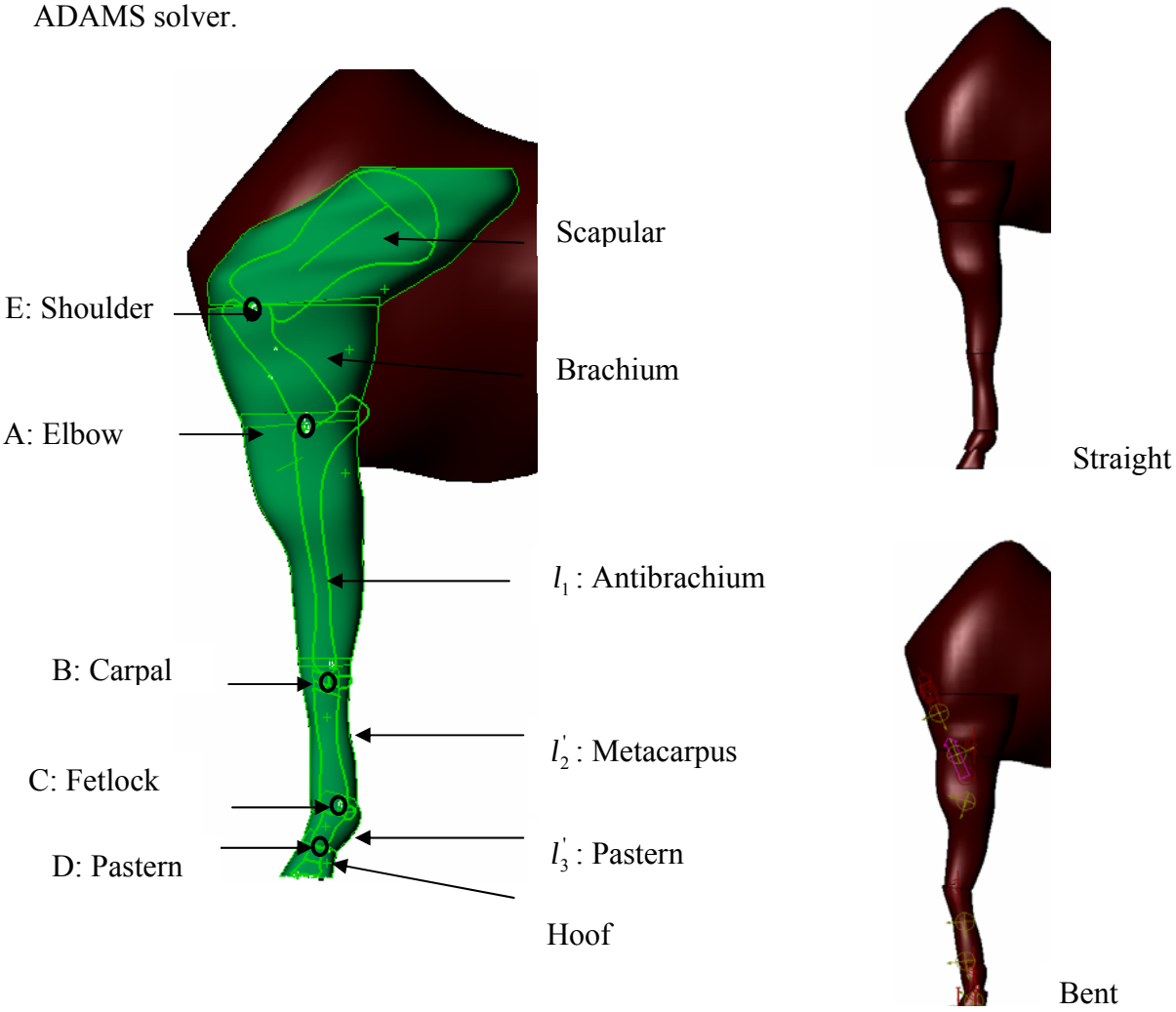

Figure 2.4: Computer model of the horse forelimb

In the computer model, the top mass in Figure 2.3 is replaced with a join upper arm part, including scapular and brachium, moving in the vertical direction. Hoof is fixed to the ground. Link1 (l_1), link2$'$ (l_2') and link3$'$ (l_3') move as a linkage system forming various patterns as shown in Figure 2.4. More details on generating the model can be found in Appendix B.

2.2.3 Kinematics of the Forelimb Mechanical Model

The mechanical model shown in Figure 2.3 has three links with three degree of freedom each (rotation and two components of translation). The linkage is fully constrained at the distal end and horizontally constrained on the upper end. The links in between are connected with two revolute joints. Therefore, the model has 3*3-2*2-2-1= 2 DOF and (in general) can be controlled by two actuation forces. However, when the biceps force is applied on l_1, $l_2^{'}$ and $l_3^{'}$ will be under tension and will always align. Thus there will be no relative rotation at joint C and the system can be simplified to a slider-crank mechanism with only one DOF. The configuration of such a system depends on only one DOF which can be defined as x (vertical displacement of joint A), α, or β as denoted in Figure 2.5. Note that now $l_2 = l_2^{'} + l_3^{'}$ and the relationships between α, β and x can be derived from the following two geometric equations:

$$l_2^2 = l_1^2 + (H - x)^2 - 2l_1(H - x)\cos\alpha \tag{2.1}$$

$$\frac{\sin\alpha}{\sin\beta} = \frac{l_2}{l_1} \tag{2.2}$$

where H is the distance between A and D in Figure 2.5 when the linkage system is stretched to align. The length of link1 and link2 in the plot are denoted by l_1 and l_2.

Angles α and β in terms of x is obtained from (2.1) and (2.2) as:

$$\alpha = \arccos\left(\frac{l_1^2 + (H - x)^2 - l_2^2}{2l_1(H - x)}\right) \tag{2.3}$$

$$\beta = \arcsin\left(\frac{l_1}{l_2}\sin\alpha\right) \tag{2.4}$$

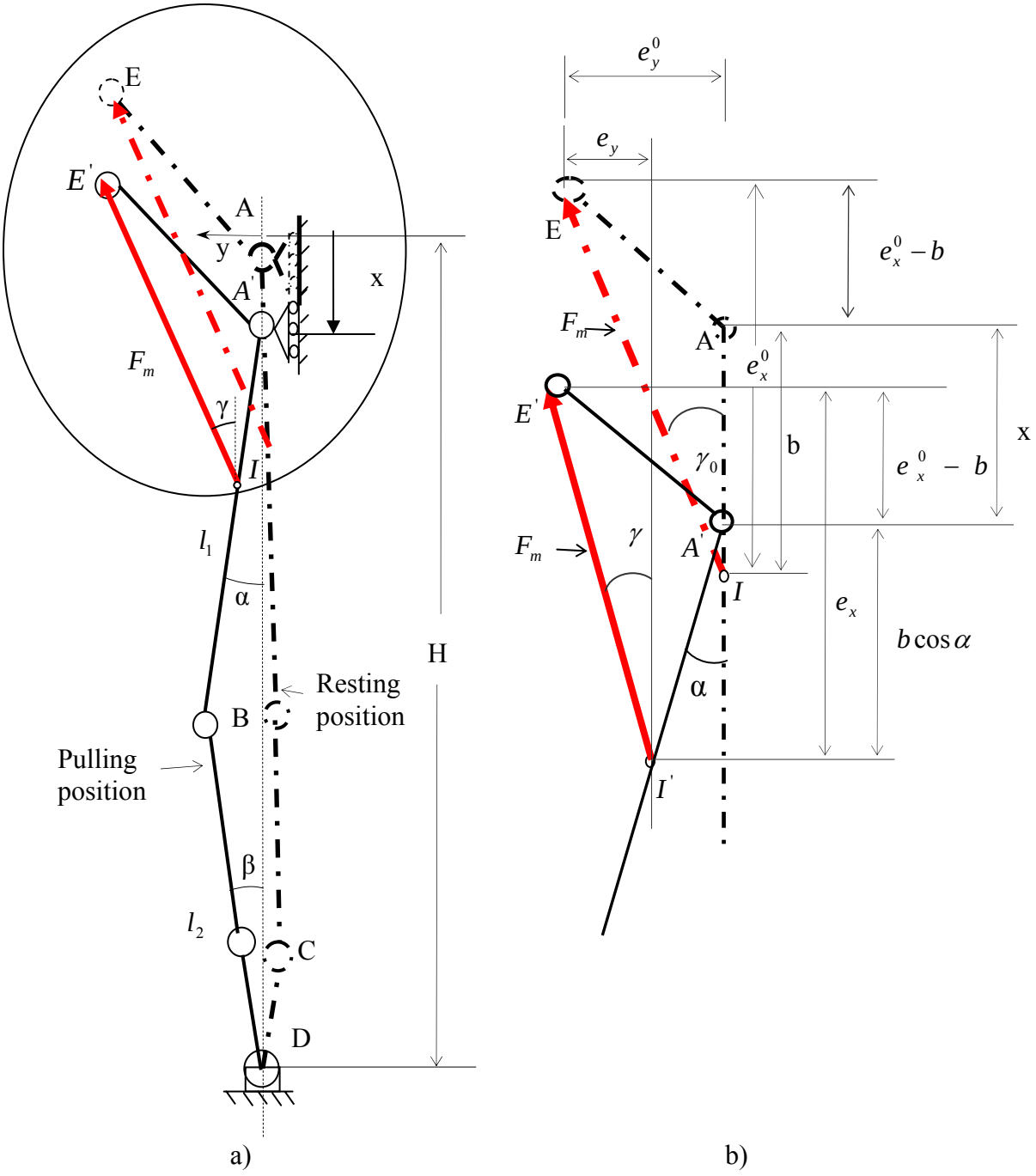

Figure 2.5: Geometric configuration of the forelimb

It is assumed that, $l_1 = 0.496$m, $l_2 = 0.356$m, H=$l_1 + l_2$ =0.852m. These numerical values were obtained from the horse picture used to create the horse model. See Appendix B for more details.

The direction of force F_m (biceps muscle force) is denoted by angle γ. The detail of geometry at the top of the linkage is shown in Figure 2.5b. In particular, the distance between the elbow joint and the biceps attachment is b = 0.111m and distances between the biceps insertion point and the shoulder joint at resting position is denoted by e_x^0=0.292m and e_y^0=0.127m vertically and horizontally respectively. The same distances are denoted as e_x and e_y in pulling position. Then one can obtain

$$\tan\gamma = \frac{e_y}{e_x} = \frac{e_y^0 - b\sin\alpha}{e_x^0 - b + b\cos\alpha} = \frac{e_y^0 - b\sin\alpha}{e_x^0 - b(1-\cos\alpha)} \tag{2.5}$$

$$\text{Thus, } \gamma = \arctan\left(\frac{e_y^0 - b\sin\alpha}{e_x^0 - b(1-\cos\alpha)}\right) \tag{2.6}$$

For x in millimeters, the values of α, β and γ in degrees are plotted in Figure 2.6a,b,c. The vertical displacement of joint A is zero (x=0) when link1 and link2 are stretched to align.

Motion at elbow (joint A) on a real horse is limited by the ROM at the pastern and hoof joint. (Joint D) Therefore, β should be smaller than 10 degrees. As a result, x should not be lowered more than 10 mm in Figure 2.6b. The corresponding limits imposed on α and γ are 7.5° and 21.2° respectively and are marked in Figure 2.6a&c.

Since the system has only one DOF, the value of angle α (or β) also defines the complete configuration of the forelimb. From all the possible patterns, the pattern to generate maximum breaking force will be determined in the next section.

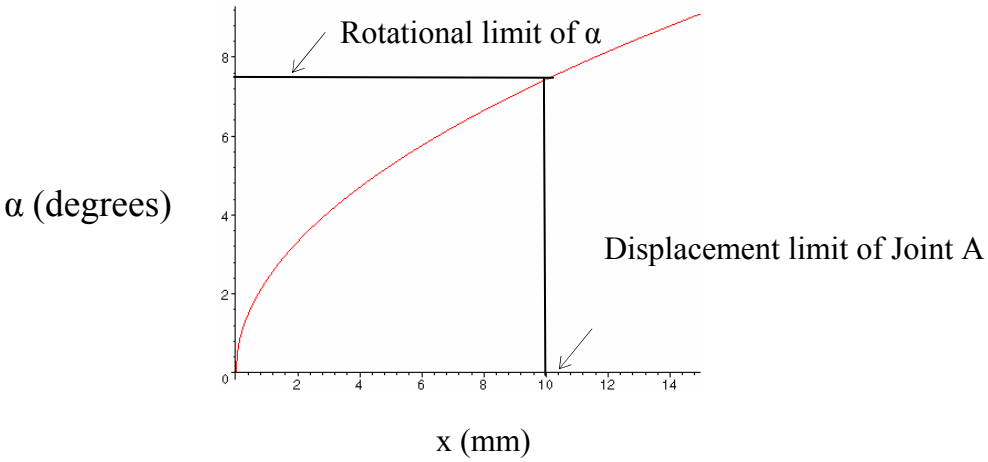

a) Angle α versus vertical displacement of joint A

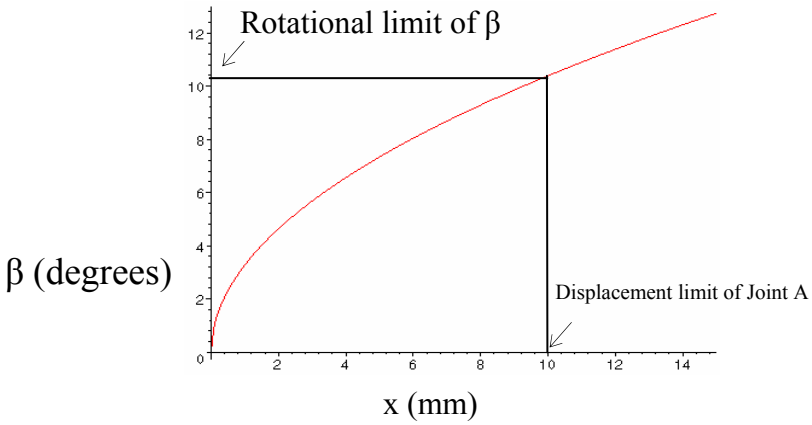

b) Angle β versus vertical displacement of joint A

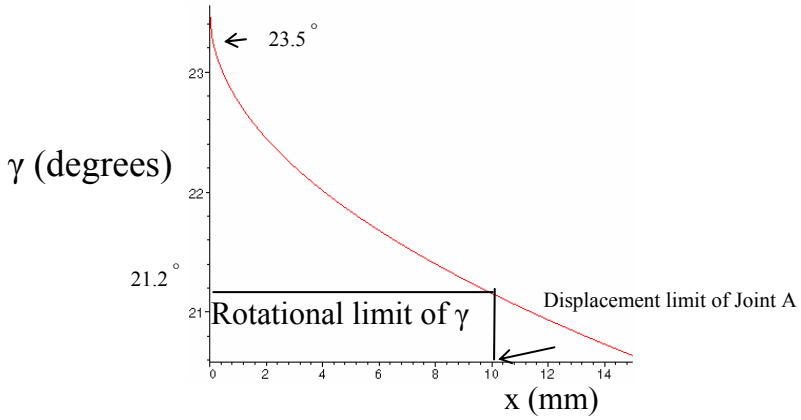

c) Angle γ versus vertical displacement of joint A

Figure 2.6: Joint angles versus vertical displacement of the forelimb

2.2.4 The Forelimb Quasi-Static Pulling

If the hoof is fixed then the pulling force, referred to as the breaking force (BF) generated by muscles may break the restraint. The ability to generate this breaking force varies with the configuration of the leg as the motion is initialized. The relationship between a configuration and the breaking force for the forelimb of the horse is analyzed in this section.

First, the quasi-static case is considered. Quasi-static pulling here means that the horse generates a breaking force by constantly pulling the leg with the biceps. Forces on the linkage system for an arbitrary configuration are shown in Figure 2.7. The bottom member of length l_2 is under tension only, therefore $F_B = BF$. Equilibrium equations for the top member of length l_1 can be written as:

$$\sum M_A = 0, \quad F_B l_1 \sin(\alpha + \beta) - F_m b \sin(\gamma + \alpha) = 0 \tag{2.7}$$

$$\downarrow \sum F_x = 0, \quad F_B \cos\beta + F_{Ax} - F_m \cos\gamma = 0 \tag{2.8}$$

$$\leftarrow \sum F_y = 0, \quad F_m \sin\gamma - F_{Ay} - F_B \sin\beta = 0 \tag{2.9}$$

where F_m is the force generated by biceps attached at I. F_{Ax}, F_{Ay} are two components of force at joint A. Force F_{Ax} when in compression may reach to the magnitude of about W/2 (half of the weight carried by forelimbs), however, the maximum tensile magnitude of it is generally small (no major muscle pulls joint A upward).

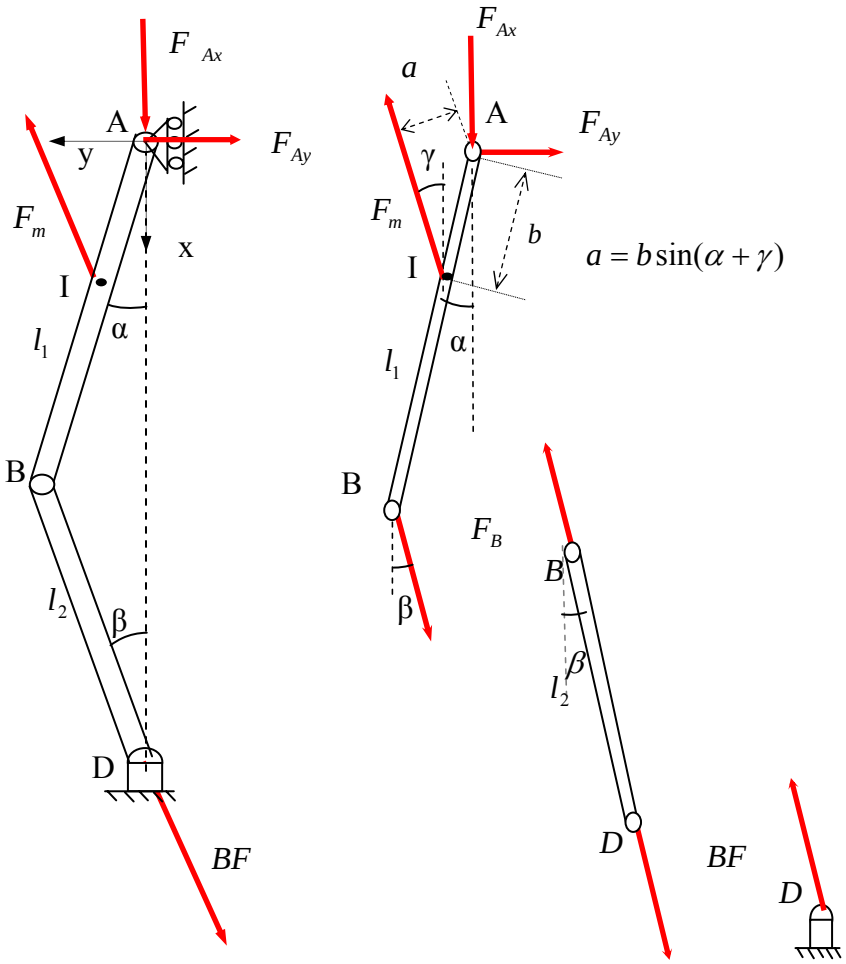

Figure 2.7: Force diagram of the forelimb in static pulling

From (2.7), one has

$$BF = F_B = F_m \frac{b\sin(\gamma+\alpha)}{l_1 \sin(\alpha+\beta)} \tag{2.10}$$

Then from (2.8)

$$F_{Ax} = F_m(\cos\gamma - \frac{b\sin(\gamma+\alpha)}{l_1 \sin(\alpha+\beta)}\cos\beta) \tag{2.11}$$

Since α, β and γ can be expressed in terms of x (by 2.3-2.6), forces BF and F_{Ax} can be written as functions of x and plotted as shown in Figure 2.8 and Figure 2.9. The plots are obtained for $F_m = 11{,}000N$.

Figure 2.8 indicates that the breaking force at the hoof increases as x decreases or as joint A elevates. However, further analysis will show that the increase of BF is limited as x becomes less than about 1mm and approaches zero.

As indicated in Figure. 2.9, the vertical force at joint A has to be a pulling force required to maintain the equilibrium when x<1mm (F_{Ax} <0). This is not realistic for a horse because there is no major muscle on the forelimb to develop this kind of force as the forelimb has already been stretched straight. Therefore, for the sake of clarity, it is assumed that force F_{Ax} can only be positive (pushing down) in this configuration. The consequence of this is that the maximum BF is developed when $F_{Ax} = 0$, which occurs when $x_0 = 1\text{mm}, \alpha_0 = 2^\circ, \beta_0 = 3^\circ$, and $\gamma_0 = 23^\circ$ as shown in Figure.2.10a, the corresponding diagram of the forces is shown in Figure 2.10b1 (solid line). Substituting these values in (2.10) one obtains $BF_{\max} = 10{,}620N$. The breaking force will not increase when joint A elevates further up (x<1mm). Joint A may move slightly in the horizontal direction as shown in Figure.2.10a (dot line). BF will stay relatively the same as BF_{Max} as explained in Figure.2.10b2. If the horse gets tired, the muscle force can drop to F_m' accompanied by the corresponding reduction of force BF.

If force F_{Ax} is pushing down, which will happen if $\beta > \beta_0$, then the diagram of forces is shown in Figure 2.10b3. One can conclude that an increase in F_{Ax} brings about a decrease in force BF.

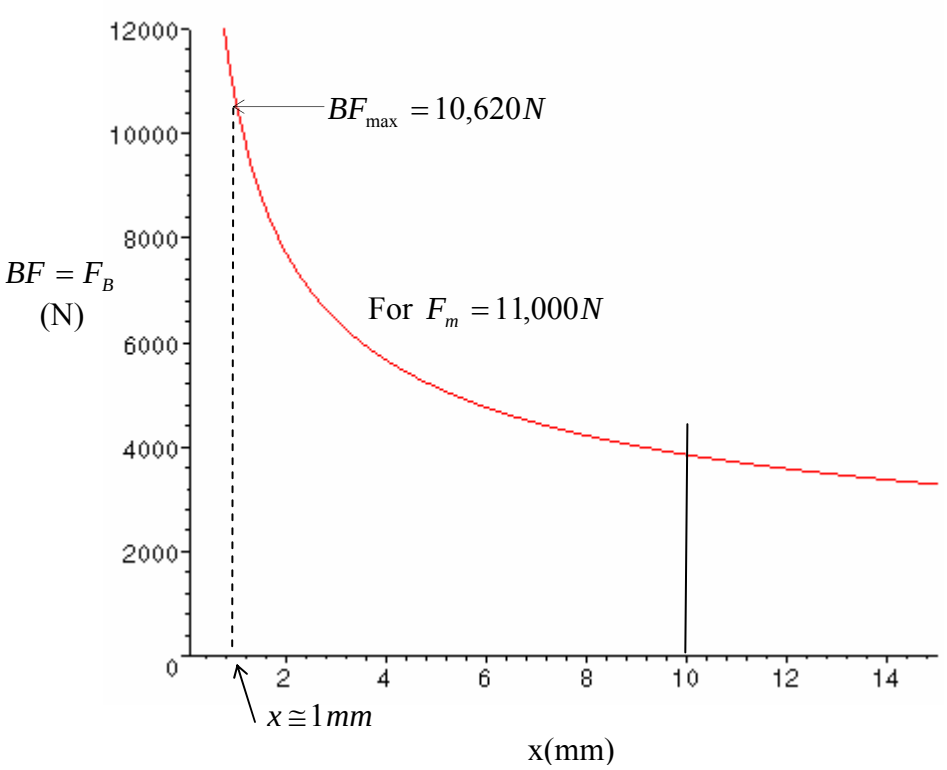

Figure 2.8: Forelimb hoof's breaking force versus vertical displacement of joint A

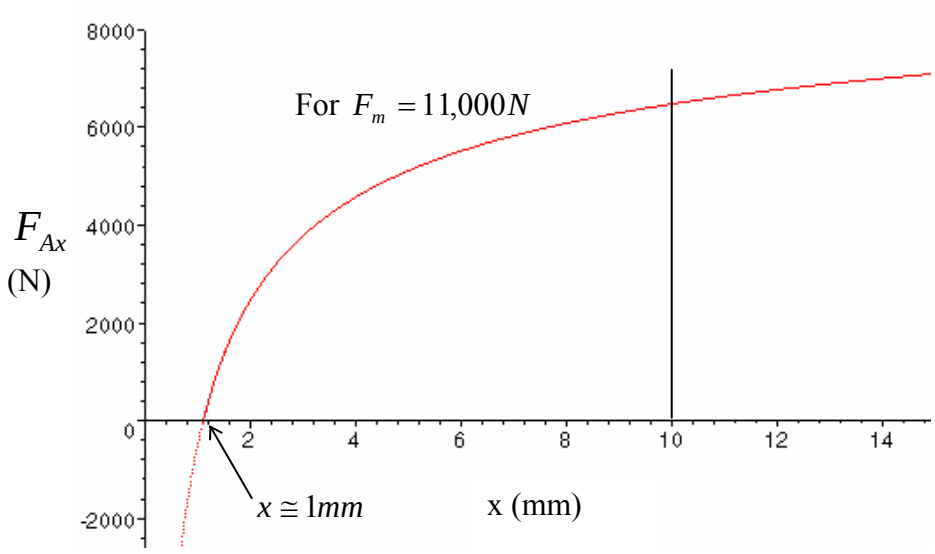

Figure 2.9: Joint reaction force F_{Ax} versus vertical displacement of joint A

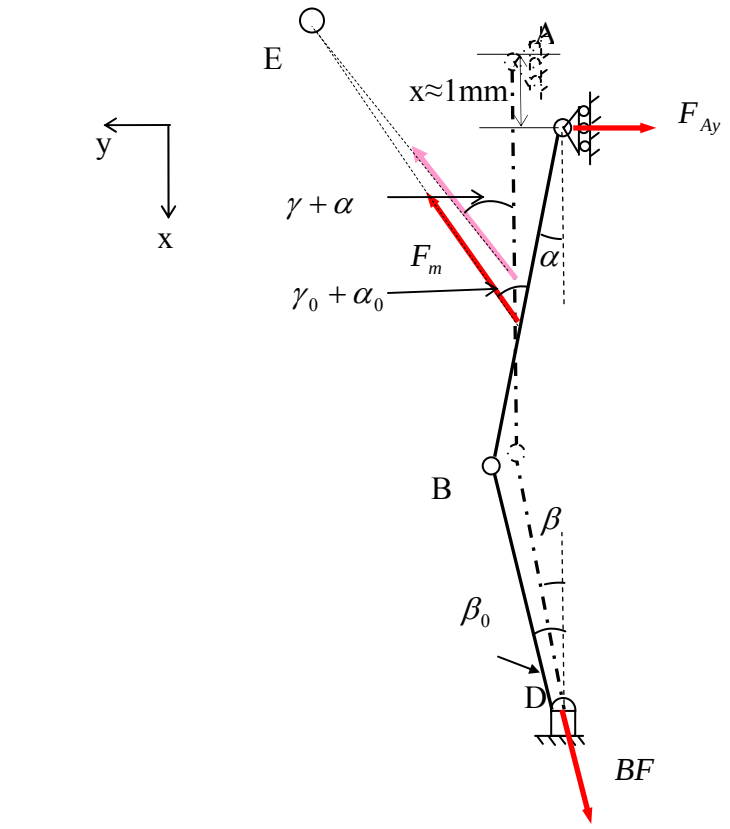

a) Geometric configuration of the forelimb approaching the top

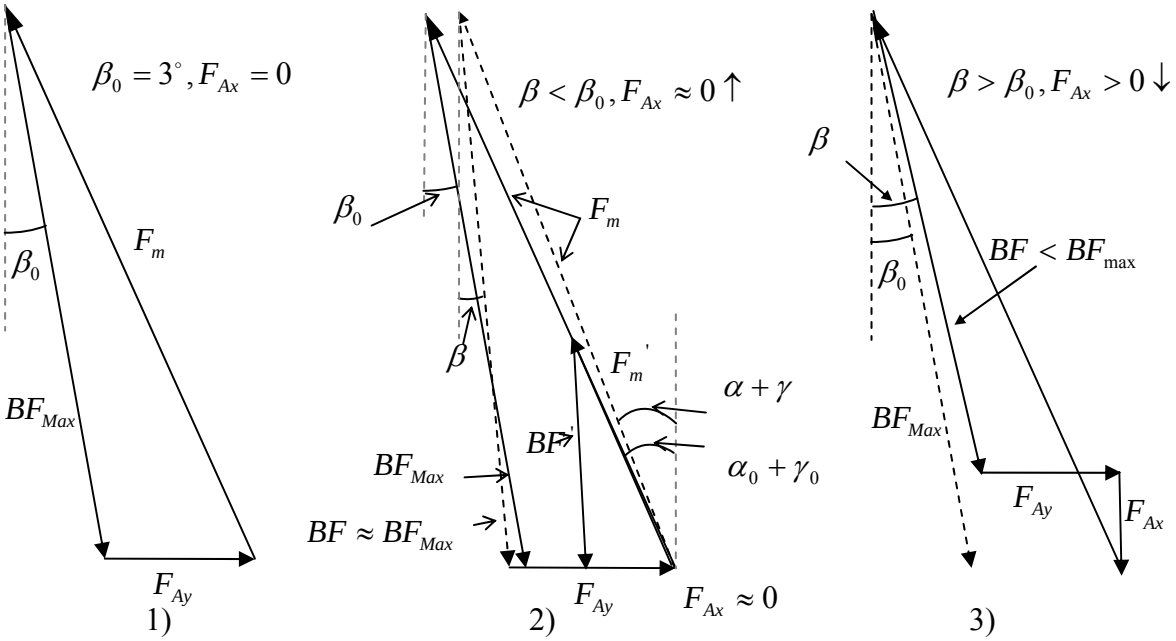

b) Force diagram of the forelimb approaching the top

Figure 2.10: Analysis of the forelimb static pulling approaching to the top

Finally, based on the analysis above, it is concluded that the maximal BF is generated when x_0 =1mm, $\alpha_0 = 2^\circ$, $\beta_0 = 3^\circ$, $\gamma_0 = 23^\circ$ and $BF_{\max} = 10{,}620$N. The corresponding BF will reduce when β is increased or decreased from β_0. Accordingly, force BF will be reduced when joint A is elevated or declined from x_0. Figure 2.11 is a re-plot of Figure 2.8 showing the decrease of BF when x<1mm or $\beta < \beta_0$.

The analytical results of the relation between the leg pattern and the breaking force generation ability are also confirmed by the simulation results from the horse model in COSMOS.

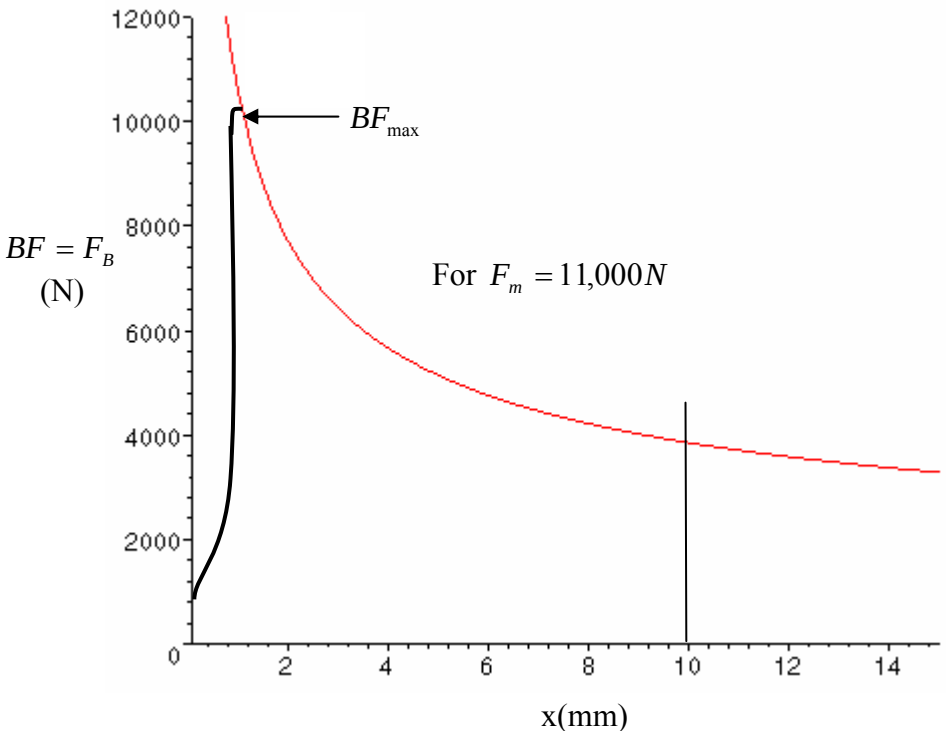

Figure 2.11: Breaking force in static pulling

2.2.5 The Breaking Force Due to Forelimb Dynamic Jerking

In the experiment, the sheep was observed to fight the hoof restraint with dynamic jerking. It is believed that the horse will behave similarly. That is, the animal may try to generate the breaking force by the dynamic jerking. The term "jerking" is used in this thesis to describe the motion of lowering and elevating the body quickly (by rotating the leg members) to generate the breaking force dynamically. The magnitude of the breaking force due to jerking will be evaluated in this section.

2.2.5.1 Forelimb Jerking by Lowering the Body (Down Maneuver)

In the sheep experiment, the animal generated jerking by lowering the upper body and elbow joint. This motion caused the antebrachium(l_1), metacarpus and proximal & middle phalanx (l_2) to rotate from initial configuration to the final configuration as shown in Figure 2.12. The rotation suddenly stopped when x = 10 mm = 0.01m. As explained in previous section, the final configuration is defined by the restriction of motion of pastern and hoof joint (joint D).

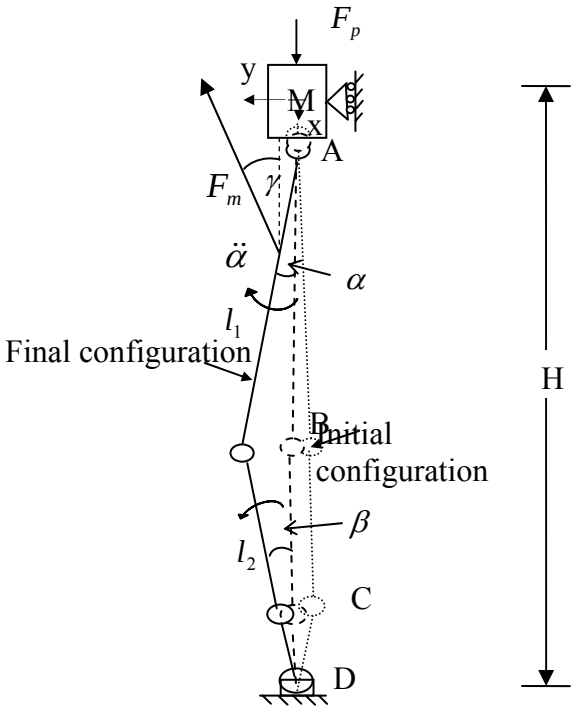

Figure 2.12: Forelimb in dynamic jerking

The dynamic breaking force due to jerking can be determined from an inverse dynamic analysis if the acceleration and deceleration of the leg during the jerking is assumed.

From a general sense of motion, one can approximate that the upper leg and body (joint A) and above move down due to gravity at the acceleration rate of $a_{down} = g = 9.81 m/s^2$. Based on the motion captured on video during the sheep restraint experiment, the deceleration of the body to stop the leg rotation is estimated to be $a_{stop} = -6g = -58.8 m/s^2$. It is assumed that horse will move at the same acceleration rate. The motion leading to the dynamic jerking can be described with plots in Figure 2.13. Figure 2.13a shows the acceleration and deceleration of the joint A. The change of the acceleration occurs at $t_1 = 0.042$s to stop the upper arm at $x_{stop} = 0.01m$ as shown in Figure 2.13c.

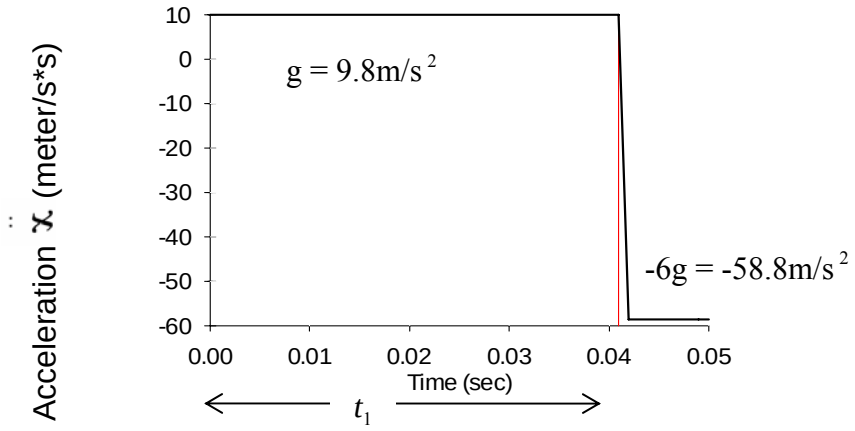

a) Acceleration of joint A

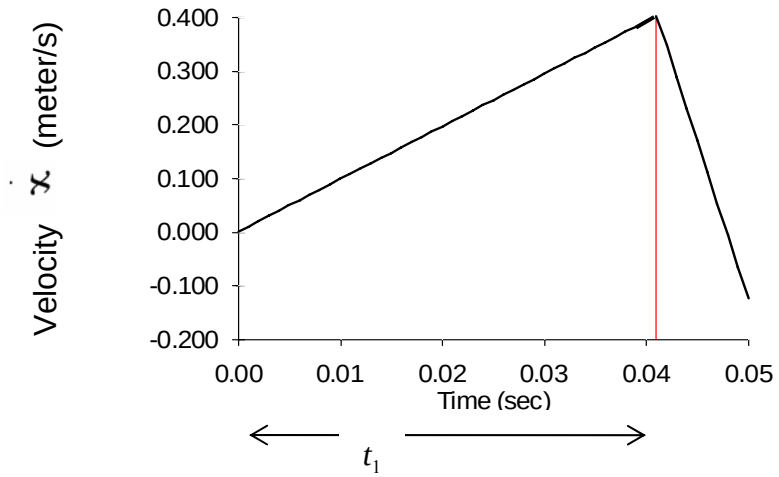

b) Velocity of joint A

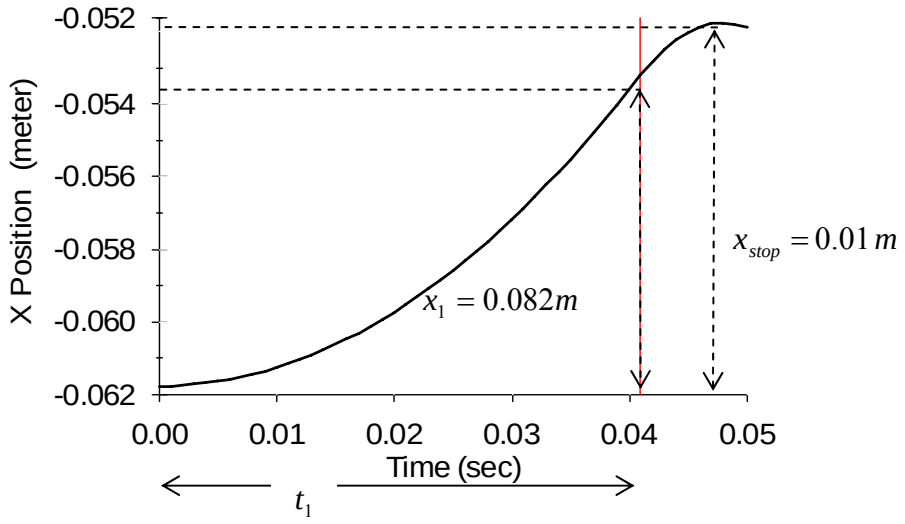

c) Displacement of Joint A

Figure 2.13: Elbow (joint A) motion in dynamic jerking (down maneuver)

In the following section, the procedure to calculate the dynamic breaking force due to jerking will be discussed.

The system in Figure 2.12 satisfies the kinematic equations:

$$x = H - (l_1 \cos\alpha + l_2 \cos\beta) \tag{2.12}$$

$$0 = l_2 \sin\beta - l_1 \sin\alpha \tag{2.13}$$

The angular velocities of link1 and link 2 can be determined by differentiates of these equations to obtain:

$$\dot{x} = l_1 \sin\alpha\dot{\alpha} + l_2 \sin\beta\dot{\beta} \tag{2.14}$$

$$0 = l_2 \cos\beta\dot{\beta} - l_1 \cos\alpha\dot{\alpha} \tag{2.15}$$

At $t = 0$ the velocity $\dot{x}_1 = v_0 = 0$ and $a_{down} = g = 9.8\, m/s^2$.
At $t_1 = 0.042$ s, $x_1 = 0.00823\, m$, $\dot{x}_1 = v_{\max} = 0.41\, m/s$.
From (2.12) and (2.13) at t_1:

$$\alpha_1 = 0.118\ rad\ (6.7^\circ),\ \beta_1 = 0.164\ rad\ (9.4^\circ)$$

From (2.14), (2.15)

$$\dot{\alpha}_1 = 2.93\, rad/s,\ \dot{\beta}_1 = 4.11\, rad/s$$

Differentiating both sides of (2.14) and (2.15) renders:

$$\ddot{x} = l_1(\sin\alpha\ddot{\alpha} + \dot{\alpha}^2\cos\alpha) + l_2(\sin\beta\ddot{\beta} + \dot{\beta}^2\cos\beta) \tag{2.16}$$

$$0 = l_2(\cos\beta\ddot{\beta} - \dot{\beta}^2 \sin\beta) - l_1(\cos\alpha\ddot{\alpha} - \dot{\alpha}^2 \sin\alpha) \tag{2.17}$$

Substituting $\ddot{x} = -6g$ into (2.16) and (2.17) results in the following angular accelerations:

$$\ddot{\alpha}_1 = -493.29\ rad/s^2,\ \ddot{\beta}_1 = -690.48\ rad/s^2$$

One can also determine the acceleration of centroids of link1 and link2 from the equations:

Link1:

$$x_{c1} = l_{c1}\cos\alpha + x = 0.852 - [l_2\cos\beta + (l_1 - l_{c1})\cos\alpha] \quad (2.18)$$

$$y_{c1} = l_{c1}\sin\alpha \quad (2.19)$$

Link2:

$$x_{c2} = H - l_{c2}\cos\beta \quad (2.20)$$

$$y_{c2} = l_{c2}\sin\beta \quad (2.21)$$

Where $l_{c1} = 0.5\,l_1$=0.248 m and $l_{c2} = 0.5\,l_2$ = 0.178 m are assumed to define the location of the centroid of l_1 and l_2 as shown in Figure 2.14 (Refer to Appendix B to determine the centroid of the forelimb part in the horse model). By differentiating (2.18-2.21) twice the following is obtained:

At t_1, $\ddot{x}_{C1} = -46.55\,m/s^2$ $\quad \ddot{x}_{C2} = -17.17\,m/s^2$

$\ddot{y}_{C1} = -93.73\,m/s^2$ $\quad \ddot{y}_{C2} = -94.74\,m/s^2$

The centroid acceleration in x, y direction together with the angular acceleration are substituted into the dynamic motion equation to calculate the breaking force due to dynamic jerking.

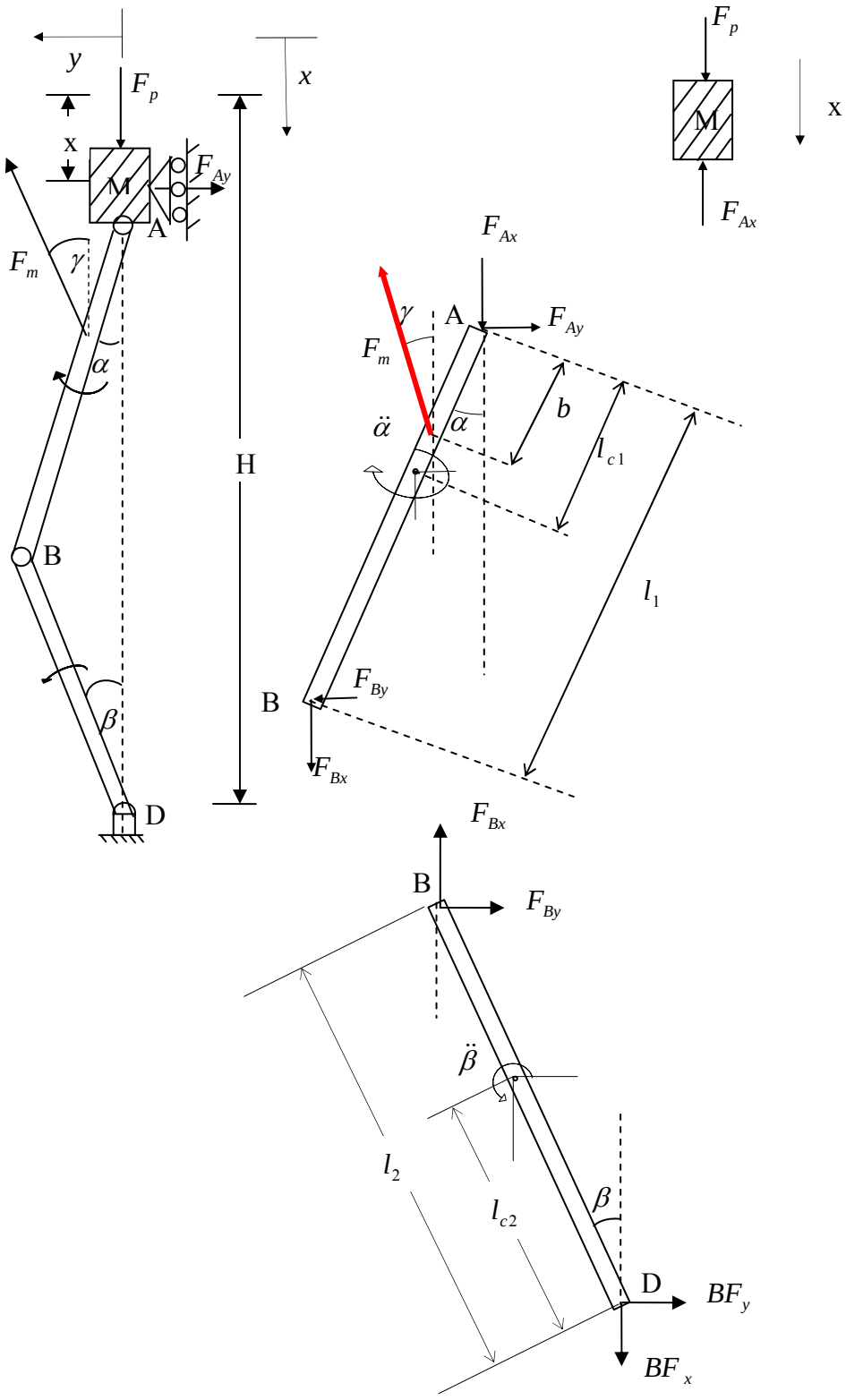

Figure 2.14: Forelimb force diagram in dynamic jerking (1)

Forces applied on the linkage system (Figure 2.14) while decelerating include the biceps force (F_m), force on top mass (F_p), horizontal force to constrain joint A (F_{Ay}) and hoof restraint force (BF). The motion equations for the top mass, link1 and link2 are:

Top Mass:

$$M\ddot{x}_A = F_p - F_{Ax} \tag{2.22}$$

Link1:

$$m_1\ddot{x}_{c1} = F_{Ax} + F_{Bx} - F_{mx} \tag{2.23}$$

$$m_1\ddot{y}_{c1} = -F_{Ay} + F_{my} + F_{By} \tag{2.24}$$

$$\begin{aligned} J_{c1}\ddot{\alpha} = {} & F_{Ax}l_{c1}\sin\alpha + F_{Ay}l_{c1}\cos\alpha - F_m(l_{c1} - b)\sin(\gamma + \alpha) \\ & + F_{By}(l_1 - l_{c1})\cos\alpha - F_{Bx}(l_1 - l_{c1})\sin\alpha \end{aligned} \tag{2.25}$$

Link2:

$$m_2\ddot{x}_{c2} = BF_x - F_{Bx} \tag{2.26}$$

$$m_2\ddot{y}_{c2} = -F_{By} - BF_y \tag{2.27}$$

$$\begin{aligned} J_{c2}\ddot{\beta} = {} & -F_{By}(l_2 - l_{c2})\cos\beta - F_{Bx}(l_2 - l_{c2})\sin\beta \\ & + BF_y\, l_{c2}\cos\beta - BF_x\, l_{c2}\sin\beta \end{aligned} \tag{2.28}$$

where $F_m = 11{,}000N$, M =100 kg, $m_1 = 6.7kg$, $m_2 = 2.41\,kg$, $J_{c1} = 0.137$, $J_{c2} = 0.025$, $l_{c1} = 0.5\,l_1 = 0.248$ m and $l_{c2} = 0.5\,l_2 = 0.178$ m, $\gamma = 21.2^\circ$.

By Substituting $\ddot{x}_{c1}, \ddot{y}_{c1}, \ddot{\alpha}, \ddot{x}_{c2}, \ddot{y}_{c2}, \ddot{\beta}$ obtained from the kinematics analysis the seven unknown forces in these equations, including six reaction forces at each joint and external force applied vertically on the top mass, can be calculated.

These forces at t_1 are:

At t_1

F_p = -2,589N

F_{Ax} = 3,290N F_{Bx} = 6,653N BF_x = 6,611N

F_{Ay} = 3,889N F_{By} = -903N BF_y = 1,196N and BF = 6,718N

Negative sign of the force means the calculated force has opposite direction of the corresponding force shown in Figure 2.14. Figure 2.15 shows the force diagram plot based on the calculated results.

At t_1, Forces in Newtons

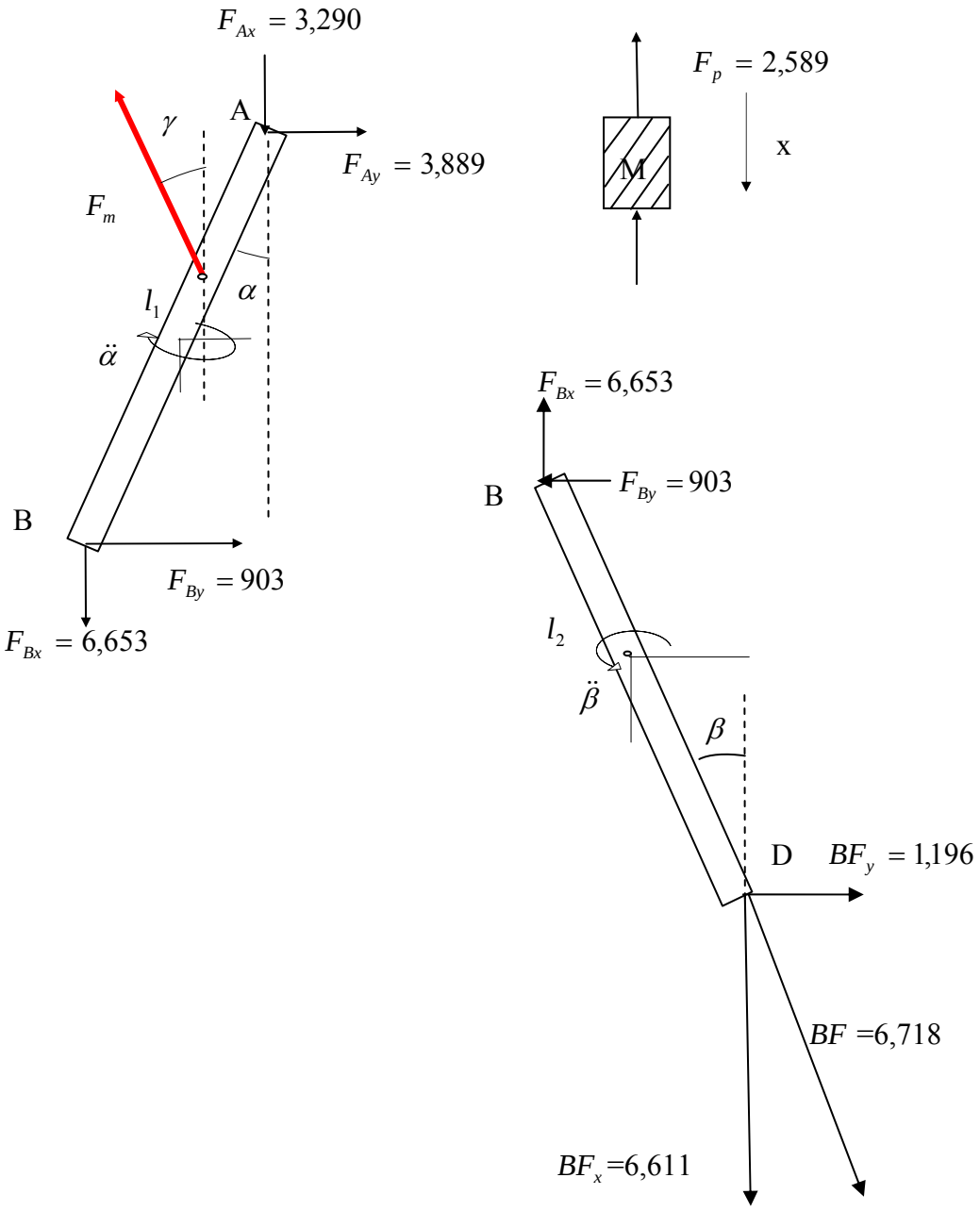

Figure 2.15: Forelimb force diagram in dynamic jerking (2)

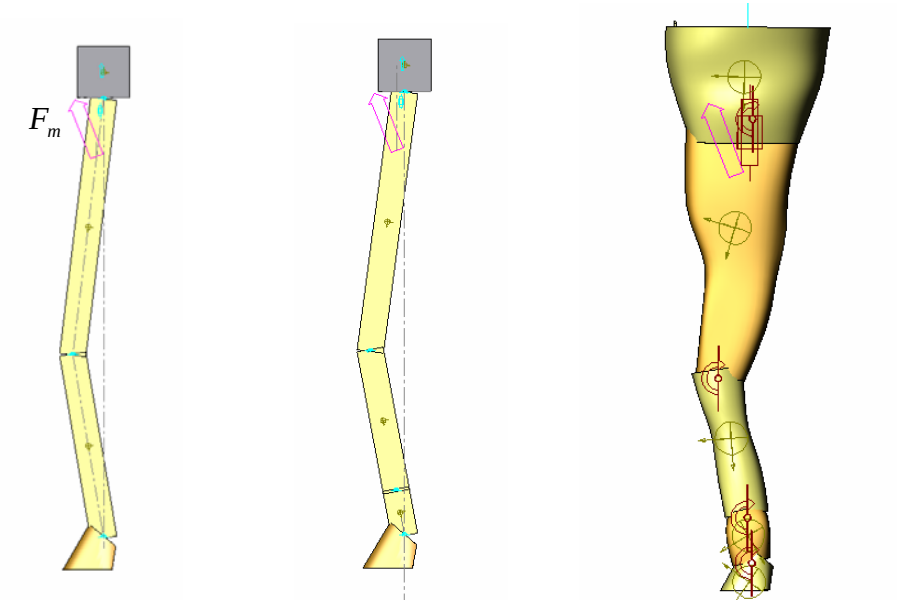

a) Two-link model b) Three-link model c) Anatomical model

Figure 2.16: Forelimb simulation models

The result obtained from a two links system descried above agrees well with the COSMOS simulation for the front leg modeled as two links system as shown in Figure 2.16a.

The breaking force obtained from this model is $BF = 6{,}705\ N$.

The breaking force ($BF = 6{,}873\ N$) obtained using the three link model is slightly different as shown in Figure 2.16b.

Furthermore, the horse forelimb was modeled with an anatomical model representing the geometry and mass distribution of antebrachium, metacarpus and proximal & middle phalanx (l_1, l_2', l_3') as close as possible. The breaking force obtained from this simulation at t_1 is $BF = 5{,}116N$.

One may conclude that these three simulation models have given generally similar results for the breaking force that can be generated by a dynamic jerking. The difference between the forces for the two link model and the anatomical model may be explained as follows: Firstly, the joint

rotation centers in the anatomical model, which is calculated automatically in COSMOS are not exactly aligned with the mass center used in the link model. Also the rotation centers are not in one straight line with the joints. Secondly, the mass center and the moment of inertia of each part in anatomical model is automatically determined in the COSMOS taking into account a specific shape of the part, while the simple link model assumes mass center in the middle. Finally, the DOFs of the two links model and the anatomical model are different. Nevertheless the results are close and simulated forces obtained from the anatomical model will better approximate the forces generated by a real horse. This shows the advantage of using a software like COSMOS for dynamics analysis with irregular shaped parts.

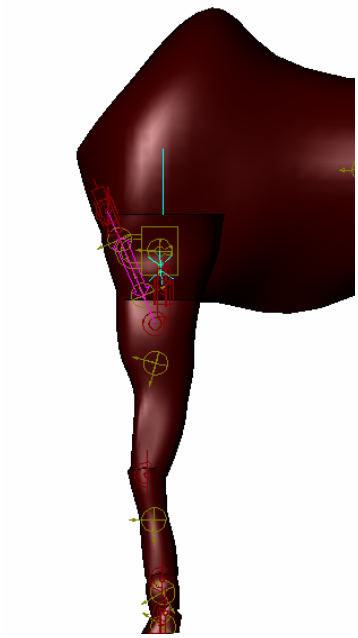

Figure 2.17: Forelimb model including the horse trunk

Finally, the anatomical model including the trunk as shown in Figure 2.17 is used in simulating the moving down process in dynamic jerking. The interaction between the massive

trunk and front leg is considered in this model and biceps muscle force is modeled as an action-reaction force between the trunk and the leg. More accurate result of the breaking force is expected from this model. Such results are shown in Figure 2.18. They indicate that during the motion described in Figure 2.13, the maximum breaking force $BF_{\max} \approx 6{,}000N$ is generated, which is about 60% of the force possible to generate statically as presented in section 2.2.4. These plots indicate that in the down maneuver jerking the force BF is not varying much. The maximum value of 6,000N is generated at the beginning of the maneuver. As the leg lowers down and rotates forward, the breaking force generated on the hoof decreases as the configuration of the leg changes, which agrees well with the breaking force and leg configuration relationship concluded in section 2.2.4. In the last phase with deceleration of -6g, the forces are higher but, due to a 'favorable' change in the configuration, they are smaller than the BF generated at the beginning of the jerking.

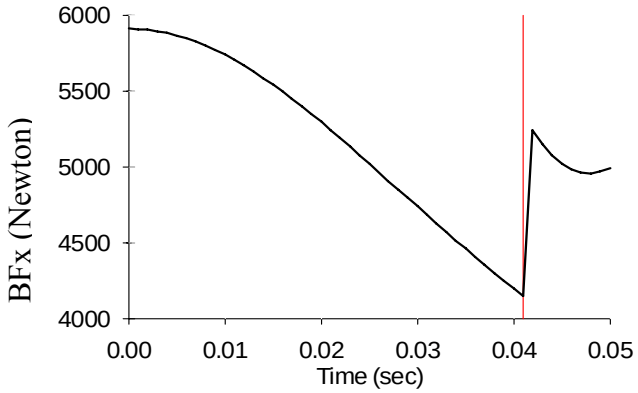

a) Force BF_x

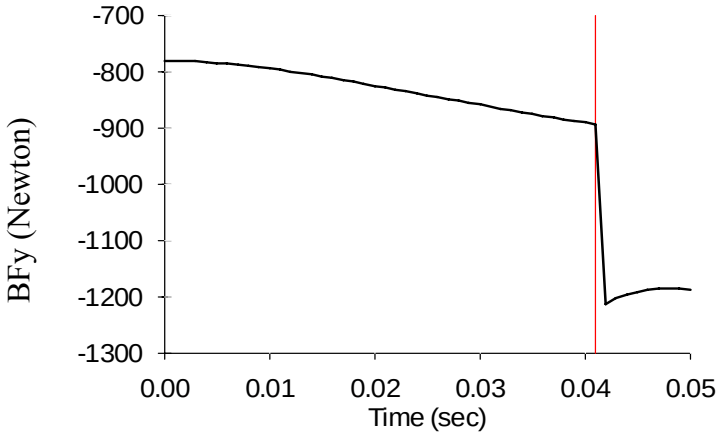

b) Force BF_y

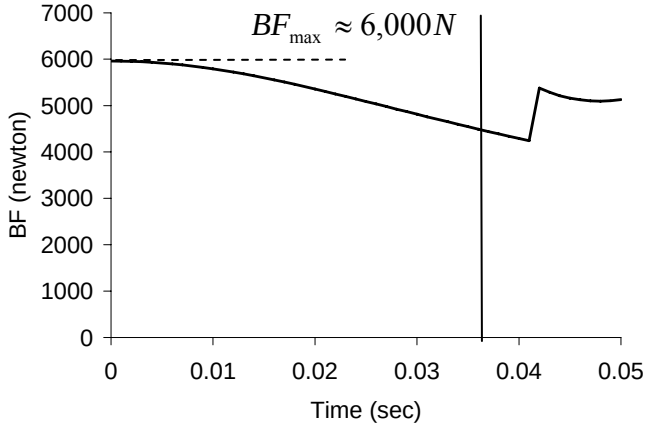

c) The hoof's force BF

Figure 2.18: The forces due to forelimb dynamic jerking (down maneuver)

2.2.5.2 Forelimb Jerking by Elevating the Body (Up Maneuver)

It was also observed that the sheep tried to generate jerking while rising up the upper body. The upper body motion starts from the lowest configuration indicated in Figure 2.12 as final configuration and stops at the highest configuration. Since the final configuration by lowering the body now becomes the initial configuration and vise versa, the jerking by elevating the body can be regarded as the maneuver which is inverse to that considerate in the previous section (jerking by lowering the body). According to the video, it takes longer time for the sheep to elevate its body than lower it. Similar situation may apply to the horse as well. Accelerate rate of elevating the body or joint A is assumed to be $a_{up} = -0.5g = -4.9\,m/s^2$. When the leg is stretched to the natural standing position, the motion will be stopped at assumed deceleration rate of $6g = 58.8\,m/s^2$. Figure 2.19 describes the motion of joint A.

The breaking force generated during the plotted motion in Figure 2.19 is determined from simulation with the model shown in Figure 2.17. The result is plotted in Figure 2.20 and it indicates that the maximum breaking force $BF_{\max} \approx 7{,}200N$ is generated when the forelimb is stopped at the natural standing position.

As can be seen, the maximum BF is now 7,200 N, higher than for the jerking down maneuver but still only about 70% of the static force generated in pulling. The main reason that these dynamic forces are smaller than the static one seems to be restricted character of motion in which the body carries a rather limited amount of kinetic energy. Jerking could be a habit the animals developed naturally when their legs were restrained. However, most probably the horse will break free by acting quasi-statically on forelimbs.

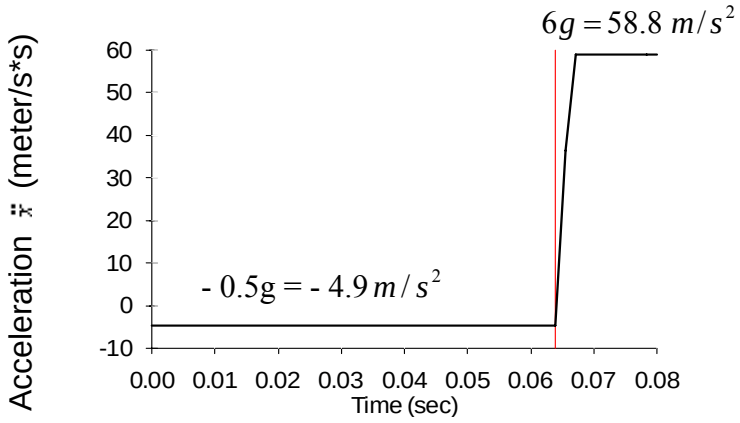

a) Acceleration of joint A

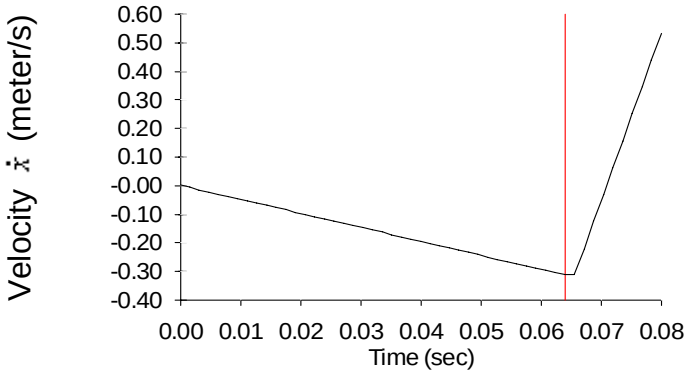

b) Velocity of joint A

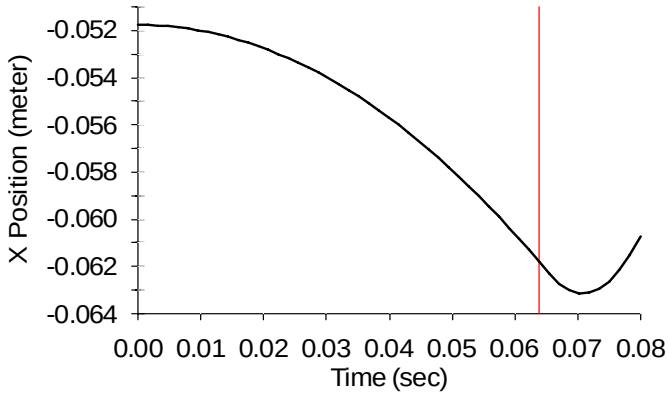

c) Displacement of joint A

Figure 2.19: Elbow joint (joint A) motion in dynamic jerking (up maneuver)

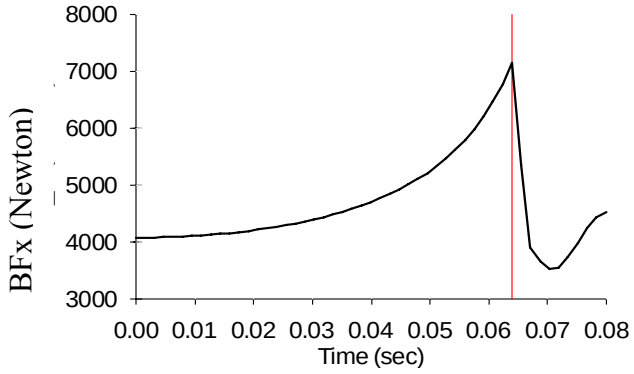

a) Force BF_x

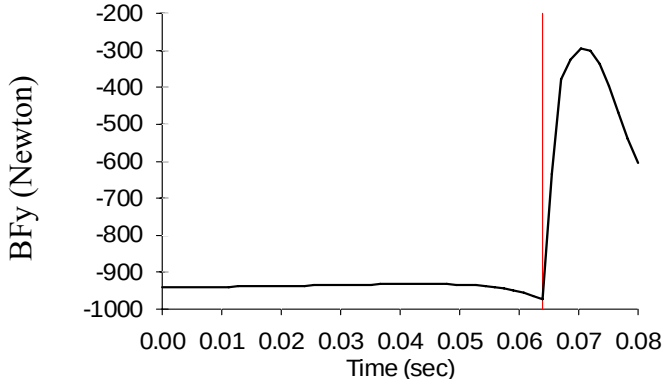

b) Force BF_y

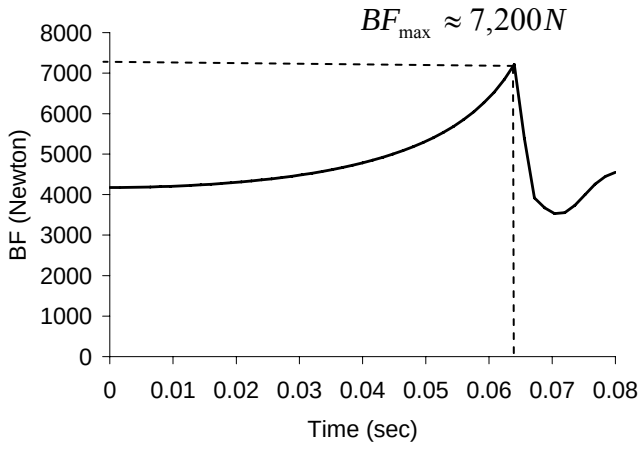

c) The hoof's force BF

Figure 2.20: Breaking force due to forelimb dynamic jerking (up maneuver)

3. REMOVING THE FORELIMB MOBILITY

3.1 Effect of Adding Additional Restraints

As mentioned earlier, when the hoof is constrained, the forelimb still has 2 degrees of freedom. The horse can generate about 10,600N of BF . In this chapter it will be shown that this force can be reduced by completely immobilizing the leg in the standing position. Removing all the mobility of the forelimb can be achieved by adding additional restraints as indicated in Fig.3.1. It will also eliminate any possibility to generate the dynamic jerking effects.

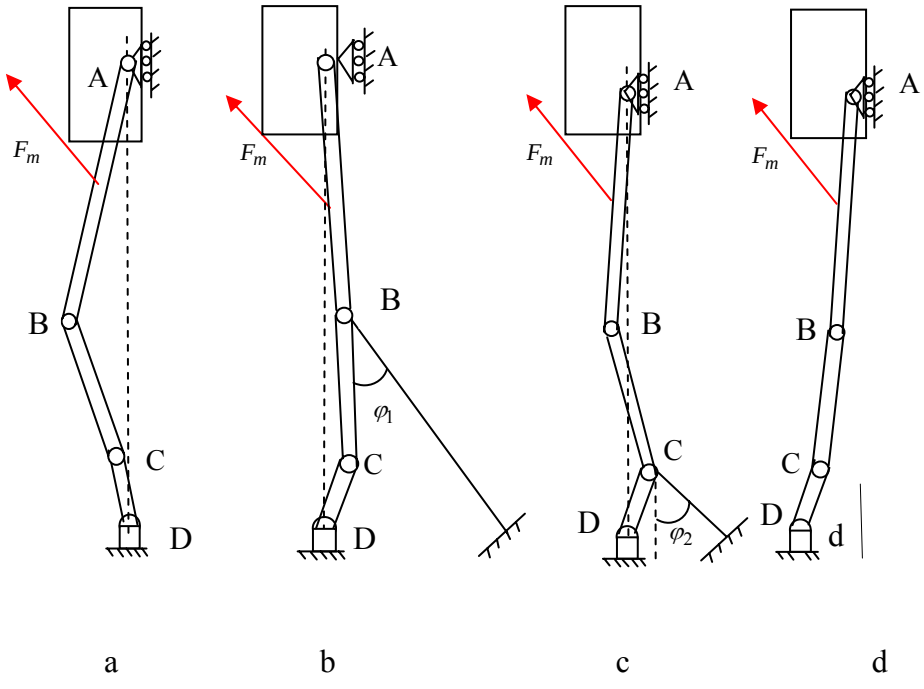

Figure 3.1: Additional restraining of the forelimb's DOFs

In Figure 3.1, the motion of links can be removed by restraining the motion of joints A, B, and C. A restraint is best applied close to a joint. Otherwise it will cause undesired bending of the links. The restraints applied to carpal and fetlock joints (joint B and C) are considered. When the carpal joint is fixed as shown in Figure 3.1b, then none of the links $l_1, l_2^{'}, l_3^{'}$ can move under force F_m. If the fetlock is fixed as shown in Figure 3.1c, then links $l_1, l_2^{'}$ can still move. Theoretically the elbow joint (joint A) could be fixed in the vertical direction but it would be difficult in practice. The spreading configuration, in which leg has to support the horse's weight, is shown in Figure 3.1d. In this configuration it's possible to immobilize completely the forelimb without additional restraints because the links cannot rotate. More details on this can be found in Chapter 6.

3.2 Forces in the Additional Restraints

Assume that the restraints are in the form of ropes that are attached to the joints under the directions φ_1 (at carpal) and φ_2 (at fetlock) as shown in Figure 3.1. For the purpose of analysis, it is assumed that the ropes are tight. Only the forces due to the action of F_m (biceps) are considered (some initial tensions in them are neglected). The restraint force required at carpal joint can be determined from the static analysis of link1 and of the joint B in the standing configuration as shown in Figure 3.2. In this figure, F_{Bx}^{U} and F_{By}^{U} are forces between link1 and joint B, F_{Bx}^{L} is the force between link2$^{'}$ and joint B, and F_1 is the restraint force at the carpal joint.

For link 1 the equilibrium equations can be written as:

$$F_{Bx}^{U} = F_m \cos\gamma \tag{3.1}$$

$$F_{Ay} + F_m \sin\gamma = F_{By}^{U} \tag{3.2}$$

$$F_m a = F_{By}^{U} l_1 \quad (a = b\sin\gamma) \tag{3.3}$$

to obtain:

$$F_{By}^{U} = \frac{F_m b \sin\gamma}{l_1} \tag{3.3a}$$

For joint B the equilibrium equations are:

$$F_{Bx}^{U} = F_1 \cos\varphi_1 + F_{Bx}^{L}, \tag{3.4}$$

$$F_{By}^{U} = F_1 \sin\varphi_1 \tag{3.5}$$

Substituting (3.3a) into (3.5) yields:

$$F_1 = \frac{F_m b \sin\gamma}{l_1 \sin\varphi_1} \tag{3.6}$$

From (3.4) one obtains:

$$F_{Bx}^{L} = F_m \cos\gamma(1 - \frac{b \tan\gamma}{l_1 \tan\varphi_1}) \tag{3.7}$$

The above formula indicates that if $b\tan\gamma \geq l_1 \tan\varphi_1$ then $F_{Bx}^{L} \leq 0$, i.e. link $l_2^{'}$ becomes compressed and the restraining force F_1 in the carpal joint is capable of completely immobilizing the leg (no restraint needed at the fetlock). For $b = 0.111m$, $l_1 = 0.496m$, and the angle of attachment $\gamma = 23.5^{\circ}$ (the same numerical values as used in section 2.2), force $F_{Bx}^{L} \leq 0$ only if $\varphi_1 \leq 5^{\circ}$. That is cable 1 in Figure 3.2 has to be tightened almost vertically which is somewhat unrealistic. If $F_m = 11{,}000N$ then under this condition the force in the rope required to satisfy the equilibrium will be:

$$F_1 \geq \frac{F_m b \sin\gamma}{l_1 \sin\varphi_1} = 10{,}093N \tag{3.8}$$

The force in cable 1 will decrease to $F_1 = \frac{F_m b \sin\gamma}{l_1 \sin\varphi_1} \cong \frac{850}{\sin\varphi_1}$ for $\varphi_1 > 5^{\circ}$. Link $2^{'}$, however, will be under tension ($F_{Cx} = F_{Bx}^{L} > 0$) that in turn necessitates the use of the fetlock's restraint. For equilibrium of joint C, it is required that

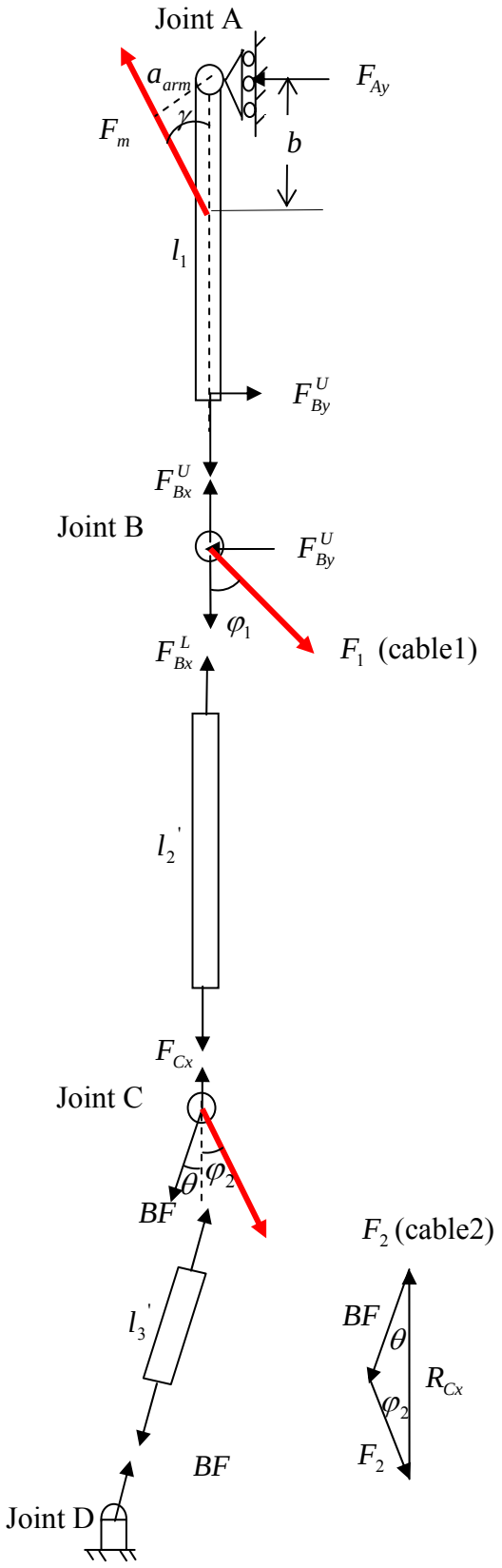

Figure 3.2: Force diagram of the forelimb with carpal, fetlock and hoof restraints

$$\frac{F_{Cx}}{\sin(180^\circ - (\theta + \varphi_2))} = \frac{BF}{\sin\varphi_2} = \frac{F_2}{\sin\theta} \qquad (3.9)$$

where θ is the joint angle at fetlock as indicated in Figure 3.2. Here it is assumed that $\theta = 25^\circ$, if horse stands in the resting position.

Therefore,

$$F_2 = \frac{\sin\theta}{\sin(\theta + \varphi_2)} F_{Cx} = \frac{\sin\theta}{\sin(\theta + \varphi_2)} F_m(\cos\gamma - \frac{b\sin\gamma}{l_1 \tan\varphi_1}), \qquad (3.10)$$

and $$BF = \frac{\sin\varphi_2}{\sin(\theta + \varphi_2)} F_{Cx} = \frac{\sin\theta}{\sin(\theta + \varphi_2)} F_m(\cos\gamma - \frac{b\sin\gamma}{l_1 \tan\varphi_1}) \qquad (3.11)$$

where F_{Cx} is the joint reaction force between joint C and $l_2^{'}$, F_2 is the force in cable 2 at fetlock joint. One can see from (3.6) that F_1 is a function of one variable φ_1, while F_2 and BF are functions of both φ_1 and φ_2 defined by (3.10) and (3.11).

The model in Figure 3.2 was verified by the COSMOS analysis performed on more detailed models shown in Figure 3.3. The 3-links model and the 'anatomical' model explained earlier were used.

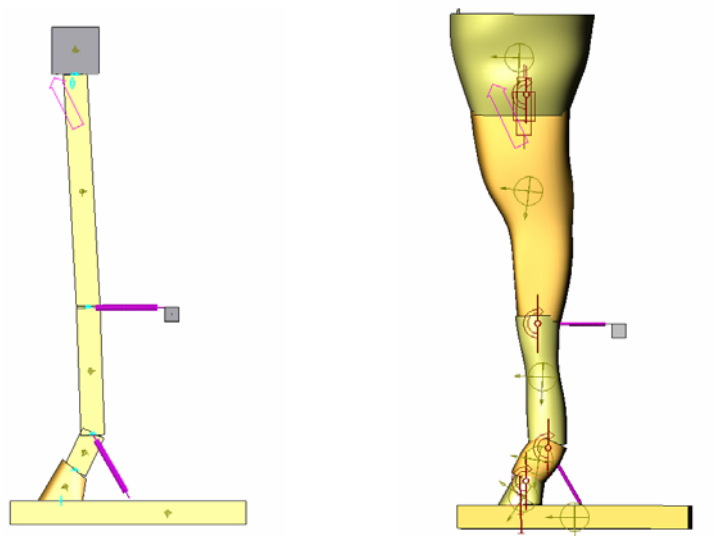

a) Three link model b) Anatomical Model

Figure 3.3: Models of restrained forelimb used in the COSMOS simulations

Forces F_{Bx}^{L}, F_1, F_2 and BF obtained from equations (3.6), (3.10) and (3.11) in terms of φ_1 and φ_2 (for the analytical model) are plotted in Figure 3.4 and compared with the findings from the COSMOS models. The three links COSMOS model results indicated by the triangle mark agree very well with the analytical results. As mentioned earlier, the simulation results from the anatomical model, denoted with circle marks, are slightly different because the properties of each part in the anatomic model are different than the three links model.

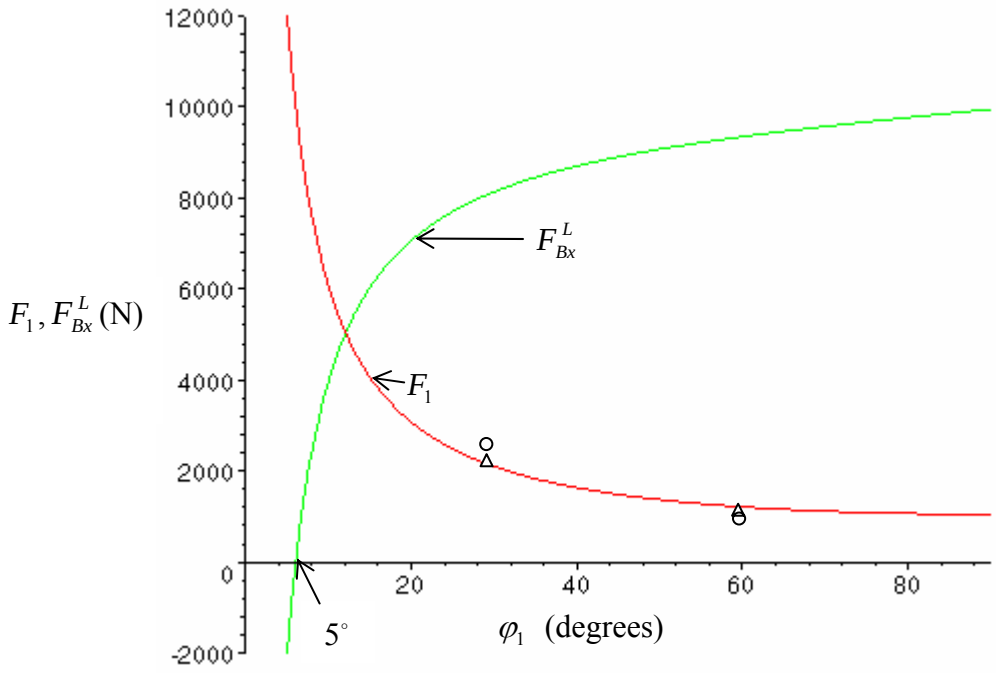

a)

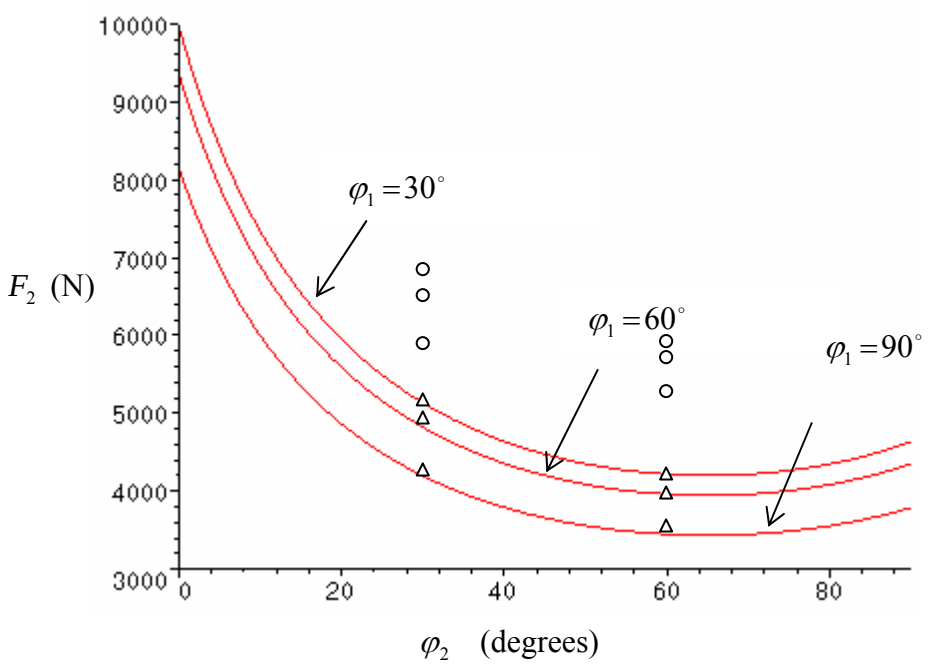

b)

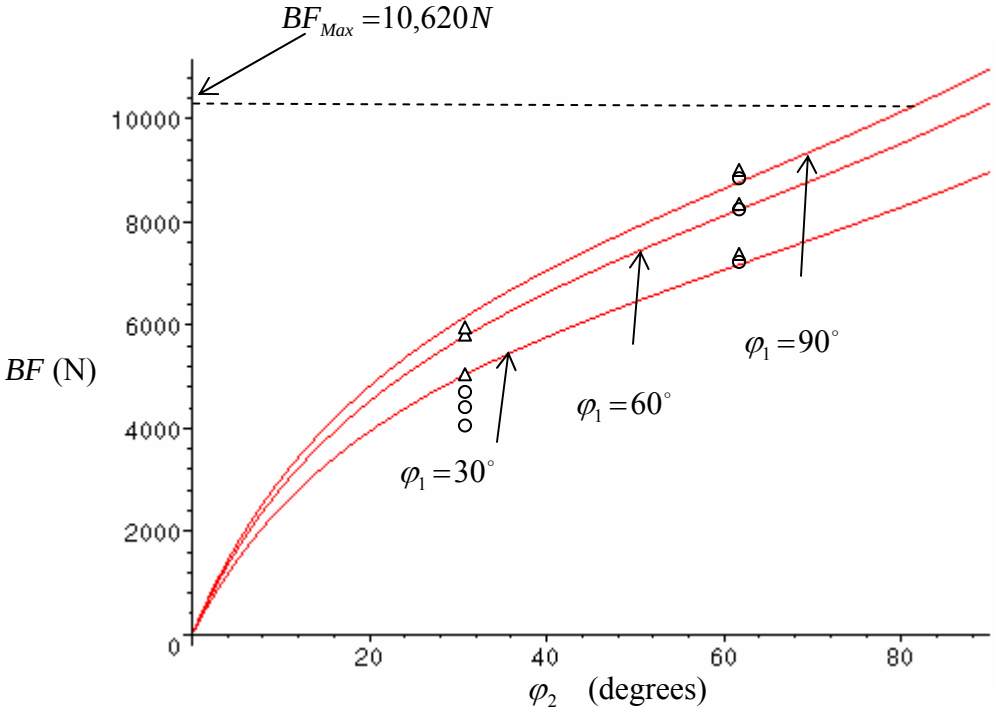

c)

Figure 3.4: Forces on the forelimb versus restraint attachment angles

△ Three links simulation result ○ Anatomical model simulation result

These results should be helpful in properly choosing the angles of attaching the carpal and fetlock ropes. The criterion should be to minimize the magnitudes of forces F_1, F_2 and BF. Also, one should take into account that some sliding of the rope is more likely to happen at the carpal rather than fetlock joint. Thus, the vertical component of F_1 should be minimized as well. The minimum of F_1 is at $\varphi_1 = 90^0$, which means that the carpal joint should be tightened up horizontally. The following results were obtained from the COSMOS simulation (anatomical model) if φ_2 is set more realistically at 30°: (Refer to circle mark in Figure 3.4)

$F_1 = 929\,\text{N}$ (horizontal)

$F_2 = 6{,}884\,\text{N}$

$BF = 4{,}768\,\text{N}$

Note that force BF is only about 40% of $BF_{\max}$ obtained in section 2 for the case of quasi-static pulling without additional restraints. This significantly reduces the risk of breaking the hoof restraint. If the ropes deformation is sufficiently small (or the ropes are sufficiently strong) then the mobility of the leg is totally removed. That is, properly designed restraining ropes and the hoof restraint should be capable of neutralizing and controlling any effort of the biceps to free the forelimb.

4. HINDLIMB RESTRAINT METHOD

4.1 Hindlimb Musculoskeletal Structure and Mobility

The hindlimb provides most of the propulsion for the horse to move forwards. The propulsion is developed by a powerful backward swing of the limb with the hoof contacting the ground. This mechanism uses strong muscle, such as biceps femoris, to develop the forces that can lift the hind hoof. It becomes the most prominent fighting pattern used by the horse in free itself from the hoof restraint.

The hindlimb of a horse is composed with Hip bone, Femur, Fibula and Tibia, Metatarsal, Proximal, Middle, and Distal Phalanges (hoof). These bones are connected at hip joint, stifle joint, hock joint, tarsal joint, pastern and coffin joint as shown in Figure 4.1. [9]

The methodology to analyze mechanics of hindlimb is similar to that used in Chapter 2 to examine the forelimbs.

The range of motion at each joint of the hindlimb is plotted in Figure 4.2. When the hind hoof is fixed, extension at stifle joint and hock joint is restricted by the extruded calcaneus. Over-extension at pastern and coffin joint is also limited. As a consequence, straightening the leg is not permitted. The only way to fight the hoof restraint is to flex the stifle and hock joint with the biceps femoris muscle as shown in Figure 4.2.

4.2 Mechanical Model of the Hindlimb in the Standing Configuration

It is obvious that the standing configuration of the hindlimb is very similar to a mirror image of the forelimb in a bent position. When the hoof is fixed, the pulling

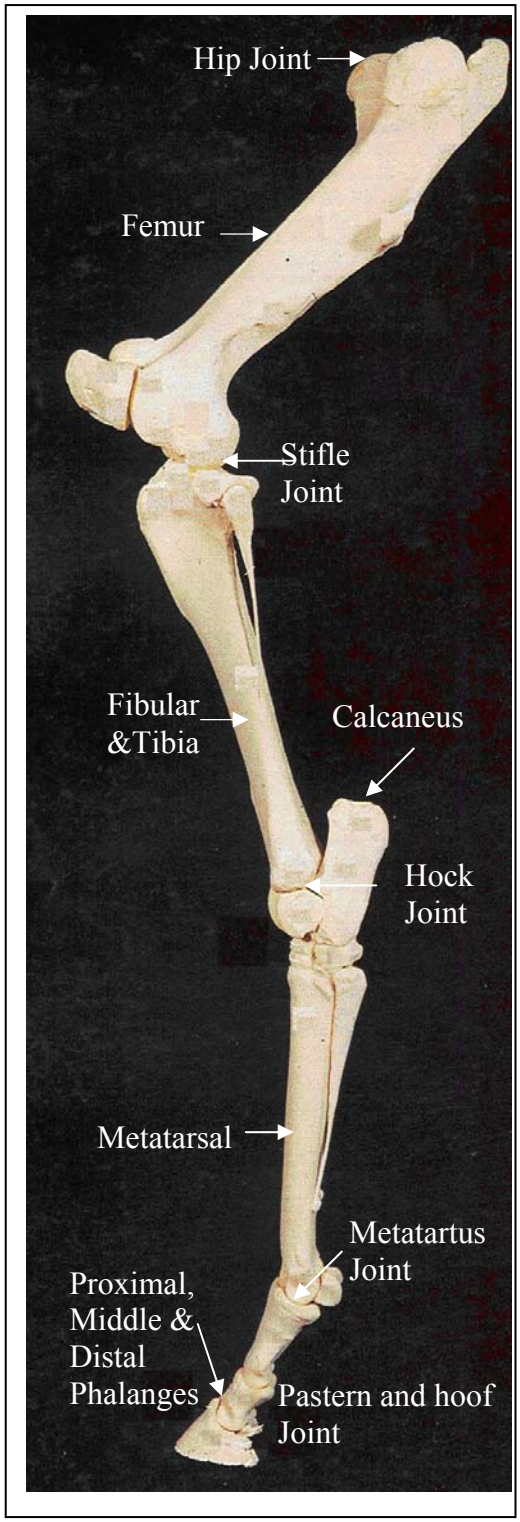

Figure 4.1: Hindlimb skeletal structure

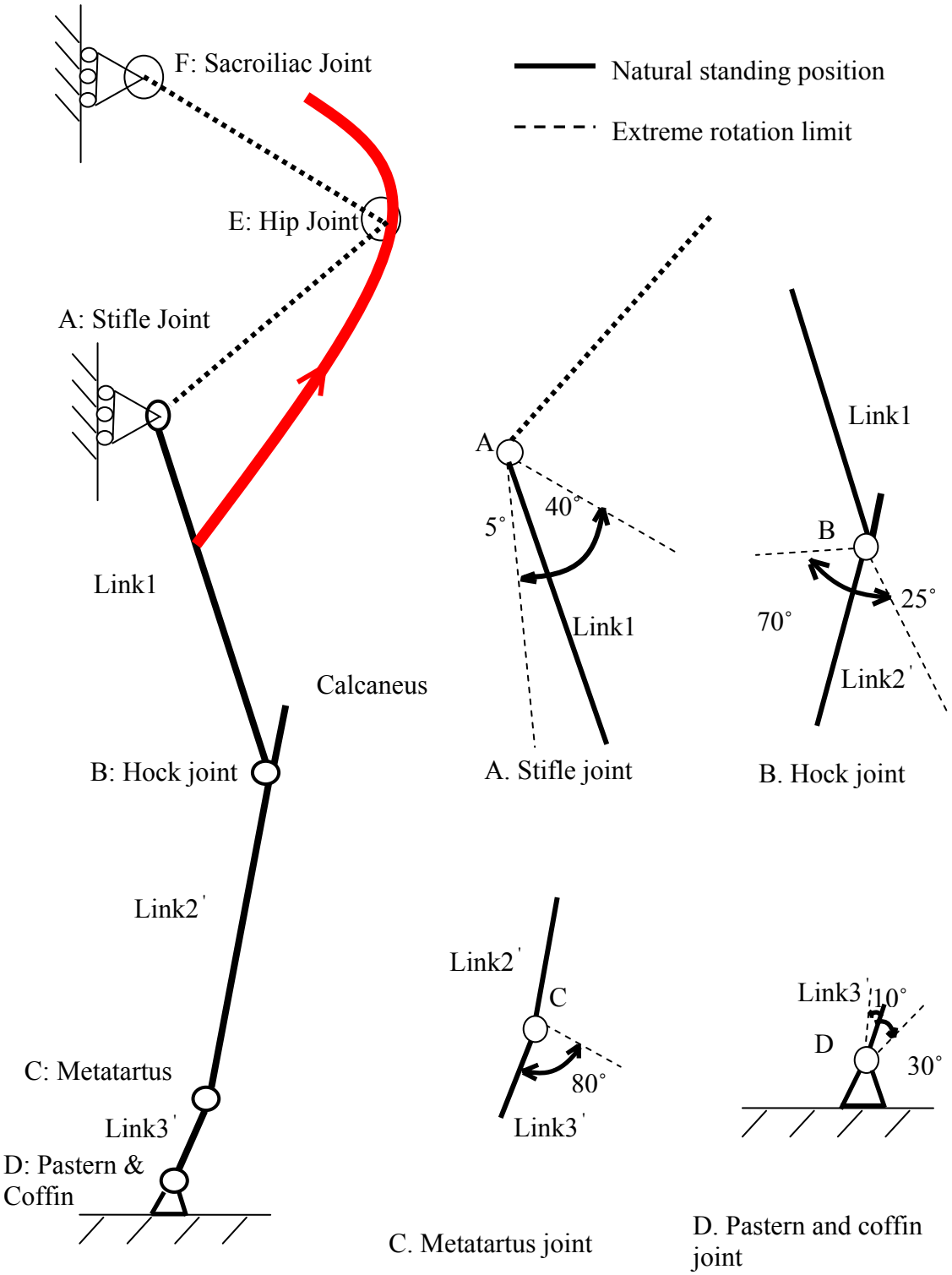

Figure 4.2: Linkage system of hindlimb and the ROM at each joint

force generated by biceps femoris and transmitted to the hoof will generate the breaking force on the hoof.

Although the biceps femoris looks stronger than the biceps muscle in the forelimb analysis, their measured PCSA is almost the same [6,7]. Force generation capacity of the muscle is also estimated at 11,000N from the muscle force and PCSA relationship function (see Section 1.3). If the hoof of the hindlimb is constrained, the forces of other muscles add very little in helping to lift the hoof. More explanation on role of various muscles on the hoof restraint can be found in the Appendix A.

Again, the breaking force generated in the quasi-static action and dynamic jerking will be analyzed. Immobilizing the hindlimb in a particularly position will be discussed in detail.

4.2.1 The Hindlimb Mechanical Model

The hindlimb of the horse is modeled as a three link system with a mass on top as shown in Figure 4.3. The mobility of the limb with the hoof restraint is driven by the force generated by the biceps femoris (F_m). The hoof is fixed to the ground and the hip of the horse is allowed to move vertically.

The top mass, estimated at 100kg, is added to represent a proportion of the horse's trunk and hip weight which may be involved in the hindlimb motion.

Link l_1, l_2' and l_3' represent, fibula & tibia, metatarsal, and proximal & middle phalanges accordingly. Joint A, B, C, D stand for stifle joint, hock joint, tarsal joint, pastern & coffin joints respectively. Each joint is assumed to be a planar revolute joint.

The action line of the biceps femoris is the line from the muscle's insertion point (I) on the tibia to the origin point at the hip joint (E).

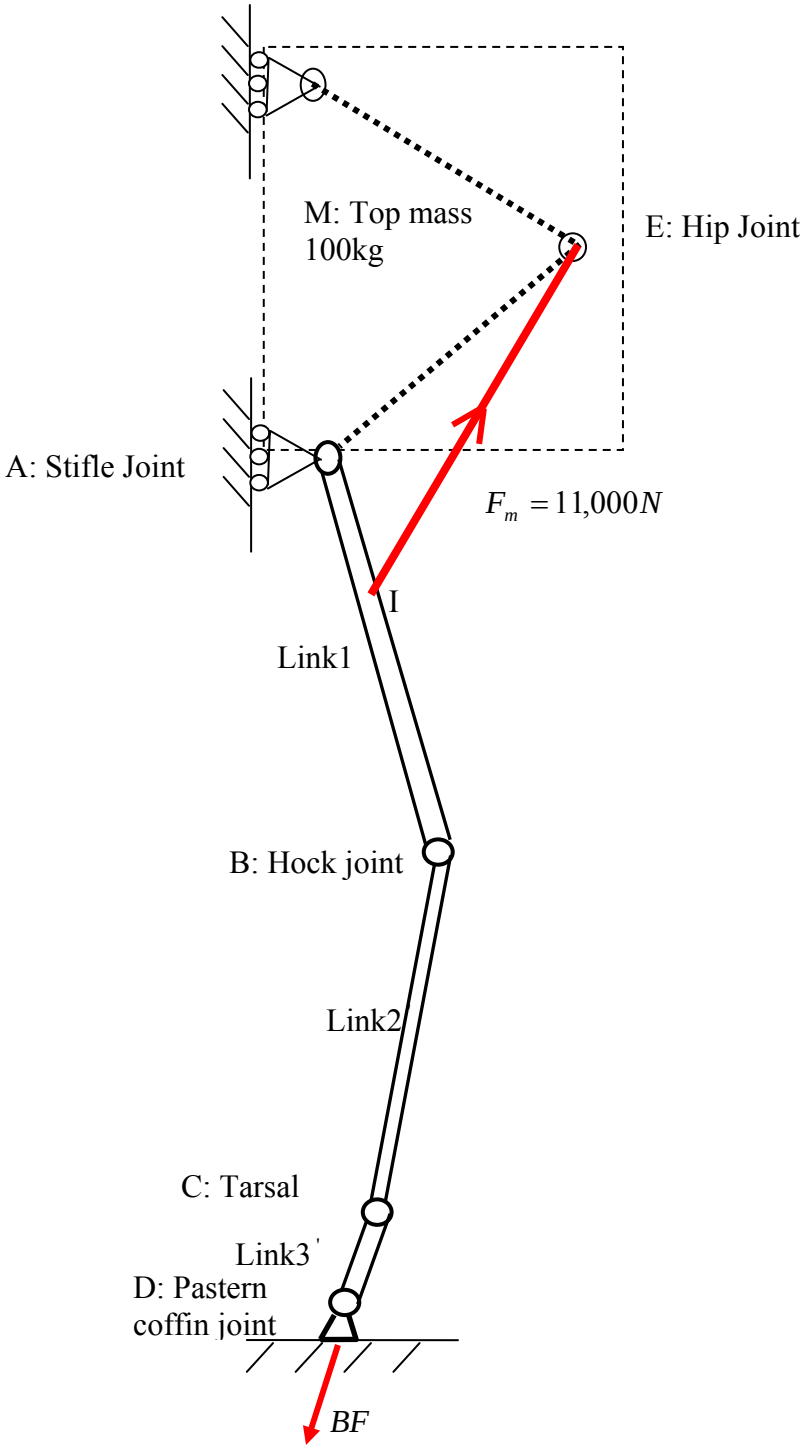

Figure 4.3: Mechanical model of the horse hindlimb

4.2.2 The Hindlimb Anatomic Computer Model

A computer model of the mechanical system of a horse hindlimb build up in SolidWorks is shown in Figure 4.4. This model also consists of essentially three links, but the links have more anatomically correct shapes.

In the computer model, the top mass in Figure 4.3 is replaced with the hip of the horse, free to move in the vertical direction. Hoof is fixed to the ground. l_1, $l_2^{'}$ and $l_3^{'}$ move as a linkage system. Geometry profile and physics properties of each part of the limb are defined in SolidWorks. Joint locations are defined based on the anatomy of average horse.

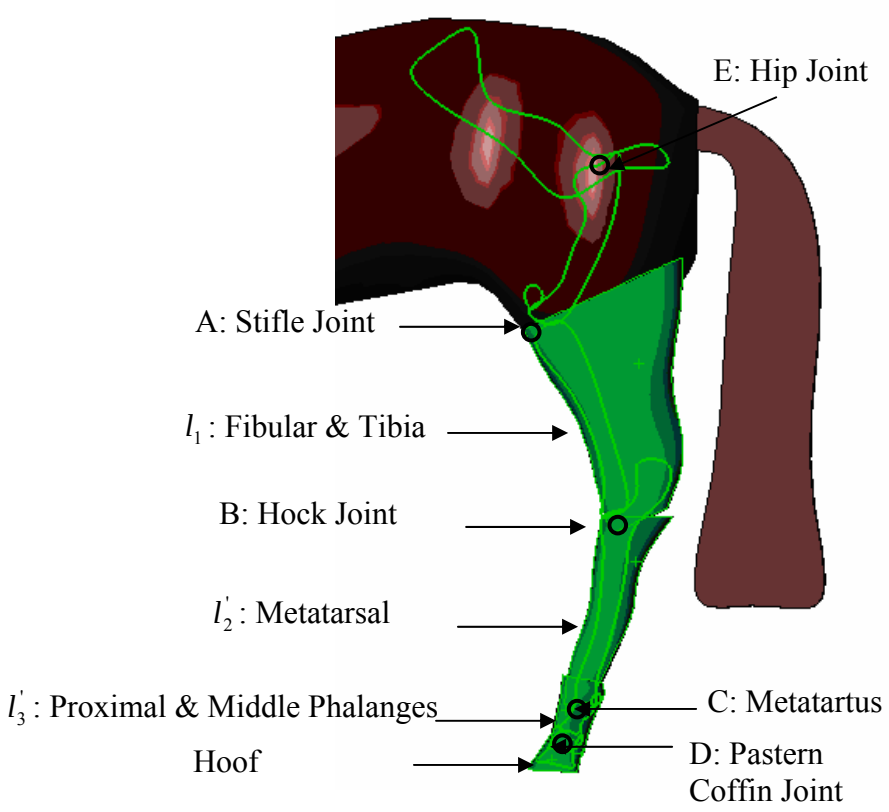

Figure 4.4: Overview structure of the hindlimb

4.2.3 The Hindlimb Quasi-Static Pulling

As mentioned earlier, the diagram of the hindlimb model shows similarity with a mirror image of a forelimb model. The biceps femoris force F_m pulls link1 (Fibular & Tibias) and generates the breaking force that may break the hoof restraint. Figure 4.3 shows the hindlimb standing configuration. In chapter 2 it was concluded that the horse generates the maximum BF if it pulls the leg straight up from the standing configuration. For the hindlimb, straightening the leg is restricted by the ROM at joint D and joint B. (refer to Figure 4.2) The force BF under the restriction will be determined from static analysis on the hindlimb.

Figure 4.5 shows the force diagram on the hindlimb. As the biceps femoris pulls link1, there will be tension in link2$'$ and link3$'$ that stretch them forming a line, or link2 as shown in the plot. Note that l_1 and l_2 denote the length of link1 and link2. H and L are vertical and horizontal distances between joint A and joint D. In particular, the distance between the hip joint and the biceps femoris attachment point (I) is b and distance between the stifle joint (Joint A) and the hip joint is denoted by e_x^0 and e_y^0, vertically and horizontally respectively.

These numerical values are obtained from the measurement with the horse model build up in SolidWorks and are taken as:

H = 0.783m, L = 0.053m, $l_1 = 0.397$m, $l_2 = 0.415m$, b = 0.211m,

$e_x^0 = 0.305m$, $e_y^0 = 0.239m$

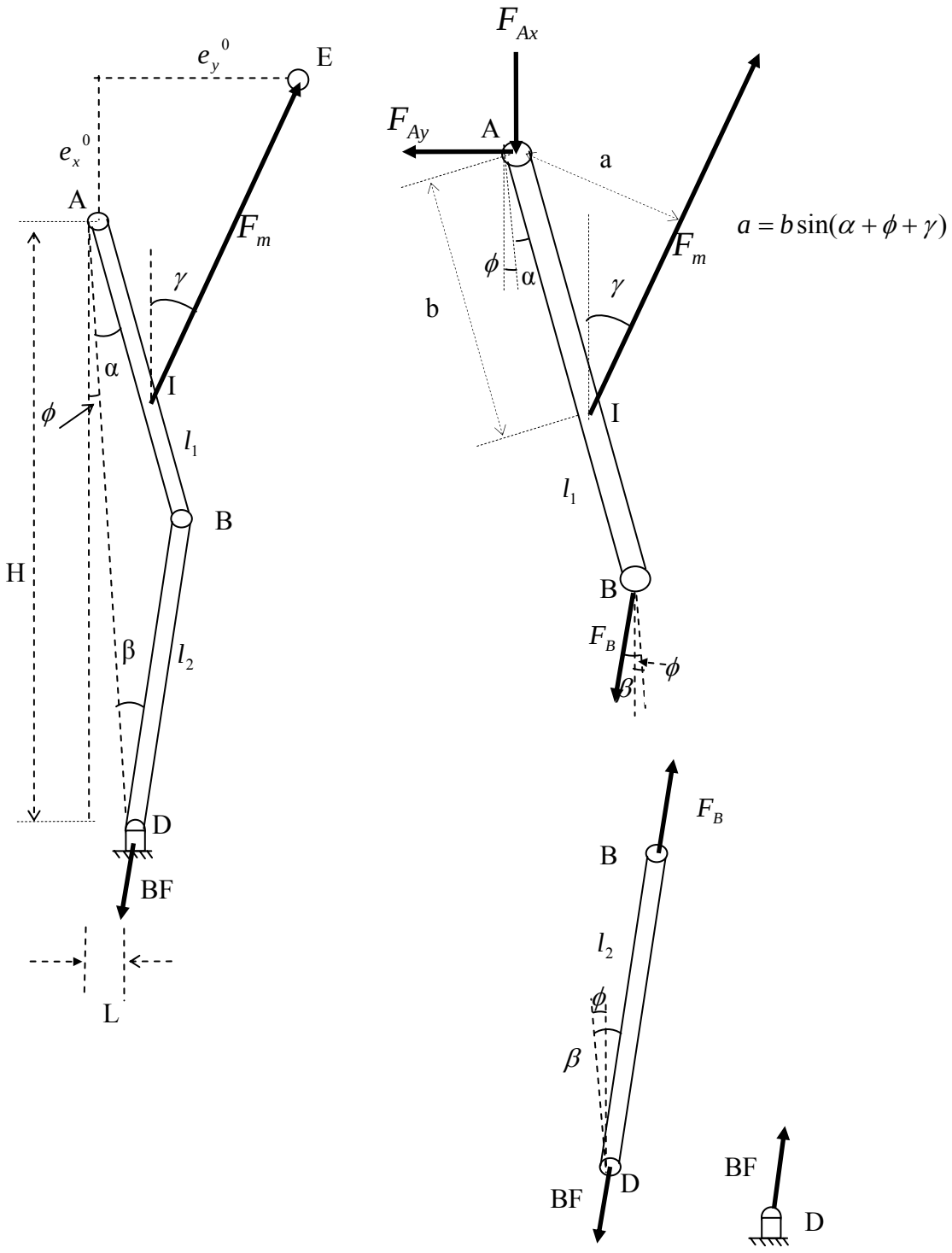

Figure 4.5: Force diagram of hindlimb quasi-static pulling

Then angles $\alpha, \beta, \gamma, \phi$ in the configuration plot in Figure 4.5 are calculated based on the geometric relations of each member. The angles are shown as:

$\alpha = 15^\circ$, $\beta = 14^\circ$, $\gamma = 18^\circ$, $\phi = 3.8^\circ$

The lower member of link2 is under tension only, therefore $F_B = BF$. Equilibrium equations for the top member of length l_1 are written as:

$$\sum M_A = 0, \quad F_B l_1 \sin(\alpha + \beta) - F_m b \sin(\gamma + \alpha + \phi) = 0 \qquad (4.1)$$

where, $F_m = 11{,}000N$. Thus, BF is obtained as

$$BF = F_B = F_m \frac{b \sin(\gamma + \alpha + \phi)}{l_1 \sin(\alpha + \beta)} \approx 7{,}150N \qquad (4.2)$$

It should be noted that breaking force that can be generated at the hindlimb is about 70% of the maximum breaking force that can be generated on the forelimb.

4.2.4 The Breaking Force Due to Hindlimb Dynamic Jerking

The sheep in the experiment was observed to move its hip up and down dynamically while trying to free itself. It is believed that it was done to generate dynamic breaking forces. The magnitudes of the dynamic breaking force are to be determined in this section.

4.2.4.1 Hindlimb Jerking By Lowering the Hip (Down Maneuver)

The animal can quickly lower hip and the stifle joint (Joint A) so that the fibular & tibia (link1), metatarsal and proximal phalanx (link2) can rotate from the initial configuration to the squat configuration as shown in Figure 4.6. The rotation will stop at the squat configuration due to ROM at pastern and coffin joint generating impact forces.

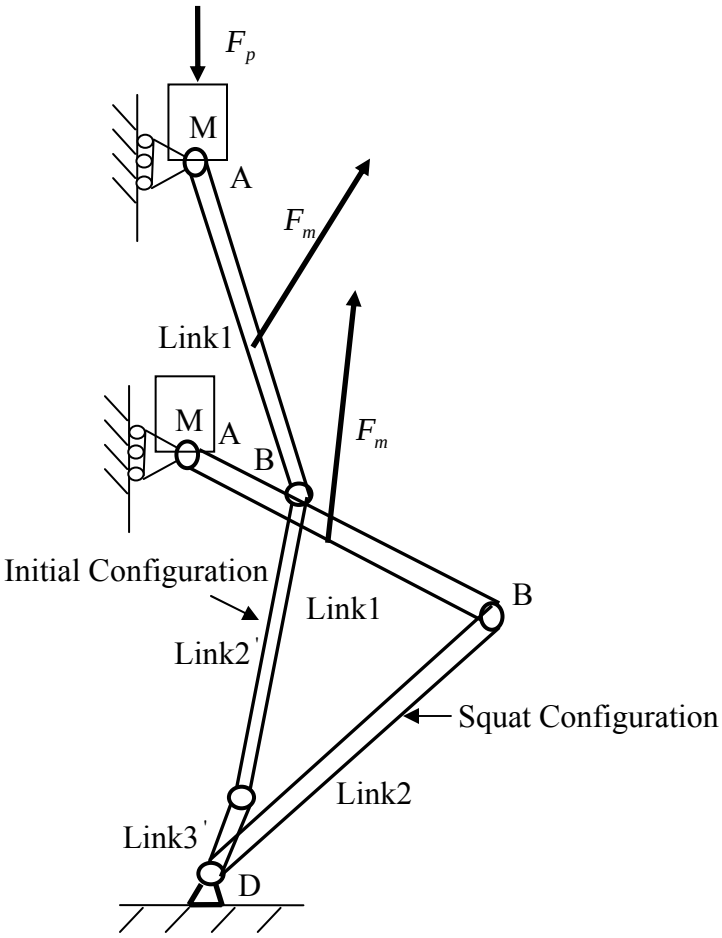

Figure 4.6: Hindlimb in dynamic jerking

Similar to the motion of the front leg, it is assumed that motion of lowering the hindlimb is initialized with the gravity force of the body at the acceleration rate of $a_{down} = g = 9.81 m/s^2$. The vertical motion is assumed to stop when joint A is lowered at $x_{stop} \approx 0.4$m with the deceleration of $a_{stop} = -6g$. Figure 4.7 describes the motion of lowering the hip in the jerking.

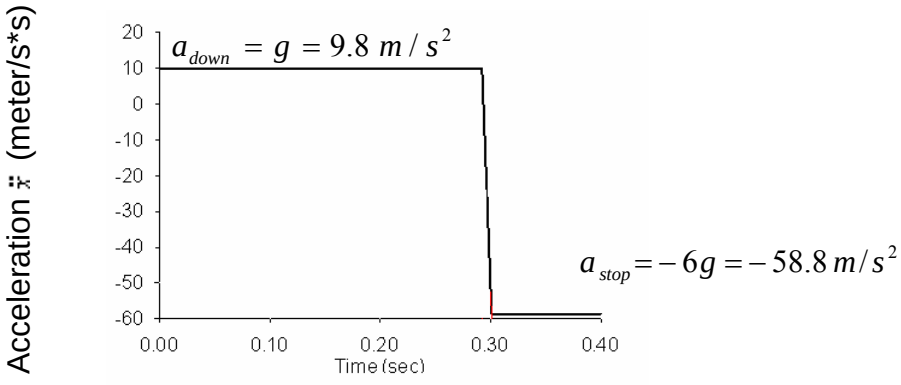

a) Acceleration of joint A

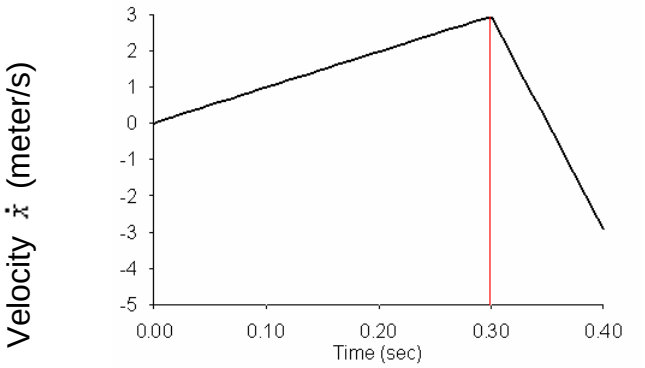

b) Velocity of joint A

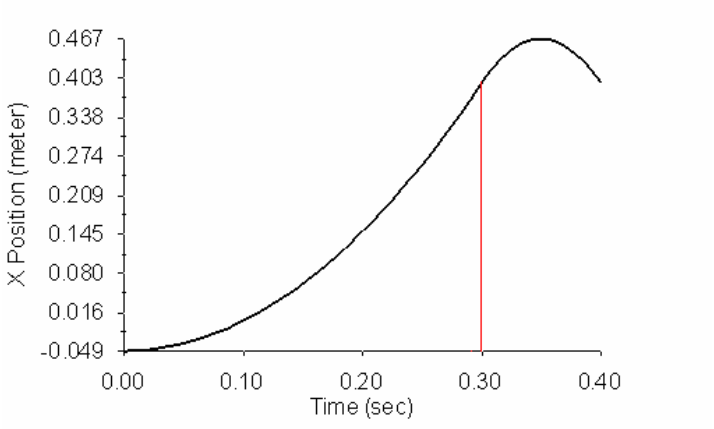

c) Displacement of joint A

Figure 4.7: Stifle joint (joint A) motion in dynamic jerking (down maneuver)

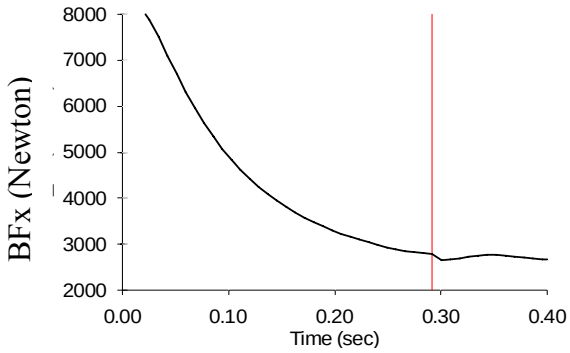

a) Force BF_x

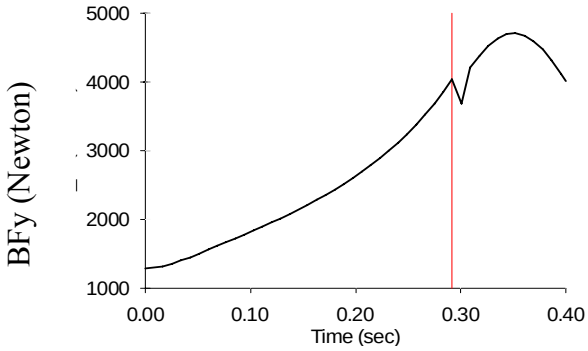

b) Force BF_y

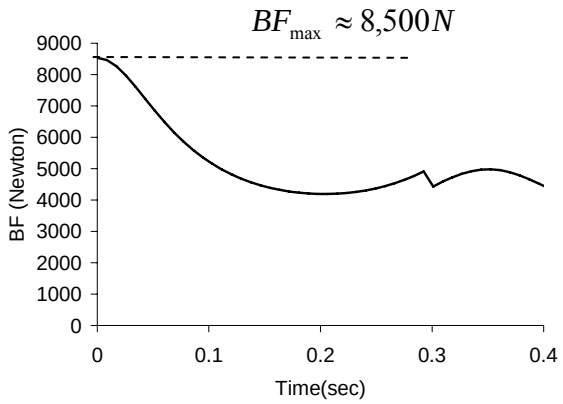

c) The hoof's force BF

Figure 4.8: Forces due to hindlimb dynamic jerking (down maneuver)

The analysis method used to determine the dynamic breaking force on the hindlimb due to jerking is identical to the one used when analyzing the forelimb in Chapter 2. In this chapter, the jerking effects in hindlimb are simulated with a model shown in Figure 4.4.

Figure 4.8 plots the breaking force due to the jerking as the hip and stifle joints move down. The simulation result indicates that maximum breaking force of $BF_{\max} \approx 8{,}000N$ is generated as the hindlimb initiates jerking at the natural standing position.

4.2.4.2 Hindlimb Jerking by Elevating the Hip (Up Maneuver)

After the leg is forced to stop at the squat configuration as shown in Figure 4.6, the horse might elevate the hip up to return to the initial standing position. For the sheep, it was observed that it takes longer to lift the hip in the jerking than lowering it down. Assuming that the horse will behave similarly, the acceleration to lift the hip is then approximated to be $a_{up} = -0.5$g. As the leg returns back to the initial standing position, a deceleration is assumed at $a_{stop} = 6g$ to stop the motion. This is described in Figure 4.9 and the maximum breaking force generated in this period is at $BF_{\max} = 7{,}100N$ when the rotation is stopped close to the natural standing position as shown in Figure 4.10.

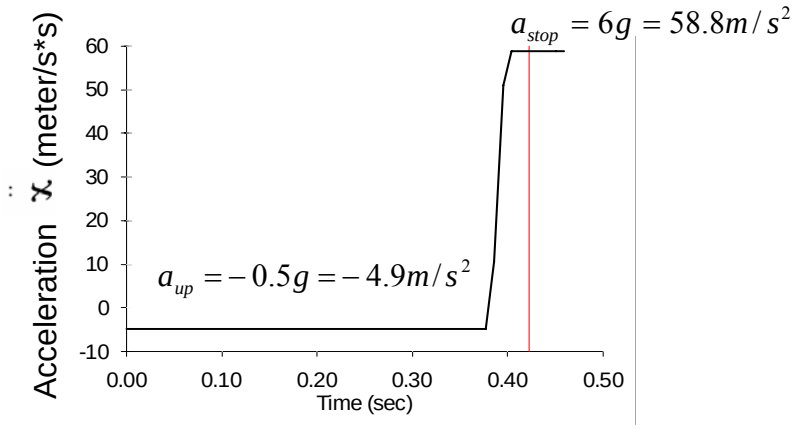

a) Acceleration of joint A

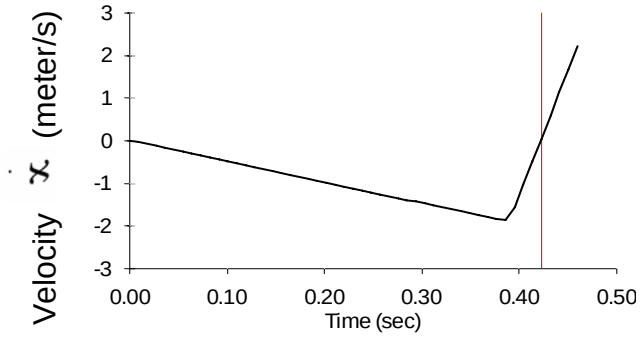

b) Velocity of joint A

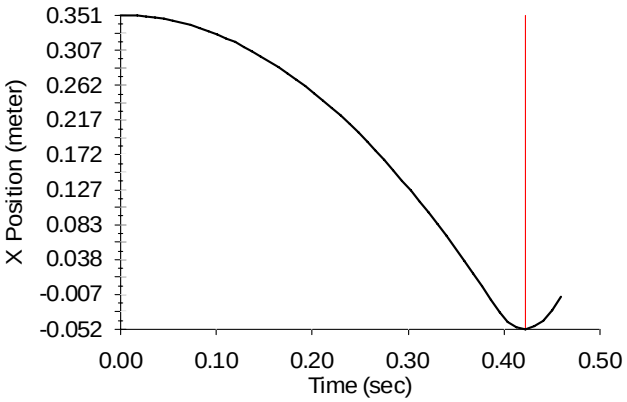

c) Displacement of joint A

Figure 4.9: Stifle joint (joint A) motion in dynamic jerking (up maneuver)

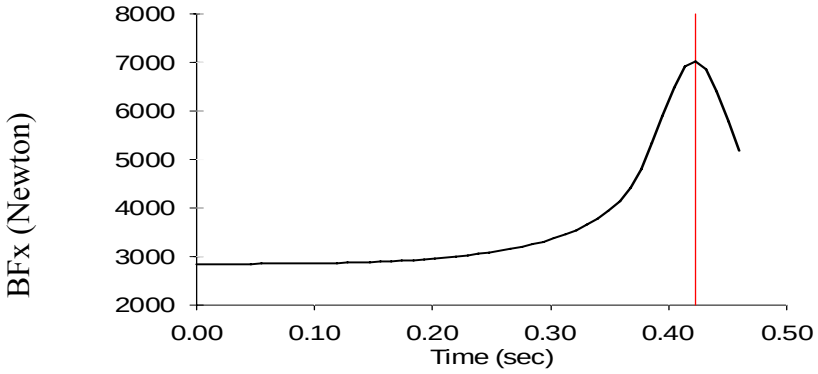

a) Force BF_x

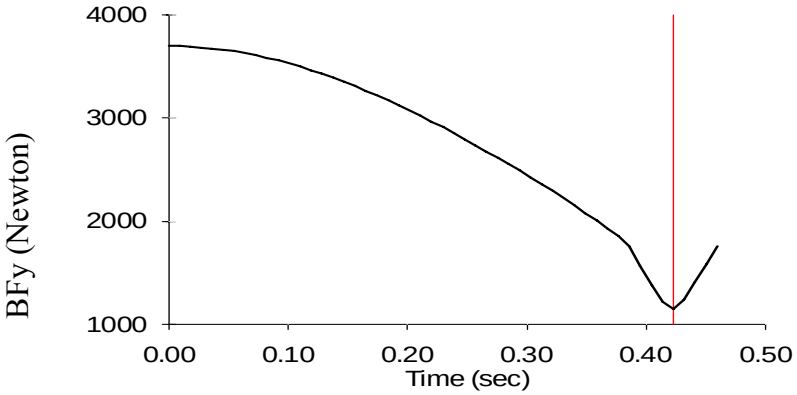

b) Force BF_y

$BF_{max} \approx 7{,}100\text{N}$

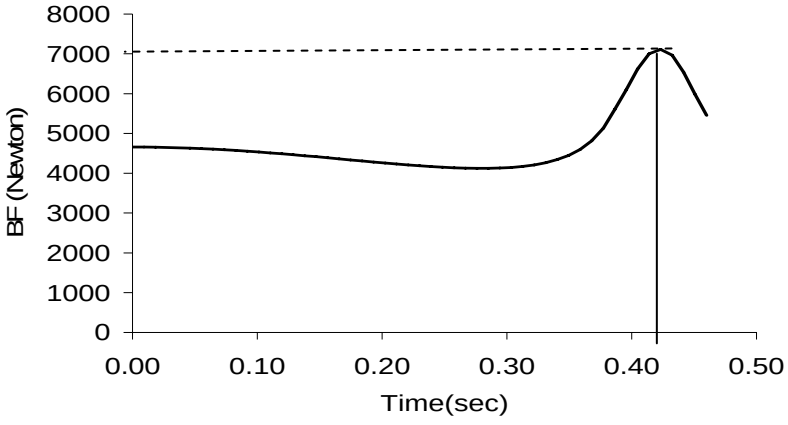

c) The hoof's force BF

Figure 4.10: Forces due to hindlimb dynamic jerking (up maneuver)

In summary, maximum breaking force generated during the jerking can reach to about 8,500 N which is about 1,300 N higher than the breaking force generated by static pulling. Thus, the jerking mechanism developed intuitively by the animal is proven to be useful in fighting the hindlimb's restraints.

To prevent the animal from generating high breaking force, more restraints should be added on the limb to immobilize it. Details of removing the total mobility on the hindlimb will be discussed in the next chapter.

5. REMOVING THE HINDLIMB MOBILITY

In this chapter, complete removing of the hindlimb mobility is considered. It has been found in the sheep restraint experiment that the hock joint restraint can immobilize the joint when adding the restraint properly. The required constraint forces in the leg spreading configuration will be investigated.

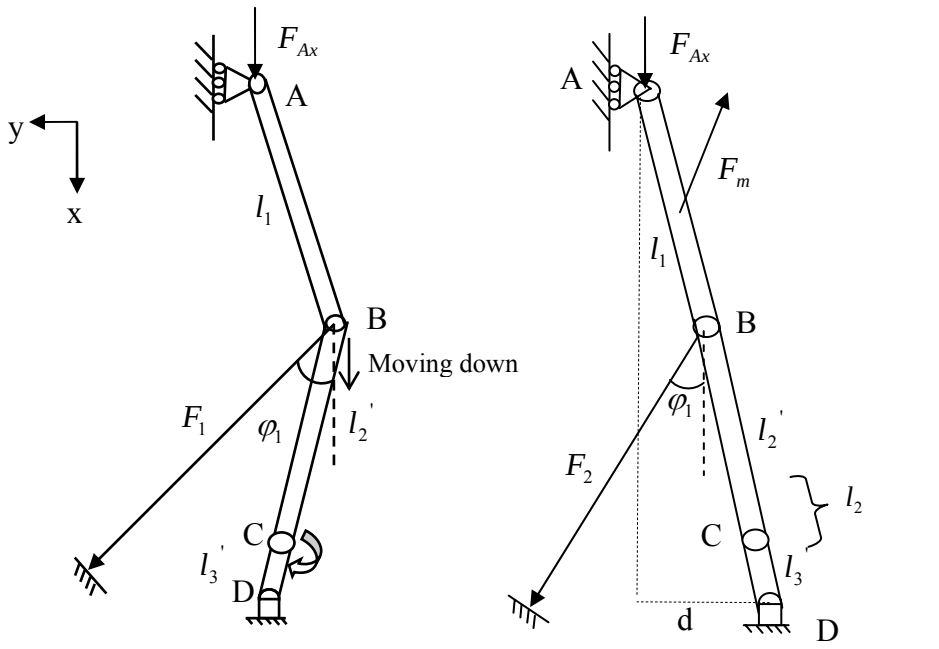

a) Natural standing position b) Stretched to align position

Figure 5.1: Adding hock restraint on the hind limb in two configurations

5.1 Effect of Adding Hock Joint Restraint in Natural Standing and Stretching Configurations

In the sheep restraint experiment, the hock restraint cannot completely immobilize the joint when sheep stands naturally in the configuration shown in Figure 5.1a because of possibility of sideways motion. However, by spreading the sheep's legs (as the configuration in Figure 5.1b) the sideway mobility of the leg seemed to have been removed and the hock restraint successfully immobilized the joint and the whole hind limb. In order to explain the above phenomena the potential motion of the limb in these two configurations is analyzed. In Figure 5.1a, hock joint (joint B) tends to move down by the gravity force F_{Ax}. The hock restraint force under the direction of φ_1 does not act contrarily to this motion. In addition, it is hard to restrain joint B as joint C can flex. Flexion of joint C can be limited when the hoof (D) is fixed at the distance d from the natural position. Also, the visual inspection of the sheep indicated that the rope at B forced link1, link2' and link3' almost to aligned as shown in Figure 5.1b. Therefore, in the analytical model these links are configured in a straight line. Details to determine the required restraint forces in the rope attached at B and the breaking force at D will be discussed in the following section.

5.2 Required Restraint Force at Hock Joint

Forces exerted on the hindlimb's links in the aligned configuration are shown in Figure 5.2. The equilibrium equations for link1 can be written as:

$$F_{Ax} + F_{Bx}^{U} - F_{mx} = 0 \tag{5.1}$$

$$F_{Ay} + F_{By}^{U} - F_{my} = 0 \tag{5.2}$$

$$F_{Bx}^{U} l_1 \sin\alpha + F_{By}^{U} l_1 \cos\alpha - F_m b \sin(\alpha + \gamma) = 0 \tag{5.3}$$

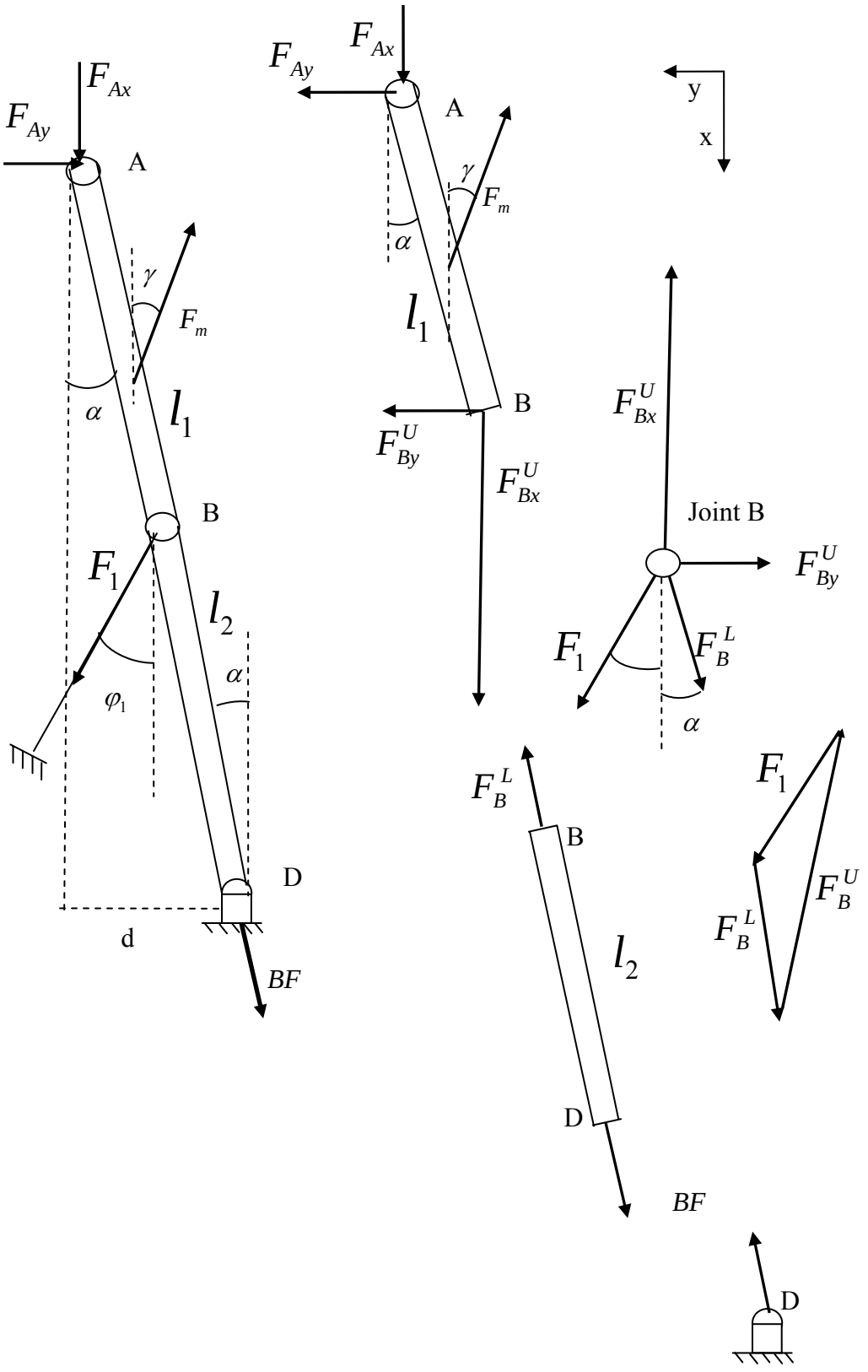

Figure 5.2: Force diagram with hock restraint

where F_{Bx}^{U} and F_{By}^{U} are joint reaction force between link1 and joint B. The following numerical values obtained from standing horse image that was used to built the model are used for the hindlimb model: b=0.211m, F_m=11,000N, $F_{Ax} = 980\,\text{N}$, $l_1 = 0.397\,\text{m}$, l_2=0.415 m, $\alpha = 19^\circ$, $\gamma = 18.6^\circ$. The three unknowns obtained from (5.1-5.3) are:

$$F_{Bx}^{U} = 9{,}444\,\text{N},\ F_{By}^{U} = 513\,\text{N},\ F_{Ay} = 4{,}024\,\text{N}$$

Substitute F_{Bx}^{U} and F_{By}^{U} into equilibrium equation for joint B:

$$F_B^L \cos\alpha + F_1 \cos\varphi_1 - F_{Bx}^{U} = 0 \qquad (5.4)$$

$$F_1 \sin\varphi_1 - F_{By}^{U} - F_B^L \sin\alpha = 0 \qquad (5.5)$$

where F_1 is the constraint force at hock joint, F_B^L is the joint reaction force between link2$'$ and joint B and is equal to the breaking force BF.

Both F_1 and F_B^L can be expressed in term of variable φ_1 as:

$$F_1 = \frac{F_{By}^{U} + F_{Bx}^{U} \tan\alpha}{\sin\varphi_1 + \cos\varphi_1 \tan\alpha} \text{ and} \qquad (5.6)$$

$$BF = F_B^L = \frac{F_{Bx}^{U} \tan\varphi_1 - F_{By}^{U}}{\sin\alpha + \cos\alpha \cdot \tan\varphi_1} \qquad (5.7)$$

Similarly as for the forelimb the COSMOS three links model and the anatomical model of the hindlimb shown in Figure 5.3 were used to validate the above formulas.

Forces F_1 and BF as functions of φ_1 according to (5.6) and (5.7) are plotted in Figure 5.4 and 5.5 with solid lines. The COSMOS simulation results obtained from three links model and the anatomical model are marked with triangle and circle marks respectively as well.

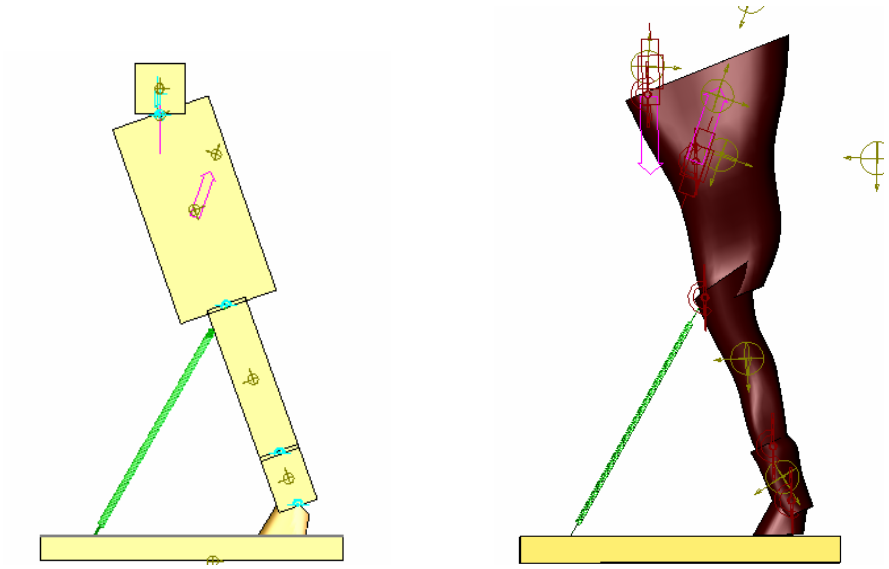

a) Three links model b) Anatomical model

Figure 5.3: The COSMOS models of hindlimb with hock and hoof restraints

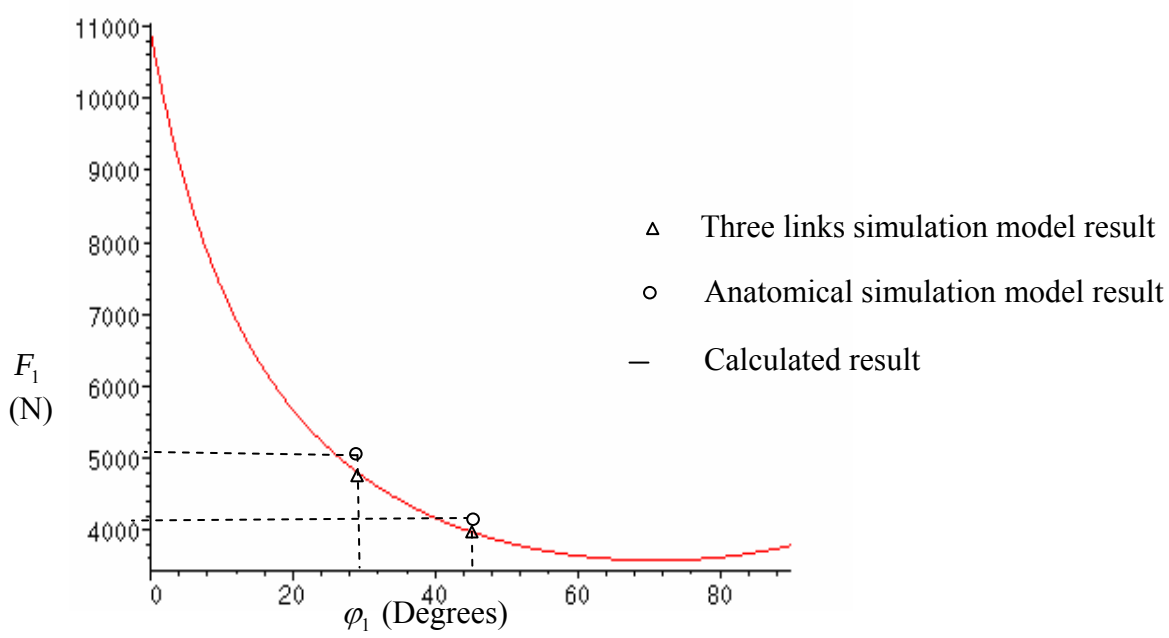

Figure 5.4: Required hock reaction forces versus the restraint attachment angle

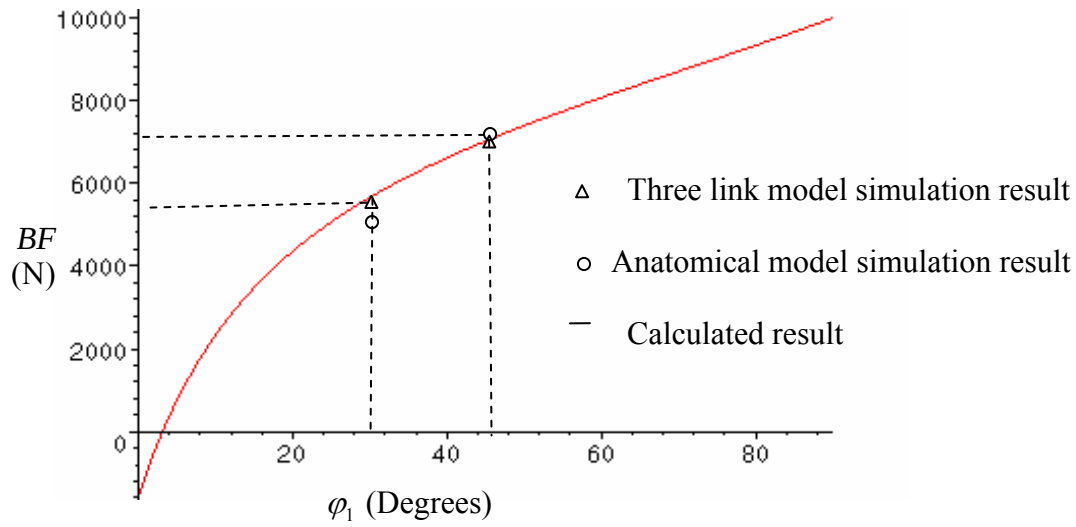

Figure 5.5: Required breaking force versus restraint attachment angle

In general, both simulation results agree well with the analytical result. These results indicate that increasing φ_1 causes the hock's restraining force to decrease and the breaking force to increase. A good compromise seems to be the range at $\varphi_1 = 30^\circ - 35^\circ$ with both the hock and hoof restraint forces are similar and equal to about 5,000N. If φ_1 increases to 45°, then F_1 drops to 3,950N, but BF increases to 7,100N.

6. THE SHEEP RESTRAINING EXPERIMENT

Because of the cost and safety involved, the animal mobility experiment is preformed with a sheep. Sheep have similar skeletal muscular system as horses, and use similar strategies to initiate motion. Also, it is believed that sheep will react somewhat similarly to restraints as horses.

The test of restraining a sheep was conducted at the Western College of Veterinary Medicine at the University of Saskatchewan on a healthy adult sheep without using any drug. The whole experiment was recorded on video for the use of further analyses.

Equipments used in the test include one general clinical purpose sheep restraint cart, a halter for constrain the sheep's head, four cleats installed on the bottom plate of the cart to fix the hooves and two ropes to restrain the sheep's hock joints.

6.1 Applying Initial Restraints

6.1.1 Sheep Cart

The sheep was first lead into a restraint cart as shown in Figure 6.1. Essentially, the sheep was restrained against sideways motion by the neck only. Standing in the cart, the sheep was still free to move in the space between the side walls.

Figure 6.1: Sheep cart

6.1.2 Hoof Restraint

The hoof restraints were critical for controlling the sheep's behavior in the experiment. It was observed that without the hoof restraint, the sheep kicked the hindlimb violently when an operator tried to lift its right hindlimb as shown in Figure 6.2.

Figure 6.2: Sheep fighting without hoof restraints

A customized design of the hoof restrain with ropes and cleats was developed. In order to fasten the restraint rope quickly and tightly, cleat was used in a way as shown in Figure 6.3a.

Each rope was attached at the coffin joint with a “bowline” knot as shown in the plot. The rope went underneath the plate of the cart through a nut preventing rough contact between the rope and the edge of the bottom plate. The rope pulled the foot down and pressed it against the floor when it was tightened up with the cleat. Cleat could lock the rope with the teeth on the surface of rollers. To immobilize the hoof the rope should be positioned precisely in mid caudal plane of the foot. Otherwise the hoof was not evenly pressed against the floor, which made the animal uncomfortable. Attention should be paid to avoid placing the rope in the interdigital space of the hoof as shown in Figure 6.3b.

a) Recommended hoof restraint

b) Hoof restraint to be avoided

Figure 6.3: Hoof restraints

6.1.3 Head Restraint

With fixed hooves but no head restraint, the sheep could generate significant back and forth body motion. Such motion was depicted in Figure 6.4. This was reduced when the head was restrained with a halter as shown in Figure 6.5. To eliminate the side movement, the ropes extended from both sides of the halter were tightened to the cart. Also it prevented the sheep from raising its head up and down. The sheep seemed to be quite comfortable with this constraint in place and tight.

Figure 6.4: Sheep body movement without the head restraint

Figure 6.5: Head restraint

6.2 Mobility of the Initially Restrained Sheep

Focus of this phase of experiment was to observe the animal's behavior with the head and hooves immobilized. The overview of the initial restraints is shown in Figure 6.6. The mobility of the forelimbs and the hindlimbs, and how the sheep would use these body parts to fight the restraints were of particular interest.

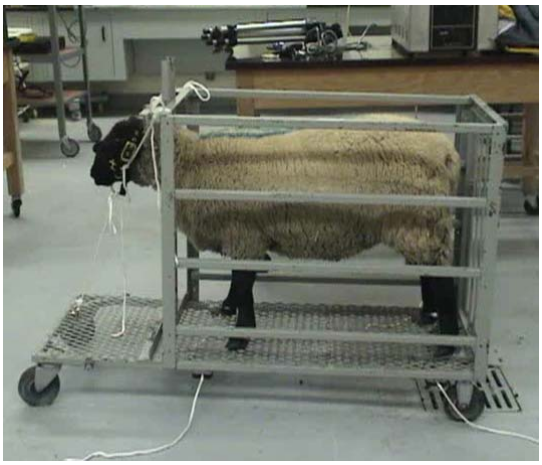

Figure 6.6: Overview of the sheep initial restraints

6.2.1 Forelimb Mobility – Quasi-Static Pulling

In Chapter 2, it was concluded that the best way for the animal to generate the maximum breaking force on the fore hoof would be to use the biceps to statically rise up and bend the forelimb. Also, it was concluded that the animal would intuitively find the best pattern to develop this force. The behavior of the sheep in the experiment confirmed the above conclusions. The sheep shown in Figure 6.7a was standing naturally under the initial restraint. In Figure 6.7b, the animal shifted all the weight on other three legs, and then raised the shoulder of the left forelimb. The quasi-static pulling pattern seen in this figure is almost identical to the 'best' pulling pattern obtained in Chapter 2 in which the maximum breaking force was generated.

a) Normal standing

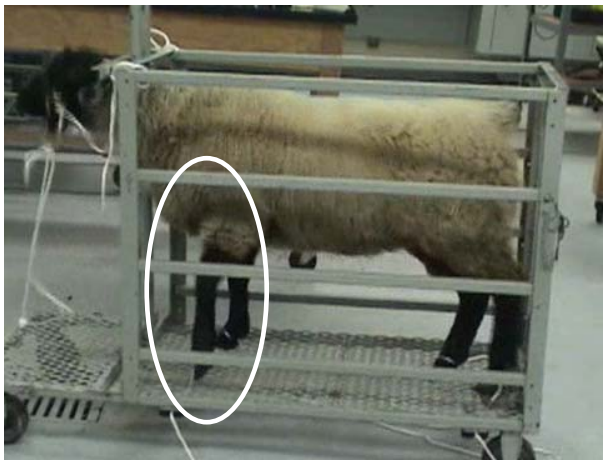

b) Slight raise and bending

Figure 6.7: Quasi-static pulling on the sheep forelimb

6.2.2 Forelimb Mobility – Dynamic Jerking

Forelimb dynamic jerking as discussed in Chapter 2 was also observed in the experiment. The limb jerked very quickly backward and forward several times in an attempt to break the hoof restraint. These movements are captured in Figure 6.8. Then the sheep returned to the static pulling. This may be considered as evidence that the latter is a better strategy to use to free itself from the restraint.

a) Forelimb jerking backward

b) Forelimb jerking forward

Figure 6.8: Dynamic jerking on the sheep forelimb

6.2.3 Hindlimb Mobility – Quasi - Static Pulling

According to the hindlimb functional analysis, the animal should try to use the biceps femoris to lift the hindhoof. However, this was not obvious on the hindlimb as seen on the forelimb. In the hindlimb, the animal would rather stay in the natural position and generate the static breaking force from this position due to the difficulties of raising the hind limb and stretching it as discussed in Chapter 4. It should be noted that no significant change of the leg pattern is needed

to do so. Therefore, it is more difficult to observe whether or not such a force is actually there and for how long.

6.2.4 Hindlimb Mobility – Dynamic Jerking

In the experiment, the sheep was seen to move its hip up and down to create dynamic jerking effect as shown in Figure 6.9. This jerking is driven by the weight on top of the limb and the pulling of the biceps femoris. Also, when the sheep jerked, the sheep cart was shaking slightly accompanied by the noise of rattling parts (the noise can be heard in the video). It indicates that greater forces were created at the bottom plate of the cart when the hindlimb was jerked than the forelimb.

Figure 6.9: Dynamic jerking on sheep hindlimb

6.3 Adding the Hock Restraint to Immobilize the Hindlimb

To reduce the dynamic jerking, hock joint restraints were added as shown in Figure 6.10. One end of the rope was tightened around the hock joint while the other end was dragged through the bottom plate of the cart by operators and tightened up.

Figure 6.10: Sheep restrained with hock restraints and hoof restraints

When the hindlimb stood in the natural standing position, the rope was almost horizontal, which makes the hock restraint not completely preventing side motions. Consequently, the sheep managed to sit down as shown in Figure 6.11.

Also, according to the analysis in Chapter 5, the joint rotation can be locked only when the hindlimb is stretched in the aligning configuration. This will be discussed in more details in the next section.

Figure 6.11: Sheep free itself from improper hock restraint

6.4 Restraining the Sheep in the Legs Spread Position

As discussed in Chapter 1, restraining the animal in the legs spread position should be a more efficient method to immobilize the animal. When the legs are spread, it is difficult for the animal to switch the weight support from four to three legs. With all four legs still supporting the body weight, it is hard for the sheep to fight the restraint.

In the experiment, first the fore hooves were fixed to the corner of the cart to spread forelimbs apart and were moved slightly forward. As a result, extra mobility of the forelimb, essentially the bending at the carpal joint predicted in Chapter 3 was eliminated in the legs spread position. Therefore additional restraint on the fore limb was not needed.

Next, the rear hooves were spread apart and fixed to the bottom as shown in Figure 6.12. In this configuration, hindlimb was stretched to align at the hock joints as shown in Figure 6.13. Joints motion was locked in this configuration. The hock restraint was tightened up with a relatively small effort of the operators. It was sufficient to immobilize the hock joint as well as the whole hindlimb.

Summarizing the experiment, the sheep seemed to be completely immobilized in the position shown in Figure 6.12. It was possible to move and turn the cart without any observable motion of the animal's body or legs (with the exception of that caused by breathing). Also there was no reaction to touching or even slightly pushing the body.

Figure 6.12: Sheep restrained in legs spread position

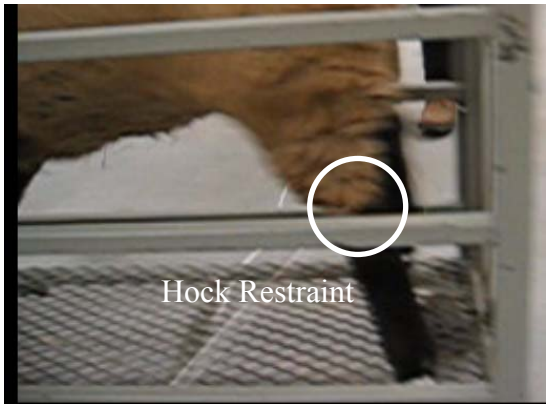

Figure 6.13: Sheep hindlimb stretched to align

The animal seemed to be comfortable with the position for about 5 minutes before it started moving and kicking again after the restraints were released. The ropes can be retightened quickly (and the hooves location can be modified) if the cleats are properly positioned.

7. CONCLUSION AND FUTURE WORK

Methods of removing the horse's mobility in its natural standing position are studied in this thesis. Various methods of restraining the horse are evaluated analytically and by computer simulation. The findings have been tested experimentally on a sheep.

The ROMs at the joints of the horse legs limit the patterns of initiating the motion especially when the hoof of each leg is fixed to the ground. A simple linkage structure is used to simulate such a motion. Forces generated by the horse and forces transmitted to the hooves (referred to as the breaking forces) at quasi-static and dynamic (dynamic jerking) attempts to initiate the motion from the natural standing position are determined. The analysis assumes that the legs' configurations can change within the limits imposed by ROMs. The results indicate that for the forelimb the static force pulling the hoof may be greater than the force generated by dynamic jerking. On the other side, the hindlimbs are capable of generating more breaking force dynamically than statically.

The horse's legs can be completely immobilized in the standing configuration by adding more restraints to particular joints (in addition to the hoof restraints). It eliminates the dynamic jerking and also reduces the static forces that the horse can generate. The analysis, the computer simulation and the experimental observations all indicate that such a method of the animal's restraining should be very effective.

The forces required to restrain each joint that are significant to the horse's mobility are evaluated. Furthermore, these forces can be reduced by optimizing the angles of

attachment of the restraining ropes to the joints. In addition, spreading the legs makes much harder for the animal to fight with the restraints. This is because it substantially limits the animal's ability to switch weight from one leg to another when preparing to initiate the motion.

All the above conclusions were confirmed by the experiment conducted on a sheep. The animal restrained by ropes that fastened all the hoofs and significant joints was standing still without any apparent discomfort for a time that seemed to be sufficiently long for the imaging application, proposed by the Biomedical Imaging and Therapy Beamline at the Canadian Light Source. This essentially proves the feasibility of the approach analyzed theoretically in this thesis.

Future plans should include testing a horse. In particular, one should examine how suitable are the ropes and cleats to immobilize the animal that is much bigger than a sheep. A sketch of a possible horse restraint platform is presented in Figure 7.1. A flat bed is needed to fix the hooves. All the ropes restraining the joints can also be attached to the bed. However, an additional structural member attached to the bed is required to immobilize the head (otherwise the horse will use it to generate some dynamic forces when trying to free itself), which can be in the form of a simple frame shown on the sketch. The horse’s head and neck will be restrained with the help of a head halter attached to the frame.

Details of the horse hoof restrains design will have to be worked out. Hoof pads that can slide on the platform may be added to assist spreading the horse’s legs apart. Also, methods of quickly attaching and detaching the ropes to the horse's joints without harming the animal should be investigated, most probably by experimentations.

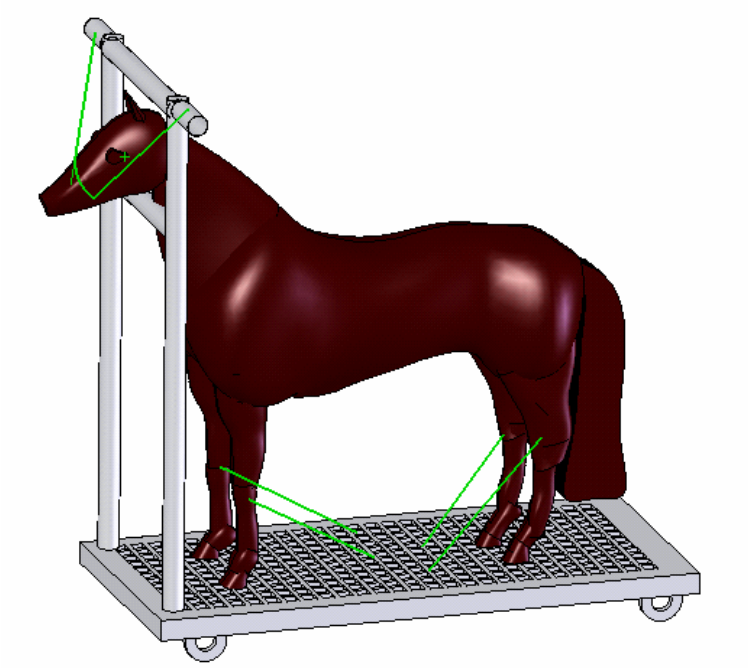

Figure 7.1: Horse restraint platform

The breaking forces to be generated by the horse during possible struggling actions were obtained 'theoretically' in the thesis. These forces could be verified experimentally by applying the strain gages or other types of force measurement devices.

If the experimental tests confirm that the horse's restrain in the natural standing configuration is satisfactory, then one may think about designing a system to restrain the horse with one lifted leg, for example. Such a position may be required for some imaging procedures.

From the computer simulation viewpoint a model that can recreate a 3D motion of the whole horse might be worth to develop. Although the horse's mobility seems to be essentially confined to the sagittal plane, a better understanding of possible sideway movements should be helpful in refining the restraint system.

Finally, the analysis and computer simulation methods proposed in this thesis could be extended to study the restraint methods for other animals, which can be done by simply modifying the anatomical structure and function used in the model.

LIST OF REFERENCES

[1] Hodson E., Clayton H.M., Lanovaz J.L., “The forelimb in walking horses: 1. Kinematics and ground reaction forces”, Equine Veterinary Journal, 2000, v 32, pp287-294

[2] Hodson E., Clayton H.M., Lanovaz J.L.,”The hindlimb in walking horses: 1. Kinematics and ground reaction forces”, Equine Veterinary Journal, 2001, v 33, pp38-43

[3] Clayton H.M., “Advances in motion analysis”, Veterinary Clinics of North America: equine practice, 1991, v 7, pp365-382

[4] van den Bogert, A.J. “Computer Simulation of Locomotion in the Horse “ PhD Thesis, 1989

[5] Dyce K.M., Sack W.O., Wensing C.J.G., “Textbook of Veterinary Anatomy”, 2nd ed. WB Saunders, 1996

[6] Payne R.C., Veenman P., Wilson A.M., “The role of the extrinsic thoracic limb muscles in equine locomotion”, Journal of Anatomy, 2005, v 206, pp193-204

[7] Payne, R.C., Hutchinson,J.R., Robilliard, J.J., Smith, N.C., Wilson, A.M. “Functional specialisation of pelvic limb anatomy in horses”, Journal of Anatomy, 2005, v 206, pp557-574

[8] Wilson A.M., McGuigan M.P., SUA, van den Bogert A.J. “Horse damp the spring in their step”, Nature, 2001, v 414, pp895-899

[9] Clayton H.M.**,** Flood, P.F., “Color Atlas of Large Animal Applied Anatomy”, Mosby-Wolfe, 1996

[10] Ramón, T., Prades, M., Armengou, L., Lanovaz, J.L., Mullineau, D.R. and Clayton, H.M., **"**Effects of athletic taping of the fetlock on distal limb mechanics", Equine Veterinary Journal, 2004, v 36, pp764-768

[11] Clayton, H.M., Sha, D.H. and Mullineaux, D.R., "Three dimensional kinematics of the equine carpus at trotting horses", Equine Veterinary Journal, 2004, v 36, pp 671-676

[12] Clayton, H.M., Singleton, W.H., Lanovaz, J.L. and Prades, M., "Sagittal plane kinematics and kinetics of the pastern joint during the stance phase of the trot", Veterinary Comparative Orthopedics and Traumatology, 2001, v 15, pp15-17

[13] Rooney, J.R., "The Mechanics of the Horse", R. E. Krieger Pub. Co., 1981

[14] Hedge, J., Wagoner, D., "Horse Conformation, Structure, Soundness, and Performance", The Lyons Press, 1999

[15] Pilliner, S. Elmhurst, S., Davies, Z. "The Horse in Motion", Blackwell Publishing, 2002

[16] Buchner, H.H.F., Savelberg, H.H.C.M., Schamhardtt, H.C., Barneveld, A., "Inertial Properties of Dutch Warmblood Horses", Journal of Biomechanics, 1997, v 30, pp.653-658

[17] http://www.imh.org/imh/bw/dwarm.html

[18] Marion, J., "Classical Dynamics of Particles and Systems", 2nd Edition, Academic Press, 1970

[19] Haug, E. J. "Computer Aided Kinematics and Dynamics of Mechanical Systems", Allyn and Bacon, 1989

APPENDIX A. EVALUATION OF LIMB MUSCLE FORCES IN FIGHTING THE RESTRAINTS

It is assumed in the thesis that biceps and biceps femoris play the most important role in generating the force to free the horse leg from the restraints. Forces generated by other major muscles on the limbs are not included in the model since their contribution in fighting the restraints are very little when compared with the biceps and biceps femoris muscles. A brief justification of the above assumptions is presented in this appendix.

A.1 Forelimb Muscles

Besides biceps, major muscles in the forelimb include Brachiocephalicus (BO), Serratus Ventralis Cervicis (SVC), Serratus Ventralis Thoracis (SVT), Latissimus Dorsi (LD), Triceps (T) on the upper arm, Extensors group (FE), and Flexors group (FF) on the lower limb. [5], [14],[15]

The upper arm muscles are used to protract or retract upper arm as shown in Figure A.1. [13]. However, ranges of protraction and retraction are not enough to stretch the leg members in tension, thus has no effect on pulling of the hoof restraints.

Lower limb extensors such as Common Digital Extensor (CDE) (Figure A.2a) may generate force to lift the hoof. But these muscles are not strong compare with the biceps and this force is ignored in the model (maximum force generation capability for CDE is about 1,000N [6]). The flexors group (Figure A.2b) has several stronger muscles such as deep digital flexor (DDF) and superficial digital flexor (SDF). When the hoof is fixed to the ground, forces pulling the leg will only push the hoof to the ground.

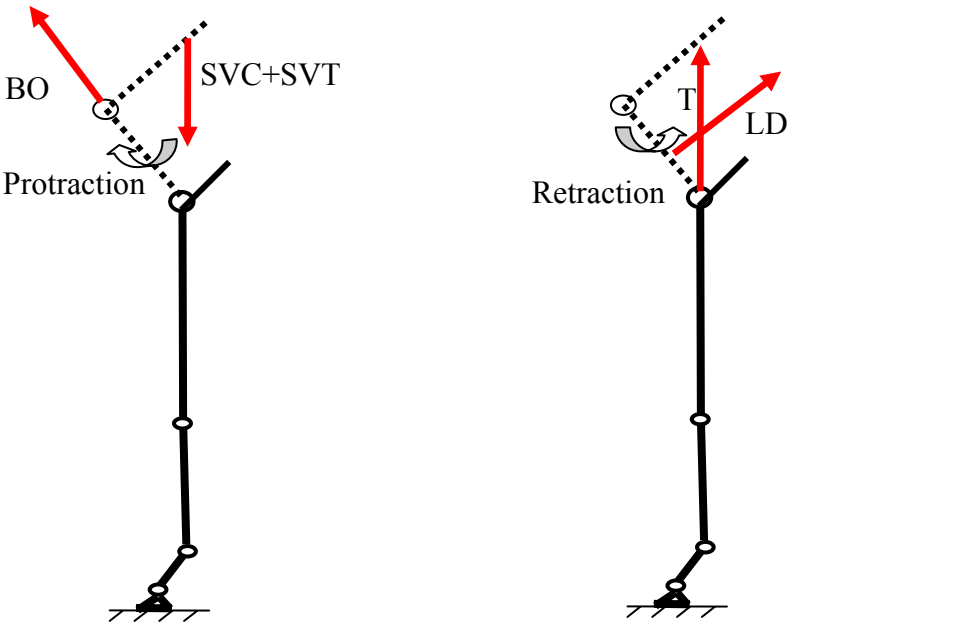

a. Muscles for upper arm protraction b. Muscles for upper arm retraction

Figure A.1: Upper forelimb muscle forces in forelimb

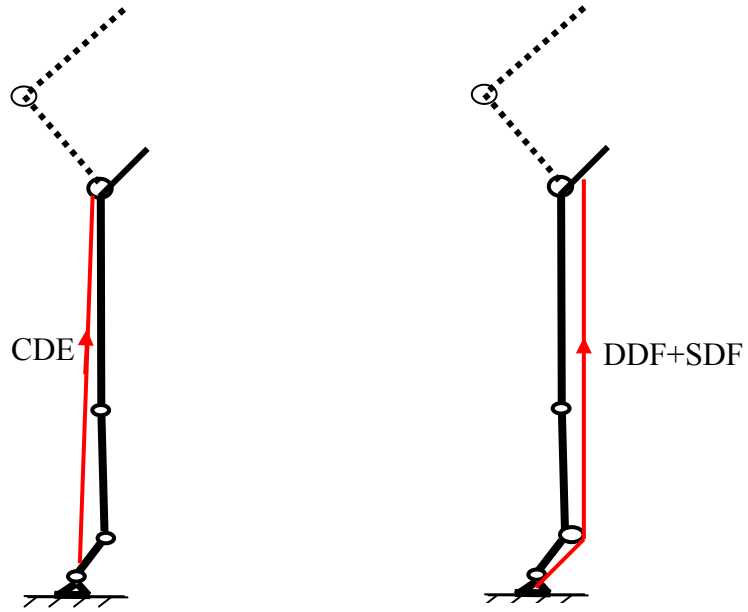

a. Extensor b. Flexors

Figure A.2: Lower forelimb muscle forces

A.2 Hindlimb Muscles

Similar situation applies to the hindlimb as well. For all muscle forces included in Figure A.3 (Glutaeus Medialis = GM, Quadriceps Femoris = QF, Semitendinosus = ST, Gastronemius = GN) [5],[14],[15] Their influence to the hoof is restricted by the rotation limit at hock joint. Just like forelimb, the force from lower extensor muscles shown in Figure A.4a (Lateral Digital Extensor = LDE) is ignored in the model [7]. The stronger digital flexor in Figure A.4b (DDF, SDF) will only led the hoof to push the ground when the hoof is fixed to the ground.

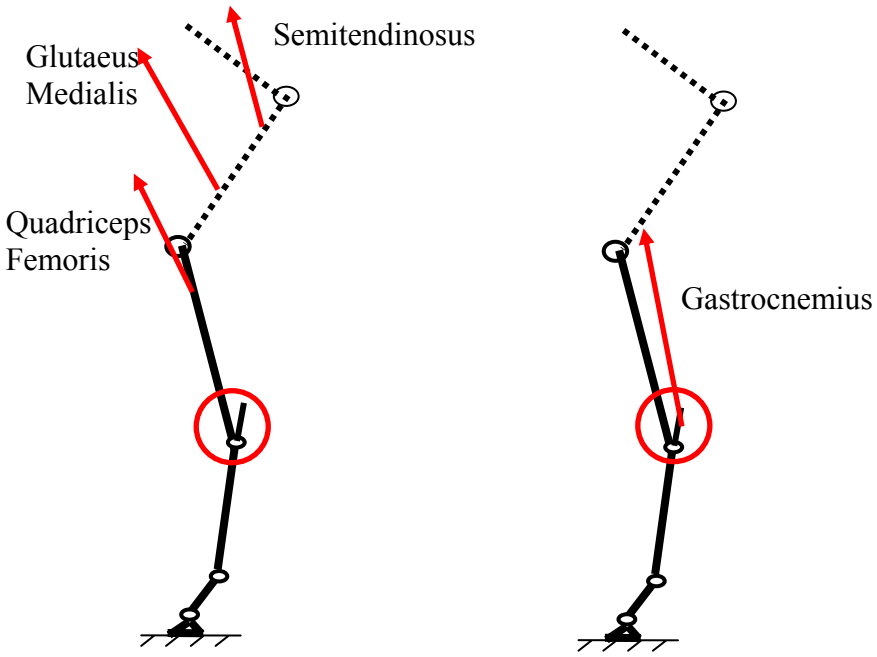

Figure A.3: Upper hindlimb muscle forces

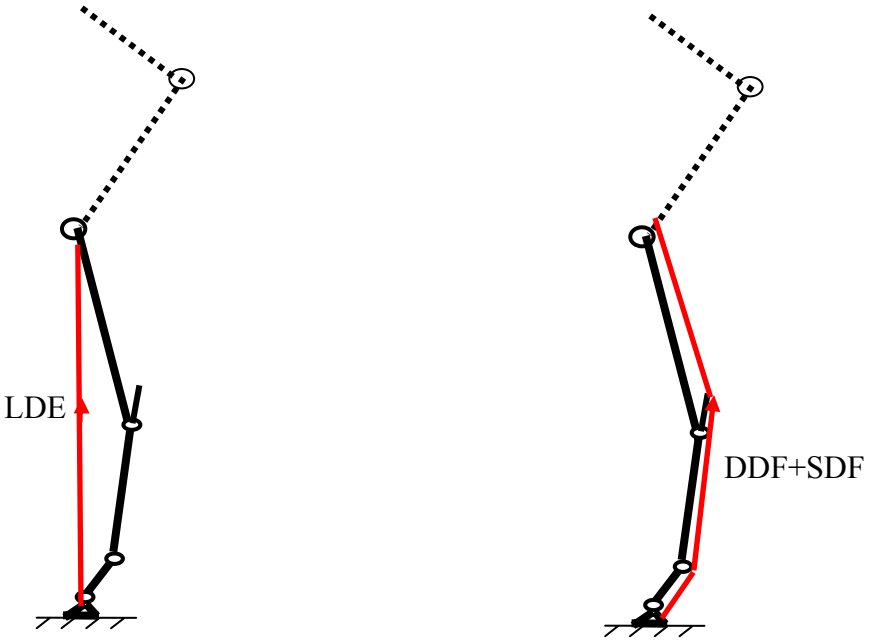

Figure A.4: Lower hindlimb muscle forces

APPENDIX B. GENERATING THE HORSE MODEL IN SOLIDWORKS

A 3D model of a horse is built up based on the twenty-six segment horse model given in Figure B.1 [16]. This is a model of a Dutch Warm Blood horse been introduced as an average horse model used in previous horse locomotion studies.

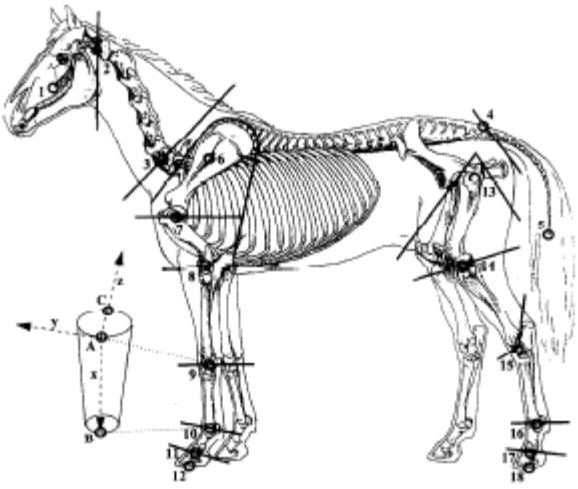

Figure B.1: Twenty-six segment model of a Dutch Warm Blood horse

B.1 Defining the Geometric Shape of the Horse

In order to create a horse computer model that is similar to the horse shown in Figure B.1, A picture of a real Dutch Warm Blood [17] horse is used as a background image in each segment's part file. In each part file, model should be scaled to read 156cm for the horse trunk as given in Butcher's note (Table 1). This procedure unifies the scale in each part file.

Table 1: Horse Body Segment Properties
(Mass, density, reference line, reference length)

Segment	n	Mass (kg)	Density ($g\,cm^{-3}$)	Reference line (A, B)	Reference length L (m)
Trunk	6	352.0 (41)	0.85 (0.05)	4–3	1.56 (0.04)
Tail	6	1.49 (0.26)	1.043 (0.026)	4–5	0.499 (0.018)
Head	6	23.1 (2.0)	1.031 (0.010)	2–1	0.302 (0.015)
Neck	6	26.8 (1.5)	1.038 (0.002)	3–2	0.540 (0.016)
Shoulder	12	20.1 (1.6)	nm	6–8	0.44 (0.04)
Scapula	12	11.5 (0.9)	1.043 (0.013)	6–7	0.274 (0.015)
Brachium	12	8.6 (1.5)	1.048 (0.013)	7–8	0.25 (0.03)
Antebrachium	12	6.7 (0.6)	1.12 (0.03)	8–9	0.434 (0.025)
Metacarpus	12	1.59 (0.09)	1.29 (0.04)	9–10	0.287 (0.011)
Digit forelimb	12	1.83 (0.21)	nm	10–11	0.130 (0.012)
Pastern forelimb	12	0.73 (0.05)	1.25 (0.03)	10–11	0.135 (0.007)
Fore hoof	12	1.08 (0.23)	1.181 (0.011)	11–12	0.099 (0.012)
Thigh	12	18.6 (2.3)	1.047 (0.007)	13–14	0.36 (0.04)
Crus	12	8.3 (0.8)	1.109 (0.019)	14–15	0.434 (0.023)
Metatarsus	12	2.84 (0.22)	1.284 (0.027)	15–16	0.353 (0.026)
Digit hind limb	12	1.87 (0.16)	nm	16–17	0.135 (0.011)
Pastern hind limb	12	0.89 (0.04)	1.23 (0.03)	16–17	0.141 (0.006)
Hind hoof	12	0.99 (0.17)	1.179 (0.012)	17–18	0.101 (0.012)

The 3D segment is created from the cross-sectional area profiles as shown in Figure B.2a. These profiles (ovals) are plotted according to the width of each segment in various height levels in the sagittal plane. Then commend “loft” is used to connect each cross-sectional profiles with smooth curves to create a 3D object as shown in the figure. The length of each segment is the distance between two joints of corresponding leg member in the background image. The entire horse is built in an assemble file gathering all segments of twenty-six part files.

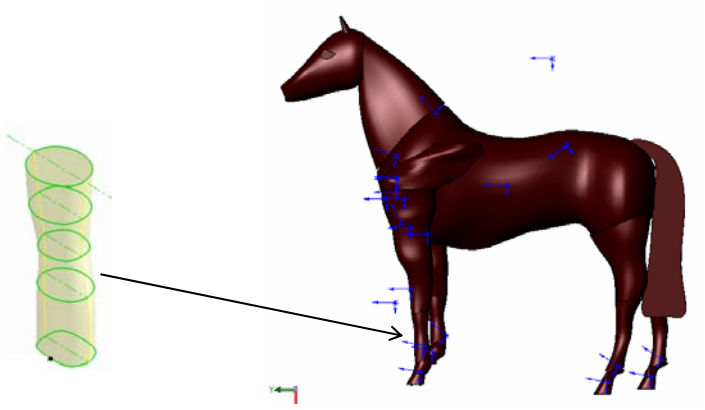

a) b)

Figure B.2: Creating 3D horse model

B.2 Physical Properties of Body Segment

Density of each part provided in Table 1 is used in the computer model. Solidworks can then calculate the mass of the segment from the product of the volume and the density of it. When the calculated mass in the computer model has significant difference with the mass listed in Table 1, the short axis of the oval shape profile will be adjusted till the mass in the model agrees with the mass listed in Table 1.

Centroid of each segment is determined automatically in Solidworks. Centroid position of some segments will be used in the simulation program to determine the dynamic reaction force.

APPENDIX C. MOTION SIMULATION

CosmosMotion, the dynamic motion simulation software can incorporate with model created in SolidWorks to simulate motion of the linkage system, representing the horse's skeletal structure. Constraints, muscle forces and some initial movement conditions and body resistance to the motion in the horse model have to be defined in the software to simulation the horse motion in restraints.

C.1 Adding Constraints in the Model

C.1.1 Joint Constraint

In this thesis, all joints are modeled as revolute joints allowing two adjacent parts to rotate in the saggital plane. In SolidWorks, these joints can be created by setting concentric and coincident constraints on two parts. Concentric constraint allows the two segments to slide along and to rotate about the *z*-axis running through the center of the parallel and concentric holes of each part. Coincident constraint allows the two segments to slide along the *x*-*y* plane, with the parallel sides sharing a common plane. It also allows the two segments to rotate about the *z*-axis. Once the revolute joints are defined, joint reaction forces can be obtained from simulation results.

C.1.2 Hoof Constraint

In this thesis, the hooves of the animal are assumed to be fixed to the ground. Fixing the horse hooves in the simulation is done by fixing the hooves with a ground part as shown in Figure C.1.

The fixing constraint is created with “smart faster” function in SolidWorks. The hoof has no DOF with this constraint and the effect is similar to nailing the hoof to the ground.

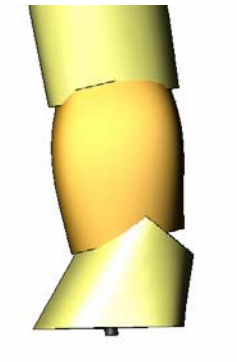

Figure C.1: Modeling of hoof restraint

C.1.3 Upper Arm and Trunk Constraint

The upper arm and trunk of the horse is assumed to be constrained in a way that only vertical movement is allowed. In the simulation, this is set with a sliding joint between the upper arm and a ground part as shown in Figure C.2. Horizontal movement of the upper arm and trunk is not allowed with this constraint.

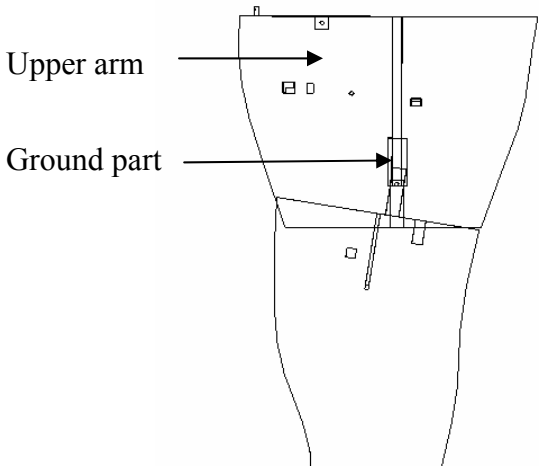

Figure C.2: Setting the translational constraint at the upper arm

C.1.4 Lower Leg Restraint

Besides the hoof restraint, restraints on lower legs are required to immobilize the whole leg. These restraints can be modeled as a cable tightening the leg with the ground. Springs with high stiffness assumed at 30,000N/mm is added to the system to simulate the cables. Spring forces required to hold leg firmly are obtained as simulation results.

C.2 Applying Muscle Force

Muscle forces in the leg are simulated as action-only forces applying on the leg. They are assumed to be constant force during the fighting period. The action line of the muscle force change as the legs rotate. This effect is created with two force direction reference bars in the model as shown in Figure C.3, an example of modeling the biceps muscle force. One bar rotates around the origin of the biceps and the other rotates around the insertion point. Their long edges are set to align during the rotation. The line between the insertion and origin of the biceps indicates force direction regardless of rotation.This edge always indicates the straight line between muscle origin and insertion regardless of the rotation. The biceps force direction is set to follow the direction of this line.

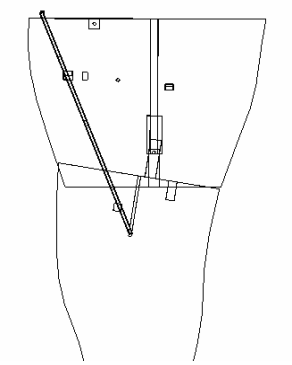

Figure C.3: Setting the biceps muscle force

C.3 Initial Velocity and Acceleration

As described in the thesis, when analyzing the dynamic jerking effect, the jerking is divided into several phases. The initial velocity and /or acceleration may be required to describe the motion. These initial conditions are input of the simulation program and can be given through motion properties page in Cosmos. Refer to the Cosmos help document for more information about setting the motion properties for the system.

C.4 Body Resistance to Motion

Several things in the skeletal muscular system may resist the dynamic motion and in turn reduce the breaking force generated in dynamic jerking. Although it is hard to evaluate their influence in the system, including these resistances in the model is necessary to avoid legs member move with unrealistically high accelerations in the simulation. Spring elements are introduced to represent the body resistance. Springs are loaded with initial compression force (3,000 N for forelimb and 5,000N for hindlimb, Figure C.4) to simulate the initial resistance. Then as the legs move up, more resistance will be generated from the spring elements (stiffness of the springs are 30N/mm for forelimbs and 10N/mm for hindlimbs). The settings for the spring elements ensure that the mass on top of the limbs can move with acceleration between 2g-3g, and leg members can have enough energy to be pulled to the highest level permitted by the range of motion during the dynamic jerking.

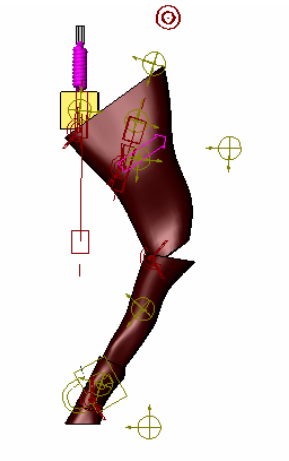

Figure C.4: Simulating body resistance to the motion

APPENDIX D. MIXED DIFFERENTIAL–ALGEBRAIC EQUATION OF MOTION

In Chapter 2 and Chapter 4, the theoretical solutions of the breaking force due to dynamic jerking are given with Newtonian equation of motion. Breaking forces are also obtained from computer simulation results in Cosmos Motion. CosmosMotion uses ADAMS/Solver as the core package in solving dynamic problems. In ADAMS/Solver, motion of the multi-linkage system is automatically described in a system of Lagrange equations. Using Lagrangian formulation in the solver enable the computer program to focus only on the dynamics of the system rather than calculating the forces acting on each component of the system. Breaking force can be determined from the Lagrange multiplies λ appears in the mixed Differential-Algebraic Equations (DAE) of motion. [18], [19]

To get a clear understanding of how the computer simulation program solves the horse motion, the procedure of generating the DAE to solve the dynamic breaking force during forelimb jerking is described as an example in detail. For a forelimb system as shown in Figure 2.14, the Lagranian L of each part in the system can be written as:

$$L = T - V = \frac{1}{2}[J_i \dot{\theta}_i^{\,2} + m_i(\dot{x}_{ci}^2 + \dot{y}_{ci}^2)] - \int M_i \delta\theta_i + F_{xi}\delta x_{Ci} + F_{yi}\delta y_{Ci} = L(\theta_i, x_{ci}, y_{ci}) \quad \text{(D.1)}$$

Where T = kinetic energy of the system, V= potential energy of the system

i = 1, 2, 3 (number of part in the system), θ_i, x_{ci}, y_{ci} are angular and centroid displacement of each part. M_i, F_{xi}, F_{yi} are external moment and force applied on each part. $\delta\theta_i, \delta x_{Ci}, \delta y_{Ci}$ are virtual displacement of each part. J_i and m_i are moment of inertia and mass of each part.

From the Hamilton's principle and the Lagrange multiplier theorem, the Euler-Lagrange equations are derived as:

$$\frac{d}{dt}\frac{\partial L}{\partial \dot{q}_j} - \frac{\partial L}{\partial q_j} + \sum_{k=1}^{m} \lambda_k \frac{\partial \phi_k}{\partial q_j} = 0 \qquad \text{(D.2)}$$

where q is the general coordinates, j =1,2,3 represent x, y and θ coordinate, λ is the lagrange multiplier, ϕ_k represents the system's constraint equations and k is the number of constraint equations.Constraint equations ϕ_k written for the linkage system shown in Figure 2.14 are

$$\begin{aligned}
&\phi_1 : x_{c1} - H + l_2\cos\beta + (l_1 - l_{c1})\cos\alpha = 0 \\
&\phi_2 : y_{c1} - l_2\sin\beta + (l_1 - l_{c1})\sin\alpha = 0 \\
&\phi_3 : x_{c2} - H + l_{c2}\cos\beta = 0 \\
&\phi_4 : y_{c2} - l_{c2}\sin\beta = 0 \\
&\phi_5 : x_{c3} - H + l_1\cos\alpha + l_2\cos\beta = 0 \\
&\phi_6 : y_{c3} - l_2\sin\beta + l_1\sin\alpha = 0
\end{aligned} \qquad \text{(D.3)}$$

Substitute (D.1), (D.3) in (D.2), the equations of motion are written as

(1) $m_1\ddot{x}_{c1} - F_{mx} + \lambda_1 = 0$

(2) $m_1\ddot{y}_{c1} + F_{my} + \lambda_2 = 0$

$$(3)\ J_{c1}\ddot{\alpha} - M_i - \lambda_1(l_1 - l_{c1})\sin\alpha + \lambda_2(l_1 - l_{c1})\cos\alpha - \lambda_5 l_1 \sin\alpha + \lambda_6 l_1 \cos\alpha = 0$$

$$(4)\ m_2\ddot{x}_{c2} + \lambda_3 = 0$$

$$(5)\ m_2\ddot{y}_{c2} + \lambda_4 = 0$$

$$(6)\ J_{c2}\ddot{\beta} - \lambda_1 l_2 \sin\beta - \lambda_2 l_2 \cos\beta - \lambda_3 l_{c2} \sin\beta - \lambda_4 l_{c2} \cos\beta - \lambda_5 l_2 \sin\beta - \lambda_6 l_2 \cos\beta = 0$$

$$(7)\ m_3\ddot{x}_{c3} - F_p + \lambda_5 = 0$$

$$(8)\ m_3\ddot{y}_{c3} - (-F_{Ay}) + \lambda_6 = 0$$

(D.4)

Then differentiate (D.3) twice and combines (D.4), one obtains the DAE of the motion of the system with 14 equations and 14 unknowns. These equations can also be written in a matrix form as shown in Figure D.1.

If the DAE is solved in Maple, lagrange multipliers are obtained to determine the breaking force.

From (D.4) (3), (6)

$$J_{c1}\ddot{\alpha} = M + (\lambda_1 + \lambda_5)l_1 \sin\alpha - \lambda_1 l_{c1} \sin\alpha - (\lambda_2 + \lambda_6)l_1 \cos\alpha + \lambda_2 l_{c1} \cos\alpha \quad \text{(D.5)}$$

$$J_{c2}\ddot{\beta} = (\lambda_1 + \lambda_5)l_2 \sin\beta + \lambda_3 l_{c2} \sin\beta + (\lambda_2 + \lambda_6)l_2 \cos\beta + \lambda_4 l_{c2} \cos\beta \quad \text{(D.6)}$$

Also the equilibrium equations of the moment for link1 can be written in Newtonian form as:

$$J_{c1}\ddot{\alpha} = -M + (F_{Ax} + F_{Bx})l_{c1} \sin\alpha - F_{Bx} l_1 \sin\alpha + (F_{Ay} + F_{By})l_{c1} \cos\alpha - F_{By} l_1 \cos\alpha$$

For link2:

$$J_{c2}\ddot{\beta} = -F_{Bx} l_2 \sin\beta + (F_{Bx} - BF_x)l_{c2} \sin\beta + F_{By} l_2 \cos\beta + (BF_y - F_{By})l_{c2} \cos\beta$$

(D.8)

Comparing D.5 and D.7, one has

$$\lambda_1 + \lambda_5 = -F_{Bx}\,, \lambda_1 = -(F_{Ax} + F_{Bx})\,, \lambda_2 + \lambda_6 = F_{By}\,,\ \lambda_2 = F_{Ay} + F_{By} \qquad \text{(D.9)}$$

Comparing D.6 and D.8, one has

$$\lambda_3 = F_{Bx} - BF_x\,,\ \lambda_4 = BF_y - F_{By} \qquad \text{(D.10)}$$

Multipliers λ are solvable with DAE, substitute the value of λ in (D.9), (D.10) , one can get $BF_x = 6{,}611\text{N},\ BF_y = 1{,}196\text{N}$, which are identical to the result obtained with Newtonian equations in Chapter 2. In the computer simulation program, DAE will be solved with specific numerical methods. More information on these can be found in ADAMS/Solver user manual.

$$
\begin{bmatrix}
m_1 & & & & & & & & & & & & & 1 & & \\
 & m_1 & & & & & & & & & & & & & 1 & \\
 & & J_{c1} & & & & & & & & & & & -(l_1-l_{c1})\sin\alpha & (l_1-l_{c1})\cos\alpha & \\
 & & & m_2 & & & & & & & & & & & & \\
 & & & & m_2 & & & & & & & & & & & \\
 & & & & & J_{c2} & & & & & & & & -l_2\sin\beta & -l_2\cos\beta & -l_{c2}\sin\beta-l_{c2}\cos\beta \\
 & & & & & & -1 & & & & & & & & & \\
 & & & & & & & 1 & & & & & & & & \\
1 & & -(l_1-l_{c1})\sin\alpha & & & -l_2\sin\beta & & & & & & & & & & \\
 & 1 & (l_1-l_{c1})\cos\alpha & & & -l_2\cos\beta & & & & & & & & & & \\
 & & & 1 & & -l_{c2}\sin\beta & & & & & & & & & & \\
 & & & & 1 & -l_{c2}\cos\beta & & & & & & & & & & \\
 & & -l_1\sin\alpha & & & -l_2\sin\beta & \frac{1}{m_3} & & & & & & & -\frac{1}{m_3} & & \\
 & & l_1\cos\alpha & & & -l_2\cos\beta & -\frac{1}{m_3} & & & & & & & & -\frac{1}{m_3} &
\end{bmatrix}
\begin{bmatrix}
\ddot{x}_{c1} \\ \ddot{y}_{c1} \\ \ddot{\alpha} \\ \ddot{x}_{c2} \\ \ddot{y}_{c2} \\ \ddot{\beta} \\ F_p \\ F_{Ay} \\ \lambda_1 \\ \lambda_2 \\ \lambda_3 \\ \lambda_4 \\ \lambda_5 \\ \lambda_6
\end{bmatrix}
=
\begin{bmatrix}
F_{mx} \\
F_{my} \\
-F_m(l_{c1}-l_b)\sin(\alpha+\gamma) \\
0 \\
0 \\
0 \\
-m_3\ddot{x}_{c3} \\
0 \\
l_2\dot{\beta}^2\cos\beta+(l_1-l_{c1})\dot{\alpha}^2\cos\alpha \\
-l_2\dot{\beta}^2\sin\beta+(l_1-l_{c1})\dot{\alpha}^2\sin\alpha \\
l_{c2}\dot{\beta}^2\cos\beta \\
-l_{c2}\dot{\beta}^2\sin\beta \\
l_1\dot{\alpha}^2\cos\alpha+l_2\dot{\beta}^2\cos\beta \\
-l_2\dot{\beta}^2\sin\beta+l_1\dot{\alpha}^2\sin\alpha
\end{bmatrix}
$$

Figure D.1: DAE in matrix